AD-A144 858 OPTICAL TURBULENCE MEASUREMENT - INVESTIGATIONS FOR ANALYSIS OF LASER DES..(U) ARMY ELECTRONIC PROVING GROUND FORT HUACHUCA AZ E C CRITTENDEN ET AL. MAY 83 1/3

UNCLASSIFIED USAEPG-FR-1226 F/G 20/6 NL

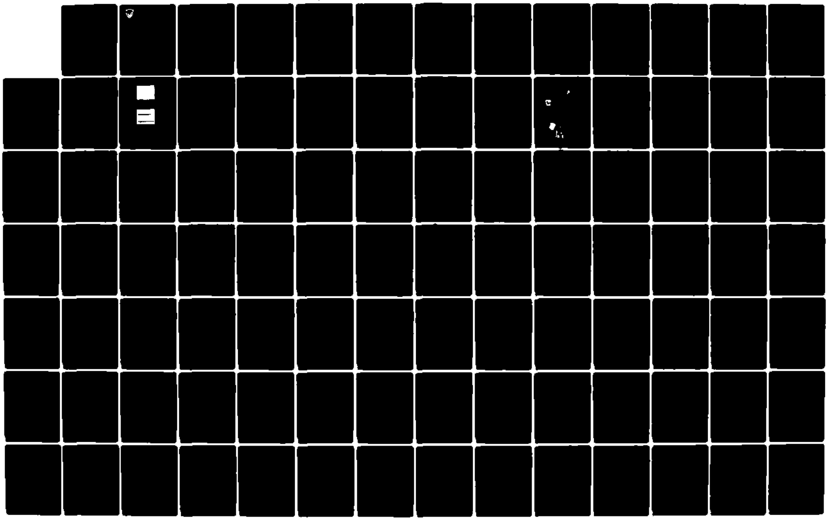

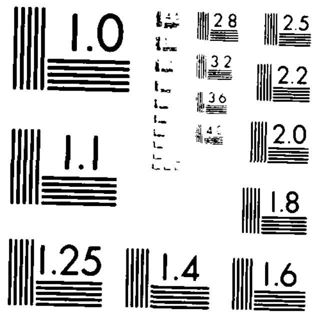

MICROCOPY RESOLUTION TEST CHART

DDC AD NUMBER

FUNDING PROJECT NO. 1T665702D625

TECOM PROJECT (TRMS) NO. 7-CO-RD1-EP1-002

TEST ACTIVITY REPORT NO. USAEPG-FR-1226

TEST SPONSOR US Army Test and Evaluation Command

METHODOLOGY INVESTIGATION

FINAL REPORT

OPTICAL TURBULENCE MEASUREMENT - INVESTIGATION FOR ANALYSIS OF LASER DESIGNATOR SPOT PATTERNS - PHASE I

BY

E. C. CRITTENDEN, E. A. MILNE, S. R. CRAGER, J. H. CONNOR, JR., N. E. PENTZ, W. M. DECKER IV, AND C. M. GIORGI

MAY 1983

DISTRIBUTION UNLIMITED

US ARMY ELECTRONIC PROVING GROUND
Fort Huachuca, Arizona 85613

DISPOSITION INSTRUCTIONS

Destroy this report in accordance with appropriate regulations when no longer needed. Do not return it to the originator.

DISCLAIMER

Information and data contained in this document are based on input available at the time of preparation. Because the results may be subject to change, this document should not be construed to represent the offficial position of the US Army Materiel Development and Readiness Command unless so stated.

The use of trade names in this report does not constitute an official indorsement or approval of the use of such commercial hardware or software. This report may not be cited for purposes of advertisement.

UNCLASSIFIED

SECURITY CLASSIFICATION OF THIS PAGE (When Data Entered)

REPORT DOCUMENTATION PAGE		READ INSTRUCTIONS BEFORE COMPLETING FORM
1. REPORT NUMBER TRMS No. 7-CO-RD1-EP1-002	2. GOVT ACCESSION NO.	3. RECIPIENT'S CATALOG NUMBER
4. TITLE (and Subtitle) Methodology Investigation Final Report (Optical Turbulence Measurement-Investigation for Analysis of Laser Designator Spot Patterns - Phase I)		5. TYPE OF REPORT & PERIOD COVERED Methodology Investigation Final Report-Jan 81-Mar 83 6. PERFORMING ORG. REPORT NUMBER USAEPG-FR-1226
7. AUTHOR(s) E. C. Crittenden, E. A. Milne, S. R. Crager, J. H. Connor, Jr. (NPS), N. E. Pentz, W. M. Decker IV, and C. M. Giorgi (TECOM)		8. CONTRACT OR GRANT NUMBER(s)
9. PERFORMING ORGANIZATION NAME AND ADDRESS US Army Electronic Proving Ground Fort Huachuca, Arizona 85613		10. PROGRAM ELEMENT, PROJECT, TASK AREA & WORK UNIT NUMBERS 1T665702D625
11. CONTROLLING OFFICE NAME AND ADDRESS US Army Test and Evaluation Command ATTN: DRSTE-AD-M Aberdeen Proving Ground, MD 21005		12. REPORT DATE May 1983 13. NUMBER OF PAGES
14. MONITORING AGENCY NAME & ADDRESS(if different from Controlling Office)		15. SECURITY CLASS. (of this report) Unclassified 15a. DECLASSIFICATION/DOWNGRADING SCHEDULE

16. DISTRIBUTION STATEMENT (of this Report)

Distribution is unlimited.

17. DISTRIBUTION STATEMENT (of the abstract entered in Block 20, if different from Report)

18. SUPPLEMENTARY NOTES

19. KEY WORDS (Continue on reverse side if necessary and identify by block number)

Methodology Investigation
Atmospheric Turbulence
Optical Turbulence
Optical Transfer Function
Laser Spot Patterns
Laser Designators
Laser Beam Propagation
Video Image Analysis
Video Image Digitizing
Electro-Optical Systems Testing
Image Wander

20. ABSTRACT (Continue on reverse side if necessary and identify by block number)

This methodology investigation evaluates the feasibility of applying video image analysis techniques and instrumentation to characterize optical path turbulence for use in assessing the field performance of laser designator systems. The effort focused on adapting a C_n^2 path weighted measurement technique developed by Dr. E. Crittenden, NPS, which uses a telescope mechanical slit scanner configuration for data acquisition. The Phase I effort

(cont)

DD FORM 1473 1 JAN 73 EDITION OF 1 NOV 65 IS OBSOLETE

UNCLASSIFIED

SECURITY CLASSIFICATION OF THIS PAGE (When Data Entered)

Item 20 (cont)

presented in this report covers a theoretical analysis and empirical measurements to include a coincident path performance comparison of the scanner and a video system in a laboratory environment. Computer programs for analyzing the video data using either a real time digitizer or a digital storage oscilloscope were also developed. The results of the investigation demonstrate that the video technique can be applied to the measurement of $C_n{}^2$ and a test plan to further validate the technique in a field environment is presented.

FOREWORD

The US Army Electronic Proving Ground was responsible for the execution of this project. Mr. C. M. Giorgi was the Activity Project Officer with assistance from Major W. M. Decker, IV. Technical guidance as well as the idea for the project was provided by the Test and Evaluation Command Project Officer, Dr. N. E. Pentz.

Dr. E. C. Crittenden and Dr. E. A. Milne, of the Naval Postgraduate School were responsible for conducting the specific technical investigations with assistance from Mr. S. R. Crager and Mr. J. H. Conner, Jr., of that organization. The material presented in this report are the results of those investigative efforts.

TABLE OF CONTENTS

SECTION 1. SUMMARY

1.1 BACKGROUND

a. The spot patterns produced by laser designators suffer from a number of defects. The patterns are broadened and exhibit wander and intensity fluctuation because of turbulence in the atmosphere. Designator spot patterns also exhibit similar defects because of internal laser instability and motion of the transmitter platform. In order to correct the latter defects, a system is needed that is capable of separating the contributions of the several effects.

b. Previous work at the Naval Postgraduate School (ref 1, 2, 3, app E) and elsewhere (ref 4, app E) has demonstrated that the effects of atmospheric turbulence on designator spot patterns can be expressed in terms of the Optical Transfer Function (OTF) of the atmosphere. This quantity is the Fourier transform of the spot profile due to the atmosphere alone. If other causes of spot broadening are present, such as laser instability and platform motion, the spot profile will be the convolution of the spot profiles due to each of the effects s. The spot profile broadening due to laser and platform instability can then be separated from the atmospheric effects by dividing the Fourier transform of the spot profile by the OTF of the atmosphere (point-by-point as a function of spatial frequency). The necessary OTF of the atmosphere can be obtained by means of a slit-scanning telescope system, which views a point laser in the target vicinity from a location near the designator transmitter. An additional imaging system, viewing the designator spot on a target screen, from a location near the target, yields the composite spot profile. Data from this imager, together with that from the telescope imager at the transmitter site, can separate the various effects. As will be described later in more detail, spot motion and spot broadening are separated by computer tracking (image centering) techniques, applied to the data from the spot profile TV camera.

c. Because designator lasers use short pulses, the previously developed mechanical slit-scan techniques cannot be used. Storage imaging systems, using TV, CCD, or CID techniques, are needed to sense the image for the very short pulse periods, and provide the equivalent of a slit-scan during the interpulse period. TV was chosen over CCD or CID techniques for this purpose because of higher interpixel uniformity for TV.

1.2 OBJECTIVES

The principal objective of the work described in this report was to demonstrate the quantitative separation of the relative contribution of the effects of atmospheric turbulence, laser instability, and platform motion, by utilization of TV imaging systems. The basic principles of this separation have been established by previous work at the Naval Postgraduate School, in terms of Fourier transform data processing. However, the previous experimental work there has been carried out with mechanical slit-scanning optics. A principal objective was thus the verification that television imaging systems can yield the same results as slit-scanning systems. The techniques were to be tested in the laboratory, but be capable of implementation in the field. The relevant field conditions to which this should apply are to include the use of a uniform reflectivity target for the designator spot. However, the techniques should also be adaptable to the case of a realistic nonuniform reflectivity field target, such as a tank. Also, although not part of the required objective, the techniques employed were to be chosen, where possible, to be extendable later to the use of moving targets. An additional objective of the work was to verify the effectiveness of the equipment chosen for the experimental program.

1.3 SUMMARY OF PROCEDURES

a. Techniques were developed and tested in a 135 meter long medium-turbulence optical tunnel for the purpose of obtaining the Modulation Transform Function (MTF), and C_n^2 (a measure of the severity of turbulence) for the path by means of a television imaging system. The system imaged a point laser source at the far end of the tunnel, simulating a laser mounted in the designator target during field tests. The television signals were recorded on analog tape, then digitized and processed later. The recording techniques were tested and found to be sufficiently linear. A computer data processing system developed for the TV data reduction was tested on the observed TV image signals.

b. A previously proven slit-scan system for measuring MTF and C_n^2 and the TV imaging system described above were then used simultaneously to view identical images of a point laser source at a distance. The images were obtained by means of a half-transmitting mirror splitter in the telescope output. The signals for both systems were recorded and data processed by Fourier transform techniques to yield values of the turbulence structure constant, C_n^2, as a quantitative means of comparing the results obtained by the two systems. The results are summarized below.

c. The procedures for digital subtraction of residual background (persisting through the laser line filter), in TV images of the laser spot pattern on a uniform screen, were tested, using a Quantex DS-30 digital image processor. The data processing to yield the MTF from the resulting background-free laser designator spot was then tested.

d. Extension of the techniques, to the case of laser designator targets with nonuniform reflectivity, was analyzed in principle, and found to be practical. Actual performance testing of this process awaits the availability of a larger computer planned for future acquisition at Fort Huachuca.

1.4 SUMMARY OF RESULTS

Measurements of the OTF of the atmosphere made by means of TV imaging systems are in agreement with measurements made through identically the same atmosphere with mechanical-line scanning equipment. Also, test of the recording systems needed for proposed field test measurements show that the recording equipment is sufficiently linear to permit data reduction to be carried out later. The general techniques are capable of separating the effects of atmospheric turbulence, internal laser designator instability, and effects of platform motion.

1.5 ANALYSIS

a. The Phase I analytical effort and laboratory experiments were designed to establish the feasibility of applying the video image analysis technique and to lay the groundwork for the Phase II field experiments. The feasibility assessment required the evaluation of the linearity of the components of the video recording system and also required the development of a computerized data analysis program to generate the C_n^2 data from the video data. System linearity was empirically evaluated by comparing the output of the video camera with the final output from the disc unit. The reproducibility achieved demonstrated the basic feasibility of replacing the mechanical slit scan system with the video system.

b. The original scope of the Phase I study did not include the setting up of a complete video data acquisition and analysis instrumentation configuration. However, the availability during the time frame of the study of a digital video analyzer, video disc unit and a desk top computer made it possible to set up a complete, self contained C_n^2 measurement system. The measurement system utilized the same components used by most test ranges to record and analyze laser designator spot characteristics. The availability of the instrumentation configuration accelerated the generation of the supporting software program to derive the C_n^2 data from the spot imagery and the results of that work are covered in detail in Appendix C. The results show that a comparison of the measured versus predicted patterns will establish the level of jitter attributable to the laser platform.

c. Improvements to the data processing capability can be made by controlling the video disc and the tape unit through an interface bus instead of manually as done for this analysis program. However, most of the currently operational designator spot analysis systems use such a bus and the software in Appendix C can be adapted to take advantage of that capability. Additionally, a significant increase in the speed of the data analysis operation can be achieved if a computer system with more speed and greater memory than the HP-9825 is used. It is currently planned to use an HP-1000 for the field test phase of the investigation.

d. The use of the beam splitter technique to compare the performance of the video system and the NPS mechanical slit scanning system represented an ideal solution to the path control problem. The commonality of both the spatial and temporal inputs to the two systems greatly simplified the analysis of the data. The data obtained during the comparison tests is covered in detail in Appendix D and it established that the video system did not produce any degradation in the signal data.

e. Due to a prior commitment for the video disc and digitizer equipments, these items were not available to use in the analysis of the comparison test data. As a result, an alternate data analysis method was used and a considerably modified computer program prepared. The alternate method, as covered in detail in Appendix D, demonstrated that a storage oscilloscope can be used for analyzing the data and that a good approximation of the point spread function can be made by recording a single TV line through the laser spot and using it to calculate the one-dimensional line spread function. The computer program generated for this data analysis is presented in algorithm form in order to facilitate its transfer to other computer systems. The use of the digital storage oscilloscope demonstrated that, if data reduction turnaround time is not critical, the video data analysis can be performed using a $6,000 instrument in place of a $60,000 video digitizer and disc system. For path weighted C_n^2 measurements not involving the high data rate laser designator spot profile analyses, the digital storage oscilloscope system represents a modest investment for the capability provided.

f. The conduct of the laboratory type system comparison tests represented an interim step between the originally planned Phase I study effort and the Phase II field tests. The successful completion of the interim step laboratory measurements has increased the probability for the successful conduct of the field tests and has also eliminated the requirement for a major portion of the preliminary technique verification tests originally planned for the Phase II field test program. The proposed field tests are covered in Appendix A.

g. By generating the analysis programs for the experimental tests for two levels of instrumentation support, the end products of Phase I study and experimental effort can be applied to a range of both laboratory and field OTF and C_n^2 measurement requirements. This includes applying the techniques to standard testing of E-O systems and devices in the field as well as for characterizing atmospheric path conditions for degraded environment testing.

1.6 CONCLUSIONS

The proposed field experiments to separate the effects on laser designators of atmospheric turbulence, internal laser designator instability, and platform motion can be successfully carried out with the techniques and equipment recommended.

1.7 RECOMMENDATIONS

It is recommended that the proposed field test experiments be carried out to separate the effects of turbulence, internal laser instability, and platform motion in laser designators.

SECTION 2. DETAILS OF INVESTIGATION

2.1 INTRODUCTION

a. The experimental and analytical program carried out has been that necessary to establish the validity of experiments proposed for a later field test program. That test program is summarized in appendix A. Briefly, the proposed field test program addresses the problem of separating the types of instability in laser designators, i.e., turbulence, the internal stability of the laser designator and its optics, and the platform instability.

b. The effects of atmospheric turbulence are broadening of the image profile, wander of the center of the beam and scintillation within the beam profile. The scintillation is the most difficult to handle in detail. However, it can be circumvented by dealing with the profile as observed in the average of a number of individual pulse profiles.

c. The effects of turbulence on beam propagation have been investigated at a number of laboratories, with perhaps the longest and most complete sustained program being at the Naval Postgraduate School (ref 1, app E). This work has led to a well-verified analytical model for the beam profile to be expected after a beam has traversed an optical path through the atmosphere. This is expressed in terms of the OTF or Optical Transfer Function of the atmosphere. Two forms of this are equally useful. One expresses the OTF for the average of a number of beam profiles without centering (or tracking) the beam. The other applies to a beam that is centered (or tracked) before averaging a number of profile measurements. In the course of centering before averaging, a tally of the offsets required gives the variance of the beam "wander." Both these quantities are functions of the turbulence constant for optical index, C_n^2, and the range, as well as the wavelength.

d. The beam spread resulting from a number of causes, such as the turbulence, designator instability, and platform instability, is the convolution of the profiles from each cause. This allows the Fourier transform convolution theorem to be utilized. This says that the transform of the convolution of several functions is the product of the Fourier transforms of those functions. This can be reversed and the functions unfolded by dividing the transforms point-by-point. This technique has been used to separate the types of broadening.

e. For the case of wander where the statistical behavior is Gaussian, the variance of the displacement is the sum of the variances of the two component wanders. This allows separation of the wander terms.

2.2 THEORETICAL BACKGROUND

a. Separation of the atmospheric contribution to the beam wander and broadening involves measuring the turbulence structure constant for optical index, C_n^2. This can be determined in a number of ways. For example, it can be determined by measuring the temperature at points along the optical path. Although, in principle, it could be measured with thermal sensors, this has not been very practical in most instances. One difficulty is that the optical properties of interest here, the broadening and wander, depend on the integrated value of C_n^2 along the optical path. Also the relative importance of C_n^2 varies with the position along the path, and this weighting factor depends on the particular type of optical property involved. The relative path-position weighting of C_n^2 is shown in figure 1, for several different optical situations. The situation for an optical beam formed by a projector lens system is shown in curve A, for the case where the lens system is on the right and the target on the left. By a reciprocity theorem, a telescope system behaves in the same way as the projector if the telescope is on the right and a point source is on the left.

b. Other methods of measuring C_n^2, for example, by scintillation, produce a path-position weighting distribution as shown in curve B. This emphasizes the center of the path and does not give the proper distribution to predict the behavior of a laser designator. In this case then, it is important to use a telescope to measure C_n^2 to obtain the weighting needed to predict the behavior of the designator.

2.3 EXPERIMENTAL PROGRAM

The experimental program to verify the practicality of the proposed field test program involved several facets. The general objective was verification of the general applicability of the use of TV imagers in place of mechanical line slit-scanners for the purpose of separating the types of spot instability. This also involved the verification of the suitability and linearity of individual components of the proposed overall test system. We will look first at the tests of system components, followed by an experimental comparison of TV and mechanical line-scanner techniques.

a. System Components

(1) Silicon Vidicon. A silicon focal plane screen is needed for the vidicon viewing the designator spot pattern in order to reach the 1.06 micrometer, near-IR, wavelength. The usual TV vidicons, or other TV cameras such as orthicons, are optimized for the visual range of wavelengths and do not reach this wavelength. A TV technique is needed because the pulse length of the designator is too short (a few nanoseconds) for a split-scanning system to function. The image of the designator spot is stored on the semiconducting sensitive surface of the vidicon. The electron beam raster scan interrogates the image to produce the usual composite TV video format. It was found on trial that each of the two interlaced "fields" of the raster completely reset the sensitive surface. The storage time is thus the 1/60 second between field scans. A test of the performance of the vidicon was carried out in the laboratory by imaging a broad spot produced by GaAs laser at a wavelength of 0.905 micrometers.

(2) Vidicon for Atmospheric OTF Measurement. A second vidicon is used to view a point laser source located in the target screen, in order to provide the data concerning the atmospheric OTF. (See fig. 1, app A.) This system is less demanding as far as pulse length is concerned, and the wavelength can be any value available in a convenient small laser, as long as it differs from the 1.06 micrometers of the designator. In practice a HeNe

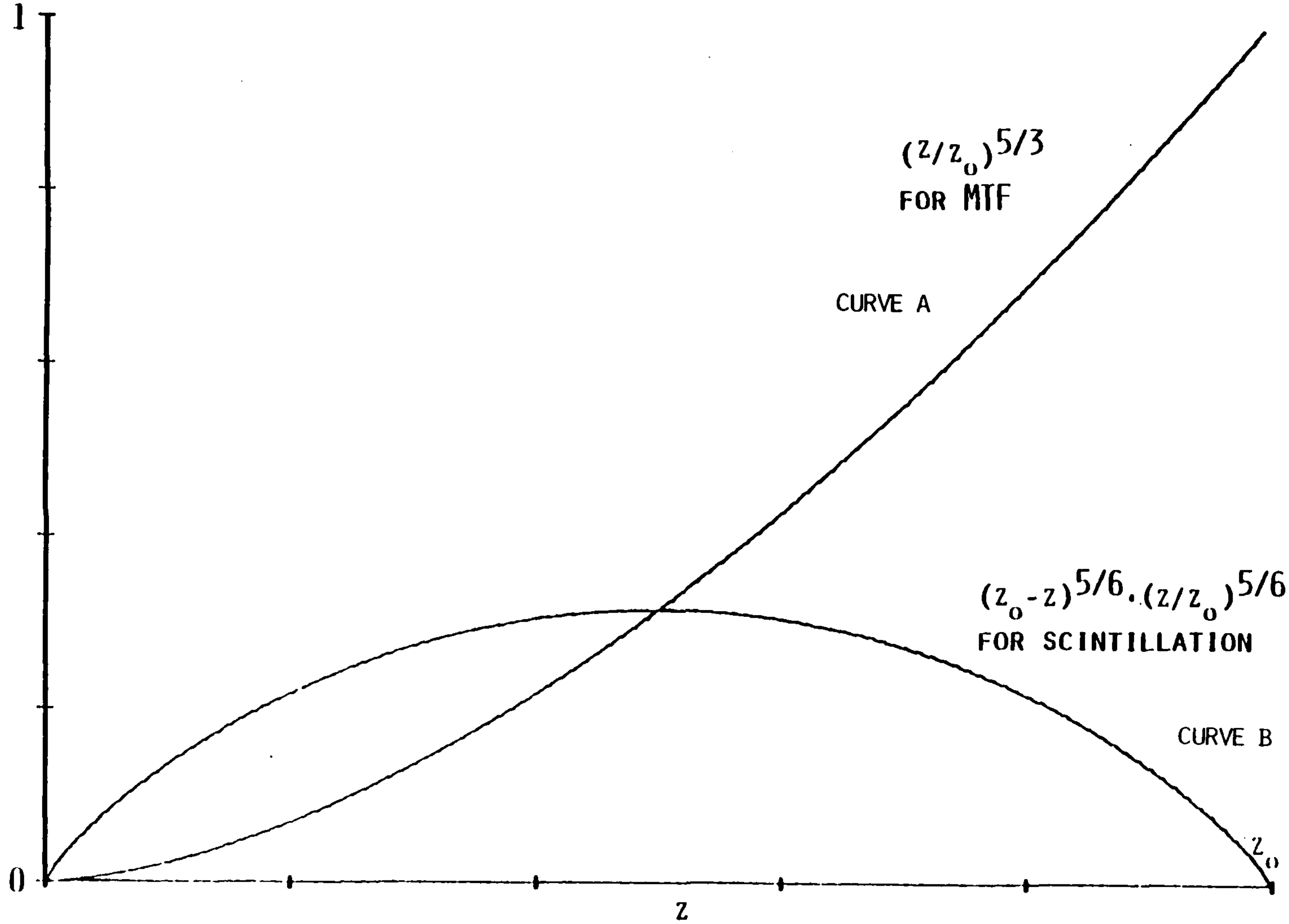

Figure 1. Relative Weighting of C_n^2 as a Function of Position Along the Path, for MTF and for Scintillation. The Telescope End of the Path is at the Right.

laser was used, emitting .6328 micrometers. A power of 1-3 milliwatts is sufficient. The viewing vidicon has a narrow-band interference filter in its optical train to reduce the background signal and exclude the designator wavelength. In order to have sufficient magnification to resolve the spread of the image due to the atmospheric turbulence, this vidicon viewed the source through a 6-inch diameter cassegrain telescope, with a 90-inch focal length. This proved to be too low a magnification so a "Barlow" negative lens was inserted just ahead of the vidicon to increase the magnification by a factor of 3. This caused the typical image to occupy a width of the order of 10 pixels, sufficient to analyze the image.

(3) Video Tape Recording

(a) The vidicon signal is continuously recorded on a Panasonic, U-Vision, type NV9240 TV tape recorder system. One matter of immediate concern in whether the tape recorder is sufficiently linear to be used for data recording. Not only must a linear analog recorder be used in the field, but it is necessary to later identify and play back with precise identification, several individual fields. This requires a disc recorder with field and frame labeling. For this purpose a Eigen, model 16-10, video disc recorder was used.

(b) To test the linearity of the complete chain of amplifiers and two recording systems, images of a point source broadened by the atmosphere were compared. Two types of signals are illustrated in figure 2. Figure 2a shows a single TV line that passes through the center of the recorded spot. The upper trace is direct from the TV. The lower trace is after the complete amplifier chain and two recording systems. The patterns are sufficiently alike to give comparable shape parameter measurements. In figure 2b, a number of successive TV lines passing through the image are displayed. Again, the top figure is direct and the lower figure is after the complete amplifier chain. The reproducibility is excellent.

(4) Background Subtraction. Although both vidicon systems have narrow-band filters to reduce background light, it is not completely eliminated. In order to remove this, the signals are digitized in a Quantex DS-30 TV frame digitizer. This system can subtract the signals of one field from that of another. This is carried out, using the field recorded signals, to obtain the image signals of the designator and OTF vidicons alone.

(5) Data Processing for Atmospheric C_n^2

(a) In order to carry out a calculation of the atmospheric C_n^2 from an image of a point source at a distance, the OTF of the atmosphere is measured. A complete curve of the OTF is also needed for the separation of the various causes of spot broadening and wander. Complete details of the video data processing techniques are given in appendixes C and D.

(b) To measure the OTF, a single TV image field is first transferred to the Quantex DS-30 from the video disc. A background field is then transferred from the video disc. This is subtracted from the image field in the DS-30. The background is ordinarily very small as the image has been taken through a narrow-band interference filter matched to the laser source wavelength.

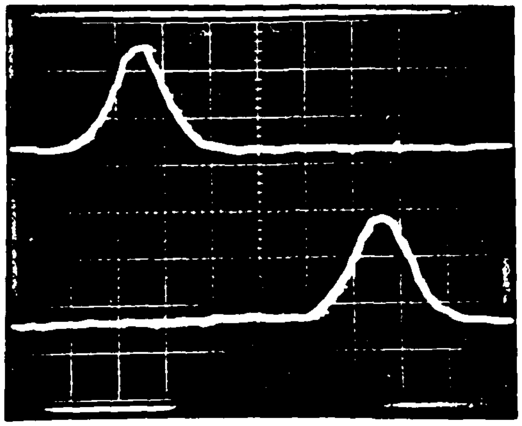

Fig. 2a. Signals for the image of a point source for the TV line passing through the image center.
Top trace: Direct signal from Vidicon
Bottom trace: Signal after recording in tape recorder, disc recorder, DS-30 digitizer and recorder, digital to analong conversion for viewing.

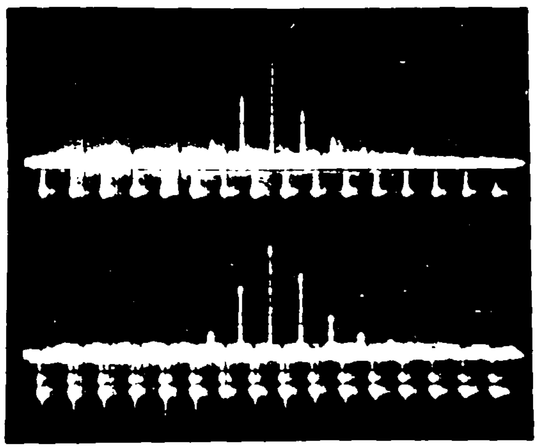

Fig. 2 b. Signals for the image of a point source for a sequence of TV lines covering the image. The envelope of these peaks is processed to give image profile.
Top trace: Direct signal from Vidicon
Bottom trace: Signal after recording in tape recorder, disc recorder, DS-30 digitizer and recorder, digital to analog conversion for viewing.

(c) After subtraction in the DS-30 of a complete background field from a complete image field that includes an image of the point laser source, a single raster line at a time is transferred to the HP-9825 calculator. The line transferred is limited in length to about twice the number of pixels required to express the image shape - usually 20 to 50 pixels. The line signal is then summed in the HP-9825. This sum corresponds to the integrated light passing through the linear slit of a slit-scanner. Successive lines are then summed similarly and the sequence of sums becomes the "line-spread function." This corresponds to the signal function obtained by a slitscanner. This line-spread function is stored in the HP-9825 memory. The next field is then analyzed similarly. To obtain the "long-term" line-spread function, successive line-spread functions are averaged in the HP-9825.

(d) To obtain the "short-term", or "image-centered line-spread function," the center of area of each line-spread function is calculated and stored in memory. The line center is then shifted to a predetermined position and the average of a number of such centered functions is the image-centered line-spread function. The RMS average of the center displacements needed to center is the RMS "image-wander" value. Its square is the variance of the wander.

(e) Next, the Fourier transforms of the two line-spread functions are carried out in the HP-9825. Each of these is then divided point-by-point by the transform of the line-spread function of the imaging telescope in the absence of turbulence. This removes the effects of the instrument. The result is two curves of the OTF of the atmosphere, the line-term, and the image-centered, OTF values. The curves can be plotted out when desired. Next, the OTF curves are fitted to the Fried model to yield C_n^2. Ordinarily, the two values of C_n^2 are identical if the image motion is due to turbulence alone, and the turbulence is not unusual. The RMS wander displacement also yields a value of C_n^2.

(f) Determination of the values of C_n^2 is not actually needed for much of the work to be carried out here, but that value is a convenient single number that characterizes the level of atmospheric turbulence along the optical path. The actual shape of the line-spread functions will be what is used in the data processing to separate the various types of line-spreads. For the wander, the actual values of the variance are also the values that will be used in the separation of various wander causes.

(6) Data Processing for the Designator Spot Pattern

(a) The details of this data reduction are provided in appendixes C and D. Before discussion of the data analysis, a few features of the equipment operation need to be mentioned. It would be desirable for the timing of the TV field initiation to be synchronized with the designator flash occurrence, in order to have the flash occur during the TV blanking and flyback. If the designator flash occurs randomly relative to the vidicon, it could occur during the period in which the electron beam is scanning the area of the image. This would make the data processing much less dependable. In practice, an occasional TV field would be lost. Synchronization would make every flash useful.

(b) The image of the designator spot taken by the close-up vidicon is next analyzed. Basically, the same data processing procedure is used as to obtain the OTF of the atmosphere. The TV image is digitized and the background subtracted in the DS-30. The average of a number of images is obtained; both the image-centered average, and the uncentered average. The process of obtaining the image-centered average also yields the variance of the image wander.

(c) The image-centered line-spread function is the convolution of the actual spread of the designator and the spread due to the atmosphere. To separate the two spreads, the Fourier transform is taken off the image-centered line-spread function. This is then divided, point-by-point, by the Fourier transform of the atmospheric line-spread function (the OTF of the atmosphere). The resulting function is then reinverted to obtain the spread due to the designator alone. This is plotted out on the plotter. This curve is one of the primary goals of the measurement. This can be used, then, as the information needed to correct errors in the optics of the laser designator system.

(d) The variance of the image wander, obtained above, is the result of both the actual wander of the designator beam and the atmospheric wander. The two can be easily unfolded, assuming that the statistics are reasonably Gaussian. The atmospheric wander of the designator, due to internal instability, would also be Gaussian. The variance of the combined wander is then simply the sum of the wanders of the atmosphere and the designator. Hence, the atmospheric wander variance is simply subtracted from the observed total wander variance to obtain the wander of the designator. This also is one of the primary goals of the measurement as this information can help in the readjustment of the laser and optics to reduce the wander.

(e) Analysis of the pattern projected on a uniform target has been demonstrated in work at the Naval Postgraduate School, using a pulsed GaAs laser source. The images have been digitized, subtracted from background, and the spot profile processed to yield a line-spread function, as well as a spot wander value. These have then been separated from the atmospheric spread and wander.

b. TV versus Line-Scanner Comparison

(1) Direct comparison of OTF values from the NPS mechanical line-scanner with those from the TV system was accomplished by use of a beam splitter in the output optics of a 270-inch focal length Cassegrain telescope. The two images analyzed were thus identical. The telescope viewed a point (HeNe) laser source at the far end of a tunnel, 132 meters in length. Turbulence in the tunnel was produced by overhead heat duct ports and amounted to moderate turbulence.

(2) The video signals from the TV system were recorded with the system proposed here for field use. The recorded signals were analyzed later by the techniques previously described in this report, with the output in the form of a plotted curve of OTF as a function of angular spatial frequency.

(3) The NPS mechanical line-scanner signals were recorded on a Precision Data frequency modulated tape recorder, with a recording bandwidth of 100 kHz. This recorder is frequently used for this purpose with the NPS line-scanner, although recently the online data processor has made this recorder unnecessary. In this case, it made careful processing possible for identically the same time interval as that used for the TV data.

(4) A pair of curves of OTF are shown in figures 3 and 4 for the NPS line scanner and the TV system, respectively. The data is for the long-term average. The output of the NPS line-scanner yields the actual data points as well as the best-fit curve from the Fried model (ref 4, app E). The output of the TV system displayed only the best-fit Fried curve, at the time of that data reduction. In the future, it will also display the actual data points. The two OTF curves can differ only in their horizontal scale because they are curves for the same model. A customary measure for comparison is the angular spatial frequency at which the OTF has decreased to a fraction, 1/e, of its initial value of unity. This point is often used as a measure of the coherence "length." For the NPS scanner, the 1/e point occurs at 26.7 lines per milliradian. For the TV system, the 1/e point occurs at 29.6 lines per milliradian.

(5) The above values are in agreement within approximately 10 percent. This corresponds to an agreement within 10 percent for C_n, or within 20 percent for C_n^2. This degree of agreement indicates that the TV system is adequate to replace the mechanical line-scanner for measurements of the OTF. That agreement is quite good, and since much of the use of the two TV systems for OTF involves use of the results of one system in terms of the other, the matched pair of two TV systems should reduce the effects of systematic error.

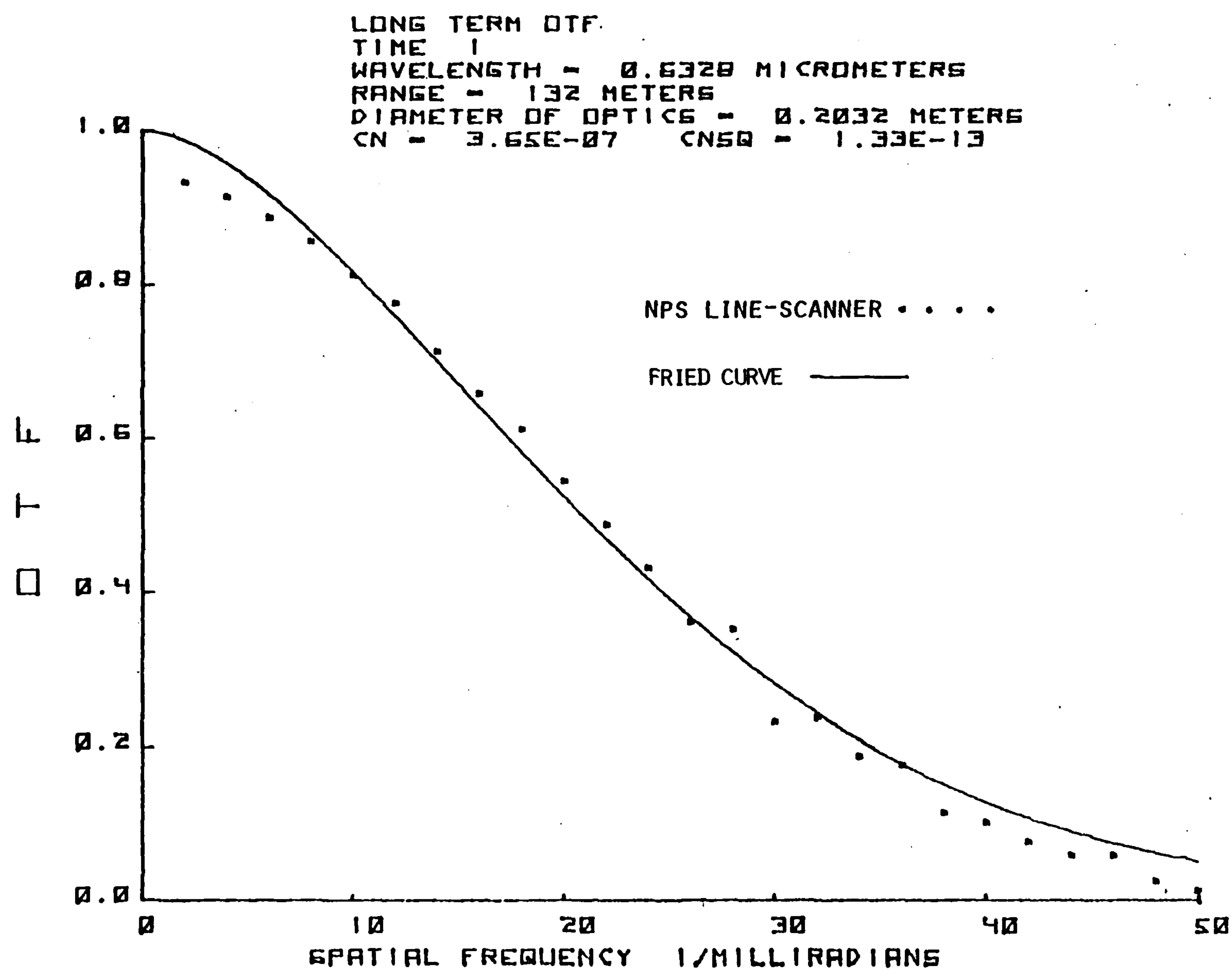

Figure 3. OTF of the Atmosphere for the NPS Line-Scanner

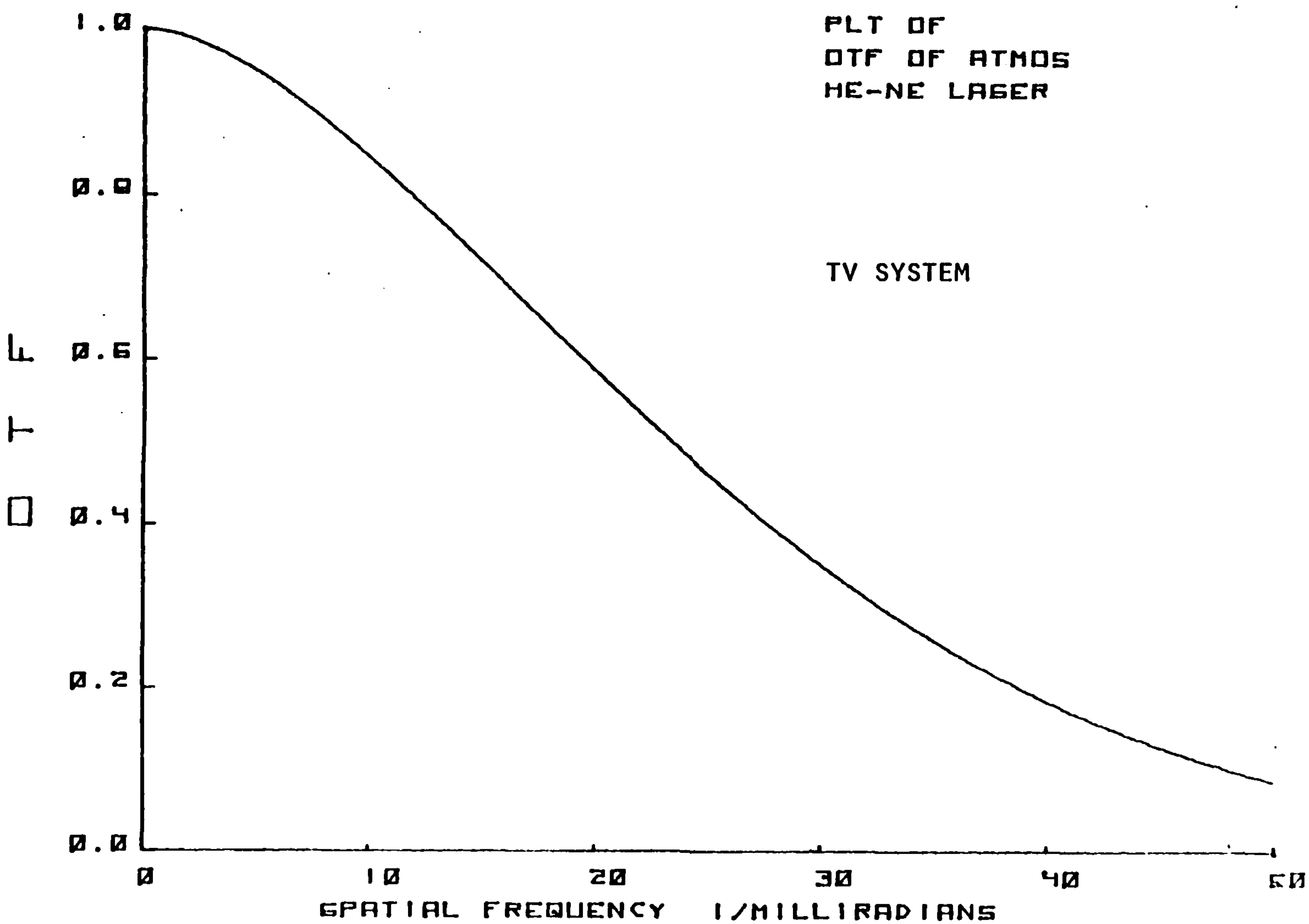

Figure 4. OTF of the Atmosphere for the TV System

SECTION 3. APPENDIXES

APPENDIX A. PROPOSED FIELD TEST PROGRAM

1. INTRODUCTION

The proposed test program has three general phases. In the first phase, a uniform reflectivity target screen would be used. These techniques would be adapted in the second phase to permit use of a real target such as a tank. The techniques utilized in the first two phases would be chosen so that they are adaptable to a third possible phase in which real targets would be in motion.

2. PHASE ONE, UNIFORM TARGETS

In the first phase of the program, field measurements would be made with a target screen with uniform reflectivity at a representative range. The equipment is planned to be arranged as shown in figure 1. The measurements and data reduction would be carried out in three successive steps.

a. Step One

(1) In the first step, field measurements would be made with a strapped-down laser designator with its spot trained onto a uniform target screen. These measurements would serve to determine the stability of the designator laser and optical system by separating the atmospheric effects from the overall effects.

(2) The target screen would be viewed with a silicon vidicon located a short distance from the screen along the line between the screen and the designator, but slightly off that line to avoid obscuring the screen from the designator location as shown in figure 1.

(3) A silicon focal plane screen is needed for this vidicon in order to reach the 1.06 micrometer, near-IR, wavelength. The usual TV vidicons, or other TV cameras such as orthicons, are optimized for the visual range of wavelengths and do not reach this wavelength.

(4) To reduce the background signal, the close-up vidicon would be equipped with a narrow-bandpass optical filter matched to the designator wavelength. The vidicon would view, alternately, the designator spot plus background, and the background alone. The video signals would be tape recorded during tests. Later, the signals for the background image would be subtracted from the signals for the background plus designator spot to give the signals for the spot alone. This subtraction would be carried out in a Quantex DS-30 video signal processor.

(5) In addition to the close-up vidicon, another vidicon, with long focal length (telescope optics), would be located near the designator transmitter and would view a point source laser located in the target screen as shown in figure 1. That laser would operate at a different wavelength from

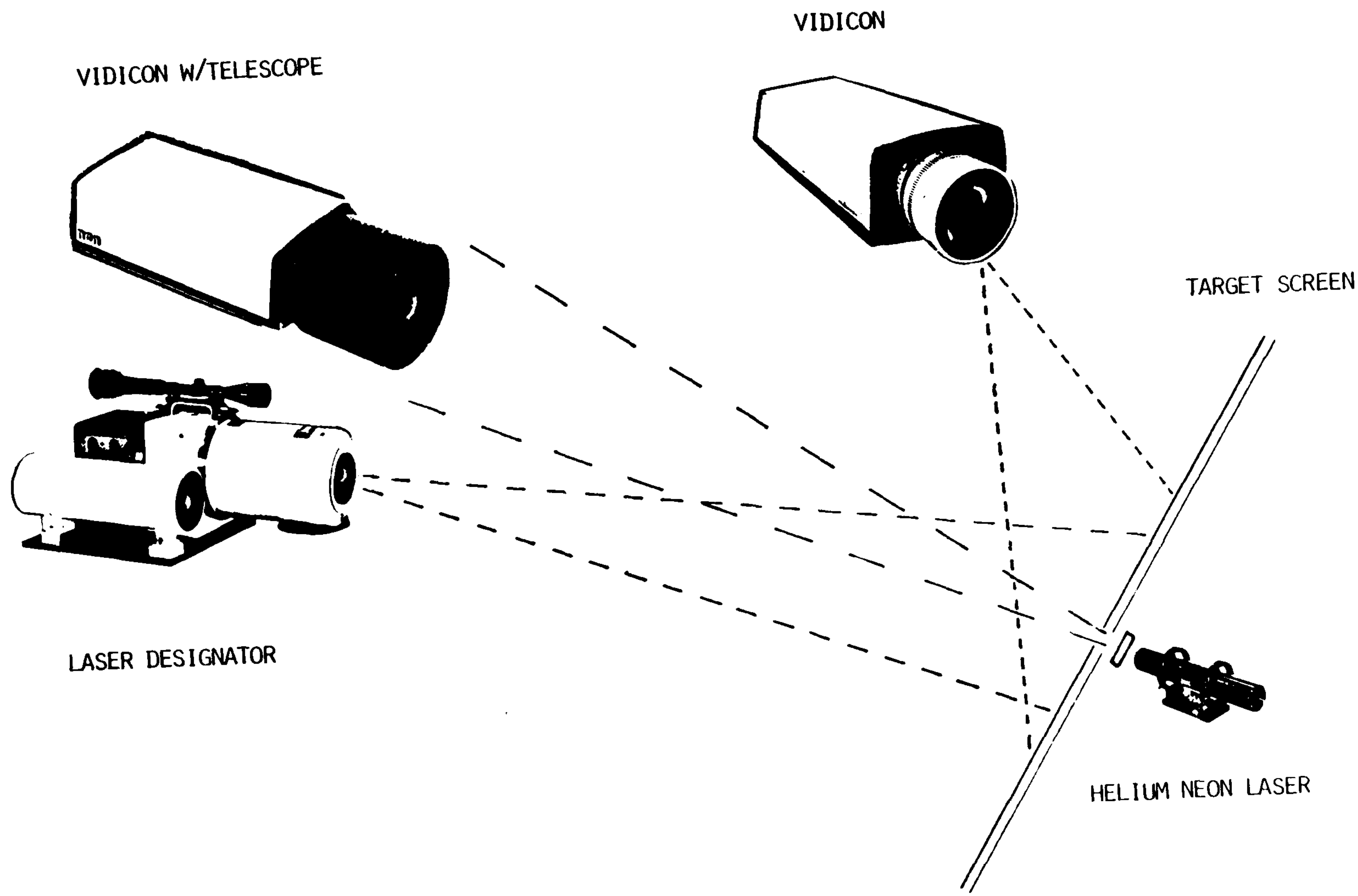

Figure 1. Optical Configuration for Field Test

the designator, e.g., HeNe, at 6028 micrometers. The telescope would have a narrow band filter to match this laser line. This will eliminate the designator signals, but not completely the daylight continuum background. Separate recording of signal and background will permit subtraction of background here in the same manner as for the close-up vidicon. This vidicon can be a more common visual range vidicon than the silicon vidicon that is required for the 1.06 micrometer designator signals.

(6) Processing of the taped data from the telescope vidicon would give a quantitative determination of the effects of the atmospheric turbulence. This data would then be used, together with the taped data from the close-up vidicon that views the designator spot on the target screen, to unfold the atmosphere effects from the designator spot width and wander, using Fourier transform techniques. The diffraction spread and any intentional geometrical spread of the designator spot would also be removed. The remaining spread (beam profile) and wander would then be entirely that due to improper laser adjustment, or instability of the laser and associated optics. This data should then make it possible to correct or minimize the defects in the designator system. Even if not corrected, the system would then be characterized, and is ready for use in the next step.

b. Step Two

In the second step, the laser designator would be placed on the unstable platform (mini RPV). The mini RPV would be mounted in as realistic a manner as possible, with engine and all systems running to simulate real operational conditions, particularly with respect to vibration, but with the mini RPV still on a ground-based platform. This is necessary so that the telescope vidicon can be mounted next to it, to view the point source in the target screen and thereby obtain a measurement of the effects of atmospheric turbulence. This would evaluate the actual beam pattern of the designator, as it would be in the air, by removing the atmospheric effects. The beam pattern would now be characterized sufficiently that it can be used in the third step.

c. Step Three

(1) In the third step, the mini RPV would be airborne, directing its laser designator to the uniform target screen. The close-up silicon vidicon would view the screen as before. In this step, the distant telescope vidicon viewing the point source is not necessary, nor could it contribute to the information, if used. It would, of necessity, be ground-based and would not look through the same atmospheric path as the beam from the mini RPV to the target. The beam from the designator on the mini RPV is now well enough known that it can be used to evaluate the atmospheric turbulence at the instant of designator firing. The data tape from the close-up vidicon would yield a sequence of beam profiles. The center of each of these is calculated and the profile centered before averaging. The averaged profile; so obtained, is then Fourier processed to remove the known designator profile; that has been determined in step two above. From this reduced profile, the atmospheric turbulence is determined. Knowing this turbulence, the expected wander of the spot center is calculated. This is then unfolded from the directly-measured spot wander to give the motion of the spot due to the platform motion alone.

(2) All of the above general processes have been proven by application in a slightly different situation, namely determining the optical properties of lasers transmitted from shipboard. A new feature in the present experiments is the use of vidicons for imaging. Scanning-slit telescopes have been used previously to carry out the same type of measurements. In the results reported in this report, data reduction for imaging with the vidicons has now been tested in laboratory work at the Naval Postgraduate School.

3. PHASE TWO, NONUNIFORM TARGETS

a. In the second phase of the program, field measurements, similar to phase one would be carried out, but with nonuniform reflectivity targets, such as a tank with natural landscape as background.

b. The measurements would differ from those of phase one in that an additional laser, with the same wavelength as the designator, would be used to provide pulse illumination of the target from a close-up location. This pulsed illumination would alternate with the designator pulses. The close-up vidicon would view the scene under pulse illumination plus background light, and then under background light alone. Both signals would be tape recorded. Later, the two images would be subtracted to yield the signals for illumination by laser light alone. The close-up vidicon would then view the scene when the designator spot is pulsed. This, again, would be tape recorded. The difference of this scene and the background would be used later for the signals for the designator alone. Later, in data reduction, the designator spot signals would be divided pixel-by-pixel by the signals for uniform laser illumination. This process normalizes the spot profile to be the same as if it had reflected from a uniform reflectivity target.

c. Steps one, two and three above would then be carried out, after the normalization, to analyze the behavior of the laser and platform.

4. PHASE THREE, FUTURE MOVING TARGETS

The systems for use in phases one and two would be set up so as to be extendable to laser designator analysis for moving targets. This will involve all the techniques of phases one and two, including steps one, two and three, plus provision of background laser illumination by flashes that follow, or lead, the designator pulses as closely as possible. In practice, this means following or leading by one TV field time interval. This is 1/60 second for standard American TV. Use of a more rapid scan TV system would improve the situation. However, the normalization operation would be improved by a lateral shift of the uniform illumination calibration image, to more exactly coincide with the image at the time of the designator flash. The proper displacement could be determined by carrying out a correlation of the two images as a function of offset, with the final offset determined by the maximum correlation between the images. This would be a time-consuming operation if both lateral and vertical offset were involved. If the direction of offset is known, for example, for a vehicle that is constrained to move on a road surface of known inclination, then the correlation operation would be greatly reduced. Carrying out this type of measurement seems well within the capability of the equipment to be provided for phases one and two, except that a larger computer will probably be needed. This should be borne in mind in selecting the computer for use in phases one and two.

March 1982

APPENDIX B. METHODOLOGY INVESTIGATION PROPOSAL

1. TITLE. Optical Turbulence Measurement

2. CATEGORY. Electro-Optics

3. INSTALLATION. US Army Electronic Proving Ground, Fort Huachuca, Arizona 85613

4. PRINCIPAL INVESTIGATOR. Colin M. Giorgi, Test Operations Office, STEEP-MT-T, AUTOVON 879-6016/6417

5. STATEMENT OF THE PROBLEM. Optical turbulence in the atmosphere can significantly degrade the field performance of both active and passive optical systems. Measurement techniques currently being used to characterize this uncontrolled and highly variable test parameter are inadequate. A measurement technique is required which will quantitatively and accurately account for the contribution of optical turbulence to variances in equipment performance during field testing.

6. BACKGROUND. The effects of atmospheric turbulence on the performance of imaging and beam forming optical systems have been well known for many years. Measured variances in beam intensity and beam position due to atmospheric turbulence have shown that the field performance of electro-optical systems, and active systems in particular, can be severely biased by the turbulence characteristics of the optical path. Because of the critical time and specific path sensitivity of the turbulence parameter, existing measurement methods are deficient in establishing the true path turbulence structure affecting a test items performance. During a recent five year investigative effort, the Naval Postgraduate School (NPS) applied optical transfer function (OTF) measurement technology to the turbulence measurement problem using a laser source and a slit scanning telescope to collect field data. The results of the study and empirical evaluation indicate that the technique developed eliminates the deficiencies of previous turbulence measurement methods. The key to the measurement is the determination of a properly path-position weighted C_n^2, the turbulence structure constant for optical index. During the review of the investigative effort by the TECOM Laser Technical Committee, it was determined that the technique had the potential of being applied to the test data correction problem by utilizing the video imaging and automated data analysis instrumentation currently used to collect spot data for laser designators. The use of a video data recording system and an automated video data reduction capability has definite advantages over the mechanical slit scanning device used in the NPS investigation but application of the technique will primarily depend on the feasibility of utilizing the test item laser as the probe source.

7. GOAL. To develop an improved test methodology for measuring atmospheric turbulence for application to the testing of electro-optical systems in the field.

8. DESCRIPTION OF INVESTIGATION.

a. This investigation will develop a test method for collecting and analyzing the modulation transfer function of atmospheric paths for the purpose of deriving the turbulence structure constant for optical index (C_n^2). The thrust of the effort will be directed at implementing the NPS image scanning technique by applying the laser spot image recording and analysis instrumentation currently being used by TECOM in support of laser designator testing. The investigation will cover both a theoretical and empirical evaluation of the application and will include the methodology essential to applying the C_n^2 parameter data to analyze test item performance data.

b. The US Army Electronic Proving Ground will conduct the investigation in two phases as follows:

(1) Survey and Analysis Phase.

(a) The initial effort will cover a survey followup to the NPS investigation to determine what additional study and experimental work has been accomplished since the conclusion of the basic investigation.

(b) The major effort during the analysis phase of the investigation will address the feasibility of applying the NPS, MTF image analysis technique to TECOM's electro-optical system's test programs using the laser spot image recording and data reduction system. The priority application will be the laser designator test programs. As the NPS measurement setup uses a one-way path and a reference laser source which is configured for the measurement requirement, a determination will be made with regard to the feasibility of using the unmodified test item laser as the probe source and a folded optical path.

(c) Following a determination of the feasibility of applying the NPS measurement technique to laser designator testing, a test plan for the field experimental phase of the investigation will be prepared. The test planning effort will include the identification of the instrumentation, real estate and personnel resource requirements to implement the field tests.

(2) Empirical Testing Phase.

(a) The purpose of this phase will be to empirically verify the feasibility of the technique application. The initial effort will require the acquisition of instrumentation support as specified in the test plan. The testing may be conducted at EPG or at another test installation depending upon the availability of representative test items and measurement instrumentation. Regarding the latter, EPG is planning to acquire a laser spot data acquisition and analysis capability by the end of FY81 in order to support the RPV test program.

Optical Turbulence Measurement (Cont'd)

(b) The data acquisition and analysis phase will include evaluating data from both the experimental setup as well as data from on-going laser test programs on a non-interfering basis.

(c) With the conclusion of the field experiments and subsequent data analysis, a final report will be prepared covering the complete effort. If feasibility of the technique is established, the report will include a detailed description of the test procedure and the data analysis program and recommendations for instrumentation development acquisition as appropriate.

c. Investigation Schedule.

MILESTONE/ACTIVITY	SCHEDULE							
	FY 81 (Qtrs)				FY 82 (Qtrs)			
	1	2	3	4	1	2	3	4
Analytical Phase								
Updating Survey	X							
Error Analysis	X	X						
Feasibility Study			X	X	X			
Test Design				X	X	X		
Empirical Evaluation Phase								
Resource Acquisition				X	X	X		
Lab and Field Testing					X	X	X	
Data Analysis					X	X	X	
Report Preparation								X

d. This investigation will result in the development of an improved optical turbulence test procedure and the determination of the supporting data acquisition and processing instrumentation and software requirements.

e. Environmental Impact Statement. Execution of this task will not have an adverse impact on the quality of the environment.

f. Health Hazard Statement. Execution of this task may involve health hazards to personnel. This task may require project personnel to participate in field tests involving the operation of laser equipment. Safety standards for laser field testing are well documented in TB MED 279 titled "Control of Hazards to Health from Laser Radiation". All field experiments will be conducted in full compliance with the regulation.

9. PROGRESS. This task received partial funding in FY81 (35k). The updating survey was initiated in January 1981 with a followup review of the NPS investigations. The major portion of the analysis and test design phases of the investigation are being performed by NPS staff scientists. The theoretical analysis and empirical measurements made to date have established the basic feasibility of replacing a telescope/mechanical slit scanner/detector unit with a video camera and a video digitizing subsystem. A prototype C_n^2 measurement system has been assembled by the NPS using EPG GFP. Subsystem interfacing has been completed and controlled laboratory tests are underway.

Optical Turbulence Measurement (Cont'd)

10. JUSTIFICATION.

a. Mission and Impact Statements.

(1) Association with mission. TECOM and EPG are assigned the mission of conducting the development testing of a wide range of electro-optical devices and systems. These include both active (laser) and passive (sensor) equipments.

(2) Present capability, limitations, improvement, and impact on test if not performed in the proposed fiscal year. The most common method used to describe atmospheric turbulence is simply a qualitative assessment of the "seeing" conditions as good, fair or poor. This imprecise and subjective criteria was developed primarily as a general measure of optical attenuation and it does not account for the time and specific path dependent nature of atmospheric turbulence. The second method employs point temperature measurements which also do not provide the key time and integrated path data essential to correlate turbulence effects. Consequently, for most EO testing, the turbulence factor remains a highly variable and uncontrolled test condition which can produce serious equipment performance data biasing. The application of the NPS technique will provide a turbulence measurement which is time and optical path coincident. This coincidence will allow the turbulence variable to be fully monitored and accounted for, thereby eliminating the biasing of test data. If this task is not completed in FY83, the capability will not be available to support the RPV laser designator test scheduled for FY83 or other key TECOM laser tests sched-uled for the FY83-84 time frame.

b. Dollar Savings. The successful implementation of a C_n^2 measurement capability is expected to reduce the extent of field testing required for electro-optical devices and systems. This reduction will result from the ability to monitor and account for an important test variable which now requires many test runs and testing at different test locations to establish a meaningful statistical base. The successful monitoring of the variable should also lead to using the data to develop performance predictions for an extended range of atmospheric conditions. This modeling capability should reduce the requirement for some field testing now being conducted. However, the generation of specific dollar saving estimates will have to await the outcome of the feasibility evaluation and the determination that image data now collected on laser tests can be directly used for the turbulence measurement.

c. Workload. The methodology will be applied initially to all laser equipment field testing to include designators, range finders, radar and illuminators. If successful, the techniques will also be applied to the field testing of all electro-optical sensors.

Optical Turbulence Measurement (Cont'd)

Examples of items anticipated for testing at EPG include:

Test Item	FY 83	84	85	86
Chaparral Night Vision Subsystem	X			
RPV Designator	X	X		
RPV Television Sensor		X		
RPV Mini-FLIR			X	
ELOCARS				X

NOTE: A number of laser and passive EO sensor tests, scheduled at other TECOM facilities during the 1983-86 time frame, will also utilize the developed methodology.

d. Recommended TRMS Priority. Refer to the workload paragraph (10.c) and the ODCSOPS priority listing.

e. Association with Requirements Documents. The ROC's for most laser and E-O systems specify that the systems will perform in a "degraded atmosphere" environment but do not quantify the degradation conditions or level. The development of the turbulence measurement methodology can be an important step towards quantifying the "degraded atmosphere" requirement.

11. RESOURCES.

a. Financial.

(1) Funding Breakdown.

Dollars (Thousands)

	FY 83 In-House	FY 83 Out-of-House
Personnel Compensation	20,000	
Travel	3,000	
Consultants & Other Svcs		34,000
Materials & Supplies	3,000	
Equipment	5,000	
Subtotals	31,000	34,000
FY TOTALS	65,000	

NOTE: No funds were provided for this project in 1983. Funding requirements and funding provided were as follows:

	Requirement	Funding
FY 81	$54,000	$35,000
FY 82	$61,000	$29,400

Optical Turbulence Measurement (Cont'd)

(2) Explanation of Cost Categories.

(a) Personnel Compensation. Covers in-house labor costs for the principal investigator and other in-house project support personnel.

(b) Travel. Travel is required to coordinate the task with other TECOM installations. Travel in FY83 may be revised if the field testing is scheduled for WSMR or YPG.

(c) Consultants and Other Services. Consultant support will be utilized to assist in performing the detailed technical feasibility analysis and to evaluate the field test data.

(d) Materials and Supplies. Recording media and incidental supplies will be required to support the field testing.

(e) Equipment. The empirical verification field tests will require a designator source. Current shortage of fielded items or spare test items indicates that a simulator unit will have to be procured. FY83 funding covers equipment contingencies including servicing and repair.

b. Anticipated Delays. A delay in EPG's acquisition of the programmed laser spot recording and data reduction instrumentation capability will extend the initiation of the field verification testing. However, an alternate support capability may be made available at WSMR or YPG to alleviate the problem.

c. Obligation Plan (FY 83).

FQ	1	2	3	4	TOTAL
Obligation Rate (Thousands)	3.0	38.0	14.0	10.0	65.0

d. In-House Personnel.

(1) Requirements.

		FY 83	
		Manhours	
	Number	Required	Available
Physicist, GS-1310	1	500	500
Elec Engr, GS-0855	1	500	500
Totals		1000	1000

(2) Resolution of Non-available Personnel. Not applicable.

Optical Turbulence Measurement (Cont'd)

12. INVESTIGATION SCHEDULE.

	FY 83											
	O	N	D	J	F	M	A	M	J	J	A	S
In-house	-	-	-	-				-	-	-	-	R
		.	.	.	.	.	.	.				
Contract		A	-	-	-	-	-	-				

Symbols: - -Active investigation work (all categories)

...Contract monitoring (in-house only)

A Award of Contract

R Final report due at HQ, TECOM.

13. ASSOCIATION WITH TOP PROGRAM. It is expected that the turbulence measurement methodology initially developed for specific commodity items such as laser designators and rangefinders will be incorporated into the existing TOPs covering those items. As more generalized procedures are developed that apply to a broad class of E-O test items, then a new TOP will be generated that can be referenced in the E-O commodity item TOPs.

FOR THE COMMANDER:

GARY L. KOSMIDER
Colonel, SigC
Director of Materiel Test

APPENDIX C

VIDEO DATA ANALYSIS USING A DIGITAL VIDEO PROCESSOR SYSTEM

ABSTRACT

This appendix presents a computer program designed to analyze the data from a TV camera for investigating laser beam propagation through the atmosphere. It uses aspects of Fourier optical theory to analyze the TV image to measure the effects of atmospheric disturbances and platform stability on the target spot. The computer program is written for a data analysis configuration consisting of a video recorder, video disk unit, digital video image processor (Quantex DS-30), and a desk-top computer unit (HP 9825).

(THIS PAGE IS INTENTIONALLY BLANK)

TABLE OF CONTENTS

I. INTRODUCTION

A. PROBLEM

A problem has occasionally been experienced in concentrating laser energy from a laser designator onto a target and sufficiently illuminating that target so a weapon sensitive to that illumination will home in on the target. Two circumstances have possibly caused this to happen; the energy is either too diffused at the target to illuminate it properly or the beam partially or completely misses the target. The aim of this study is to develop a computer program to aid in determining which part of these effects is atmospheric and which is the instability of the laser and stabilization system in the illuminating aircraft.

B. METHOD OF APPROACH

The analysis of the problem requires two general types of systems. One system evaluates the performance of the designator using some techniques from Scott [Ref. 1]. A silicon vidicon views the successive pulsed designator spots on the target from a location near the target. A line spread function of the spot on the target and the standard deviation of the wander of the laser beam is produced. The other system provides measurement of C_n^2 for atmospheric turbulence along an optical path adjoining the designator optical path. The laser on the target is viewed by a silicon vidicon located near the designator's optics. The value of C_n^2 obtained is inherently properly path weighted to express the atmospheric effects on the designator spot. Techniques from Fourier optics theory use the measured value of C_n^2 to predict the intensity pattern of the laser beam on a distant target. The results from the two systems can then be analytically compared to determine the causes of spot wander and broadening.

The sponsor-supplied hardware includes an HP-9825 calculator with 23K bytes of internal memory for equipment control and data processing; an HP-9885 disc memory used for additional storage space; and a Quantex DS-30 Digital Video Analyzer used for digitizing the analog video input from an Eigen video disc; a Panasonic NV-1240 video tape recorder for initial recording of video from the target on a silicon vidicon camera. After analysis, output is in the form of plots produced on an HP-9862 plotter.

The sequence of analysis is currently as follows. Modulation transfer functions (MTF) of the laser output and optics are measured or calculated and stored on disc. A video recording of the target being illuminated by the designator is made for a number of video frames, the target alone is also recorded, for later subtraction from the total picture to produce an image of the laser spot alone. The video recording is then played through the DS-30, controlled by the HP-9825, to digitize the information for use by the HP-9825. The HP-9825 takes the digitized video of the target, produces a line spread function (LSF) of the image, subtracts the background, and averages a number of frames to produce a short term measurement of the laser energy on the target. The amount that each laser spot wanders from the others is also stored. In the second phase, the HP-9825 uses the MTF's of the laser, optics, and atmospheric measurements to produce a total system predicted MTF, LSF, and wander. These results of the target spot measurement and the baseline studies can be compared for possible correlation.

The laser pulse is timed so that it occurs on the fly-back of the TV signal. This will cause the laser spot to appear on one field of a frame. For accurate results the DS-30 needs to digitize a single field for each pulse of the laser. The videotape unit currently used will not allow this capability. For this reason the tape recording video is transferred to an Eigen video disc, which has the capability of displaying each frame or field (1/2 video frame interlace) individually and of selecting any one frame or field for viewing.

II. BACKGROUND AND PROGRAM DESCRIPTION

A. THEORETICAL DESCRIPTION

In order to combine the individual optical components of the laser to the target system, some elements of Fourier theory must first be remembered. The Fourier transform represents the one dimensional position variable g(y) expressed in the spatial frequency domain U(v). The inverse transform repeats the operation in the opposite direction. Their forms are commonly represented as follows:

$$U(v)=\int_{-\infty}^{\infty} g(y)\exp(-2\pi ivy)dy=\mathcal{F}[g(y)]$$

$$g(y)=\int_{-\infty}^{\infty} U(v)\exp(2\pi ivy)dv=\mathcal{F}^{-1}[U(v)]$$

The program calculates the value of the integral at a preset number of points and yields a discrete Fourier transform. A theorem from Fourier theory that allows us to compute the line spread function as presented in Fried [Ref. 2] for one of the elements in the system given the others is the convolution theorem stated as follows:

$$\begin{aligned} &\text{If} && \mathcal{F}[g(y)] = G(v) \\ &\text{and} && \mathcal{F}[h(y)] = H(v) \\ &\text{then} && \mathcal{F}[g*h] = GH \end{aligned}$$

(* - convoluted with)

The first element in the system we are analyzing is, of course, the laser itself. The radial intensity output of the laser is generally Gaussian of the form $A=A^{o}\exp(-r^{2}/2\sigma^{2})$ as shown in Figure 1. This can be calculated for each laser for approximate results but was usually measured directly in this study.

The above radial distribution of intensity must then be integrated over x to produce a one dimensional line spread function for the source. A Fourier transform is then used on this LSF to yield the MTF of the laser. The MTF is a measure of the spatial frequency response of a system compared to the input. A "perfect" system response would be 1.0 out to its limit (large spatial frequencies) and then dropping to zero.

The optics associated with the laser is basically diffraction limited. The "Airy function" is used to calculate the diffraction point spread function for the laser optics. This point spread function is then converted to a line spread function, Fourier transformed to get the MTF and then combined by the convolution theorem into a laser system Fourier transform.

The next step is to calculate the effects of atmospheric turbulence on the laser beam. The value of C_n, "the index of refraction turbulence structure constant," as expressed by the relationship from Tatarski [Ref. 3] and Ochs et. al. [Ref. 4]:

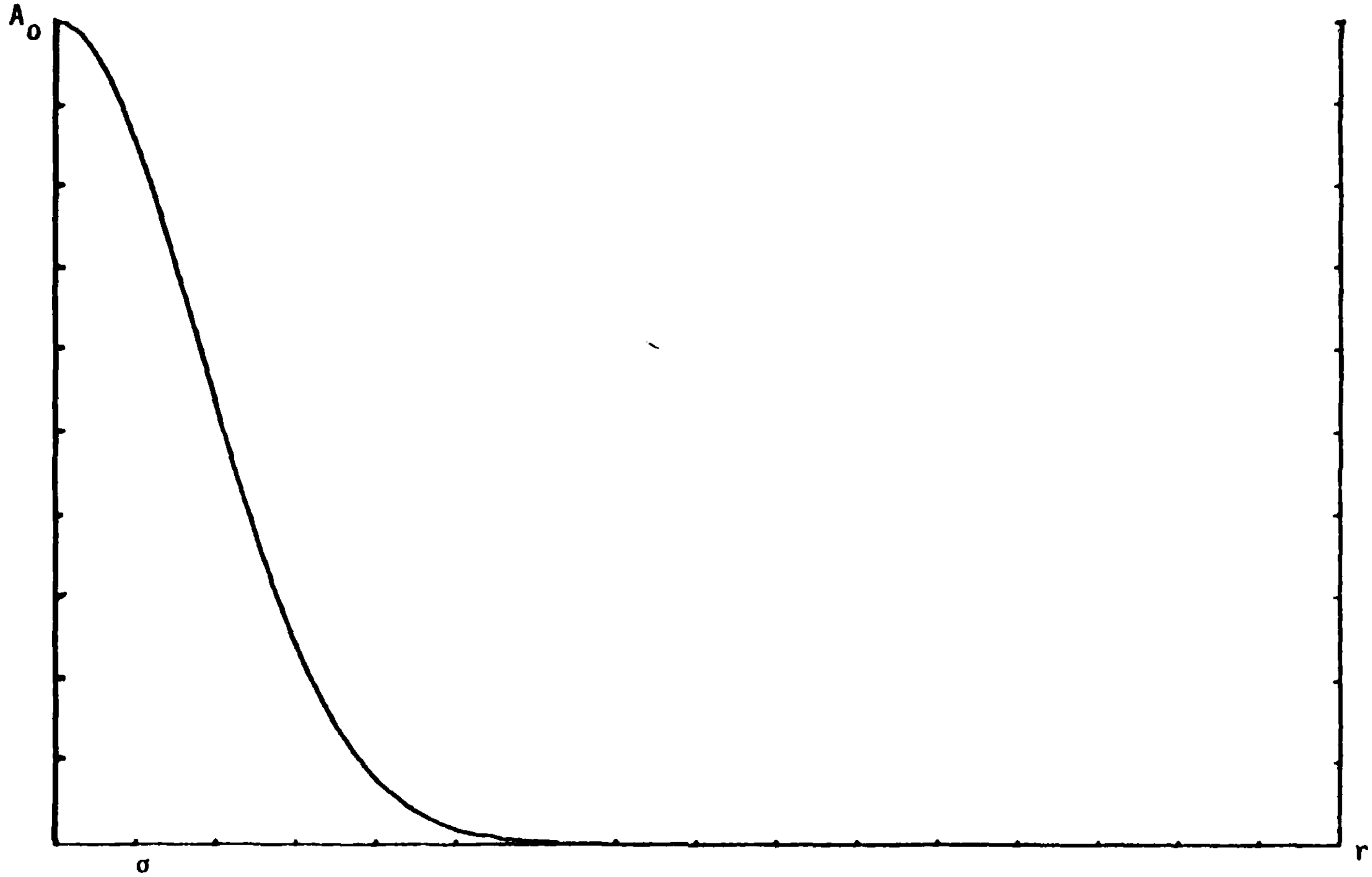

FIGURE 1. IDEAL LASER INTENSITY OUTPUT LINE SPREAD FUNCTION

$$\langle (T_{r1}-T_{r2})^2 \rangle = r^{2/3} C_T 2 \quad \text{and} \quad C_n = 79\times10^{-6} p/T^2 C_T$$

where $T_{r1}-T_{r2}$ is absolute temperature at two points separated by a distance r and p is pressure in millibars; is used to predict the MTF of the atmosphere over the path between the laser and the target. Measurements made along the path are inputs to the C_n equation which predicts the turbulence effects on the MTF and wander of the beam. In the field, however, plans are to measure C_n by optical methods decribed in Crittenden [Ref. 5].

The theory then, according to Fried [Ref. 2], shows that the total effect of the atmosphere and the laser can be found by the product of the two transform functions:

$$G\ \text{total}\ (v) = G\ \text{optics}(v) \times G\ \text{atm}(v)$$

The inverse transform then will yield the line spread function of the total system, the LSF as predicted on the target.

Crittenden et. al, [Ref. 5] describe the process of converting the one dimensional LSF to a circular symmetric PSF using the Abel transform, from Griem [Ref. 6]. The power inside a circle of radius R can then be obtained by integrating the PSF out to R. For the purposes of comparison in this study, however, the resulting system LSF is used to compare the prediction with measured values.

B. HARDWARE USE AND LIMITATIONS

The HP-9825 calculator used for this program had an internal capacity of 23K bytes. This was quite adequate for program storage but because of the great volume of digitized video data that was involved, the inclusion of an HP-9885 disc drive system was necessary. The Quantex DS-30 can store and rapidly transfer a maximum of 512 lines of video with 512 pixels (picture elements) per line, easily exceeding the HP-9825's memory capability. The large overflow of data was reduced by storing each image into a quarter of the memory, thus limiting the amount of data that needed to be transferred. This also made disc storage more reasonable and sped up program running time.

The DS-30 was also capable of taking the difference on a pixel by pixel basis between a reference image and the input and storing that in memory. Differencing was necessary in order to remove the background from the recorded image for processing the laser spot alone. Normally, it is necessary to divide the image by the background to offset the effect of the non-uniform reflectivity of the target. This was not possible with the DS-30 so these steps need to be performed by the computer. The division was not possible to do at this time because of the memory limitations of the HP-9825. This must be done pixel by pixel since division by the LSF is not equivalent. The memory limitation was als~ he reason why the HP-9825 used the LSF instead of pixel by pixel subtraction for this process.

All the peripheral equipment to the HP-9825 was controlled through an IEEE standard 8 bit interface bus. This allowed control of all aspects of data acquisition and processing to be modified by software. The video recorders were the exception to this and provided the only real manual manipulations required after the program had begun. Each frame of video needed by the program had to be selected when requested by the program because of the lack of interface control.

The linearity of the recording system was checked and found to be almost distortion free. A signal from an image was passed directly to an oscilloscope from the vidicon and compared side by side to a signal from the same image which had been recorded in the tape recorder, transferred to the video disc and then passed through the DS-30 circuitry to a digital analog converter for viewing. Crittenden et. al. [Ref. 7] present photographs of the two images for comparison and further discussion.

Variable usage became a problem as the program grew, which was due to the limitations of the HP-9825. The HP-9825 has available twenty-six variables (A-Z), twenty-six variables for arrays (A-Z), a subscripted variable (r) with as many elements as the memory has space for plus a subprogram variable (p) for use in passing parameters through "called" subprograms. One of the usage problems was using identifiable variables in passing from main programs to subprograms. A good number of the subprograms originally were designed for other programs and the variables often conflicted. The r variable is nice to use here because of its practically unlimited numbers. A more serious problem, though, was the inability of HPL, Hewlett Packard's version of the Basic language, to allow an entire array to be used as a parameter to pass to a subprogram. This at first made necessary extra internal storage for additional arrays to be used only within a certain subprogram, with the variable name being changed through a lengthy process upon entering or leaving that subprogram. A much faster and easier way was using separate storage files on the disc for each major array manipulation. When entry into a subprogram was needed the array could be stored in the file assigned to that subprogram, which could then be read out and labelled as any array needed for each subprogram.

The programming to use the DS-30 also was primarily a language problem. The DS-30 was very sensitive to the format in which it received data or commands. All leading zeroes and carriage return/line feed commands had to be suppressed. The address of command locations within the DS-30 also had to be encoded in hexadecimal nibbles (one-half byte) and sent in reverse order to load the registers properly. Commands to the DS-30 were sent as ASCII character strings. Data was output from the DS-30 to the HP-9825 via a fast read buffer which allowed a very fast data transfer rate. In use, a block of 256 bytes at a time were transferred representing one horizontal TV line of the quartered memory space. This was done in a loop which went back and took 256 lines, completely transferring the image.

It was decided that output would be on the HP-9825 plotter so that direct visual comparisons could be made between measured and predicted intensity LSF's. This was much more dramatic and easier to see than tabular output which then would have to be compared on a point by point basis for a correlation.

III. SUMMARY

This program can be useful in solving the problem that spurred this study. It will be able to show how much wander can be expected out of a laser designator beam as it travels through the atmosphere from the laser to the target. Based on the video recording of the actual image on a target it will show comparatively the amount of wander actually present in the laser. Plans are to unfold the results analytically, but at present, a visual comparison of the measured and predicted patterns is made to determine if there is any excess wander or "jitter" attributable to the laser platform itself. This determination will be helpful in setting specifications for the stability needed in the system to remove as much excessive spot movement as possible. It will also allow testing to determine if those specifications are being met.

This program can also be used to verify atmospheric problems when both the laser and target spot are fixed and known. Essentially, any of the laser to target elements can be determined by knowing the others and calculating the unknown using adaptations of the program. The beginning part of this program can be used to digitize and store any video image and produce an LSF of the image. This may be useful in recording and testing the output of several different lasers and optical aperatures for comparative analysis.

This computer program was designed in the initial stages of a continuing project studying the described problem. If desired, changes can be made to the program to adapt to changing field conditions and analysis requirements. In particular, the program now requires a greater understanding of its internal operations and operator interaction than is necessarily needed. More complete cueing prompts and data entry parameters may be worthwhile changes. Adaptability to other hardware may provide more program control, especially if control of the video disc or tape can be handled through an interface bus instead of manually. Also, improvements in output design can be foreseen to expand its usefulness and adaptability.

Finally, the speed of program operation could be increased through use of a faster computer with a greater memory capacity. The HP-9825 is comparatively slow and has insufficient memory. The use of a faster system such as the HP-1000 is recommended for actual measurements.

ANNEX A

USING THE COMPUTER PROGRAM

The analysis program requires considerable preliminary set up and operator interaction. Before the program is started there should be several items already recorded on videotape. The first item is a TV camera shot of the laser output. This is normally taken with a long focal length lens and filters to reduce the intensity without losing the beam pattern. A part of this recording should include a known diffraction grating through which the beam passes in order to measure the scale of the data for each system of lenses used. The diffraction pattern should extend in the vertical as seen on a TV screen for proper output on the plotter. Also needed to be recorded is, of course, a sequence of laser spot images on the target. Part of this recording should have the target only as a background reference for later calculations.

The next step that needs to be taken is to compute and record the square atmospheric turbulence index (C_n^2), then record the following system data for later program entry; wavelength of the laser, diameter of the optics objective lens, ratio of the obscuration to the diameter of the objective lens, distance to the target, and the extinction coefficient.

The first cue the program asks is for the input/output parameters. Table 1 lists the parameters and the different function each one is used for.

If the laser source pattern is not to be computed the next cue requests that the laser pattern be displayed from the video disc for transfer to HP-9825 memory. A cue is also presented asking for the horizontal width of the images to be taken from the DS-30. The first value should be the left most pixel desired, the second being the furthest right pixel to be used. The first value must be less than the second, with the first no less than 1 and the second no more than 256. This cue is also presented below before either the scale image or the target image is taken.

If the scale of the source data is to be determined the next cue requests that a frame be displayed on the video disc of the laser output with the diffraction grating in place. When this has been done continue the program and it will plot out an LSF of that image whereby the scale of the data can be determined in microradians per point.

The next cue alerts the operator to ensure that a frame of background video is displayed from the video disc for use in the difference process.

The program will then ask for the number of total frames that the user wishes to average for the measured target spot LSF. The value should be in the range from 1 to 600. The latter value being the greatest number of frames the video disc can hold at one time. The program will then proceed to record and process images from the video disc and DS-30. The program will provide a cue when it wants the next image to be sequenced on the video disc.

The program will alert the operator when it is about to produce a plot. If the HP-9862 plotter is not ready simply stop the program until a piece of plotting paper is in place.

The program will request the system data after the measured image spot data has been plotted. The data format is not critical but should be in the correct units as follows:

Wavelength	Meters
Diameter of objective lens	Meters
Obscuration/objective	None
Scale of data	Microrads per point
Range to target	Meters
C_n^2	Meters$^{-2/3}$
Extinction coefficient	Inverse meters

If the source pattern is to be computed the program requests peak amplitude and standard deviation of the intensity distribution.

The program will then continue computations without further inputs until it has run through with the initial parameters. The I/O parameters will determine at which steps output is plotted. After one run through, the program will request a new C_n^2, range, and coefficient. If the input range is positive the program will again run through from the atmospheric calculations with the new range. If the range is negative, the branch is to the beginning of the prediction phase where all new system inputs are requested. If the range input is zero, the program ends.

ANNEX B

PROGRAM VERIFICATION AND FLOWCHARTS

I. MEASUREMENT PHASE

Section I (steps 0 - 50) consisted of program setup information and the DS-30 function command programming. This section was easily verified by observing that all initializing functions were accomplished and the response of the DS-30 could be visually noted.

Section II (steps 51 - 86) consisted of transferring the contents of the four quarters of the DS-30's memory to the HP-9825 and producing an LSF of each image. For testing, an image consisting of all black (8 bit binary ones) or all white (8 bit binary zeroes) was placed in each of the four quarters of memory, each quadrant was then read out to the HP-9825. The values received by the HP-9825 corresponded to the contents of the DS-30 memory quadrant and did show proper changes when the subject quadrant memory was inverted from black to white. The LSF was produced by averaging the pixels in each horizontal line of video, each line producing a point value as the image was scanned vertically from top to bottom. Examples of LSF's produced for a "black" and a "white" image are in Figures 2 and 3.

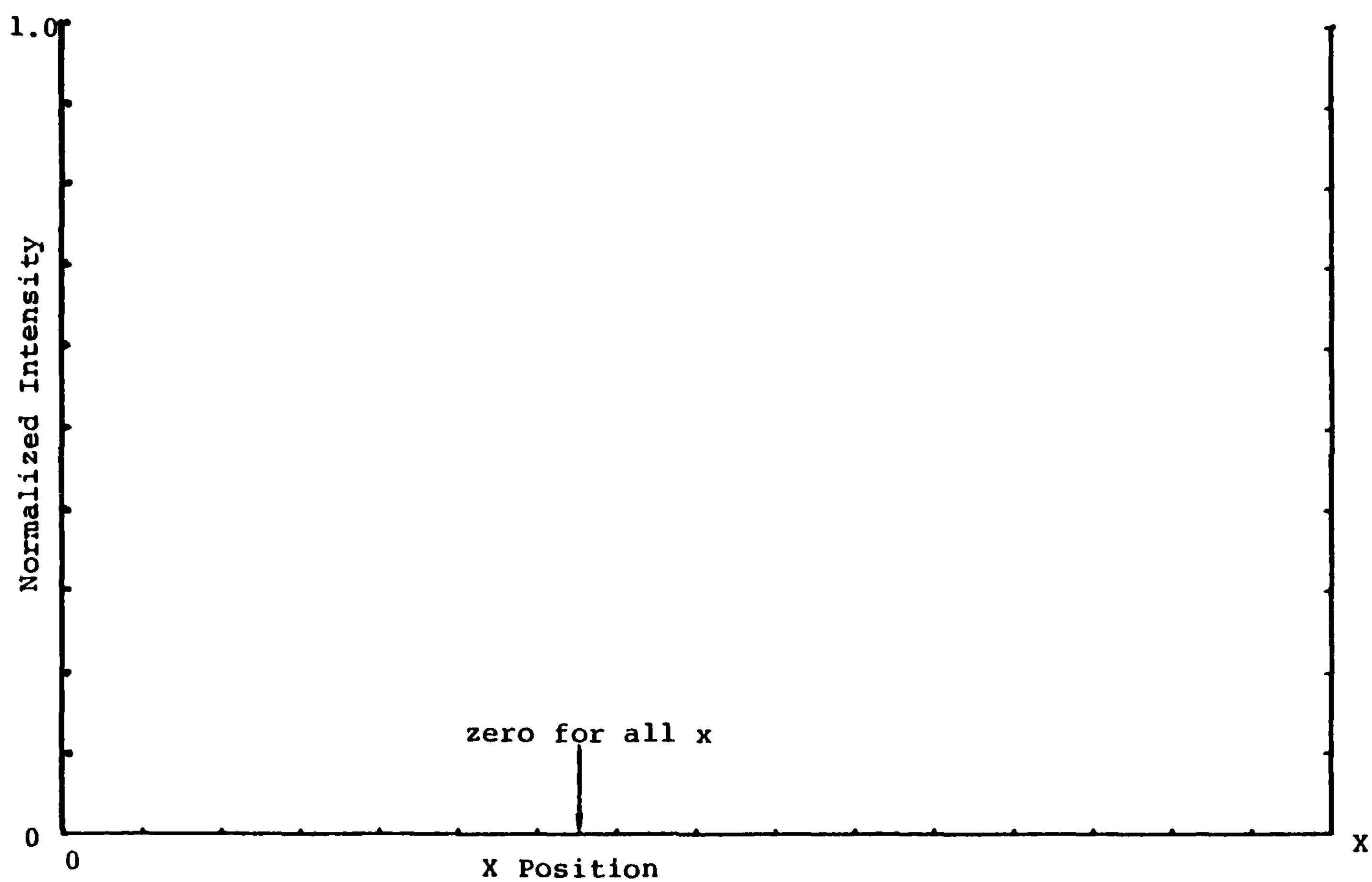

FIGURE 2. "BLACK" IMAGE LSF

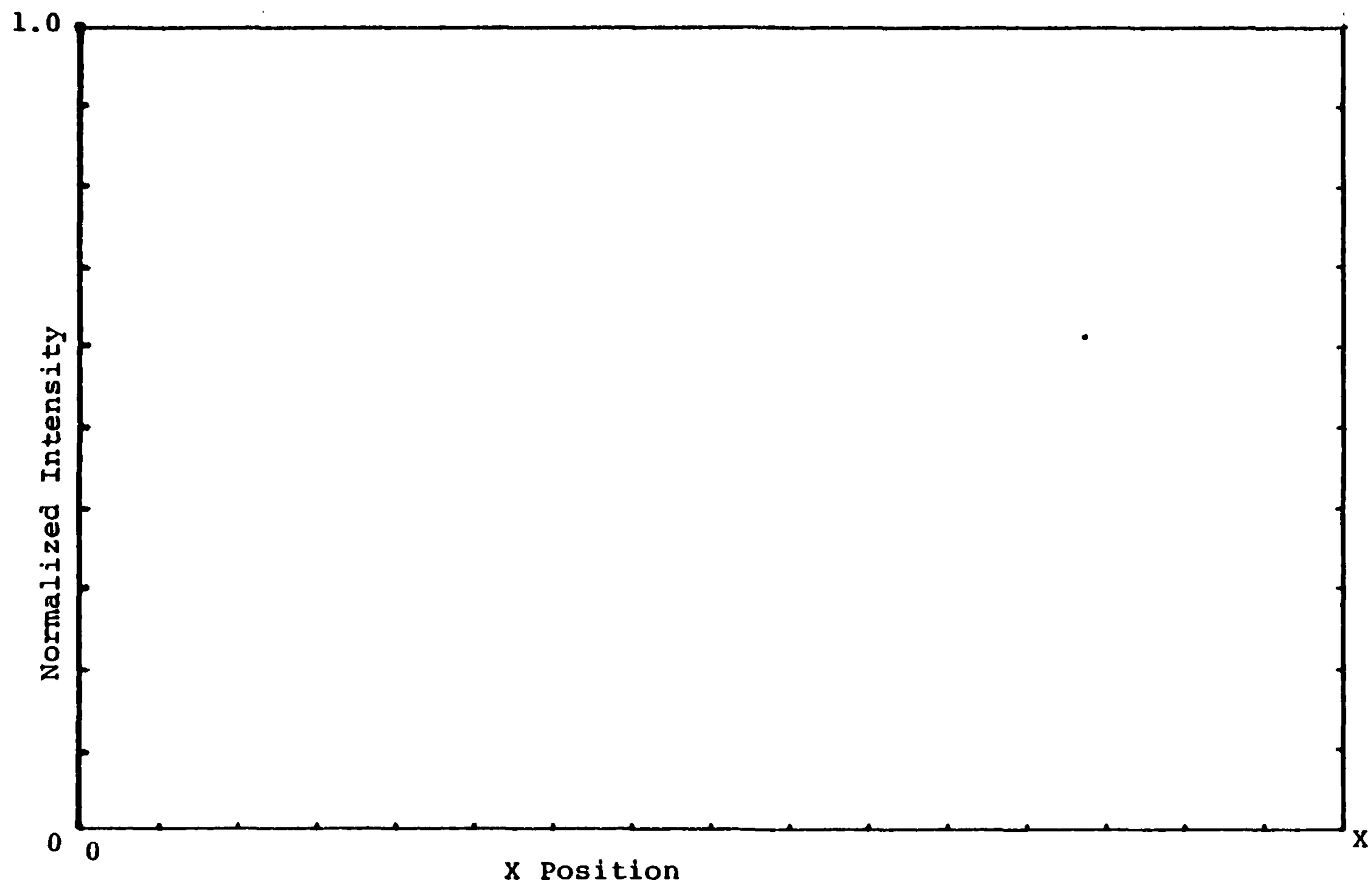

FIGURE 3. "WHITE" IMAGE LSF

Section III (steps 87 - 118) subtracted a reference background from an image to yield a difference image, then shifted the resulting LSF so that the center of area under each image was centered on zero. In this way the wander from each succeeding image could be determined, removed, and the total frames used could then be averaged to show the short term atmospheric action on the laser spot image. Proper operation of this section can be seen in Figure 4 where two images of slightly different position and intensity were averaged to yield an LSF halfway between the two image functions as expected. Figure 5 shows a differenced LSF where a small laser spot was added to a reference background. The result is almost entirely the laser spot with a small amount of "video noise" caused by the camera and associated electronics.

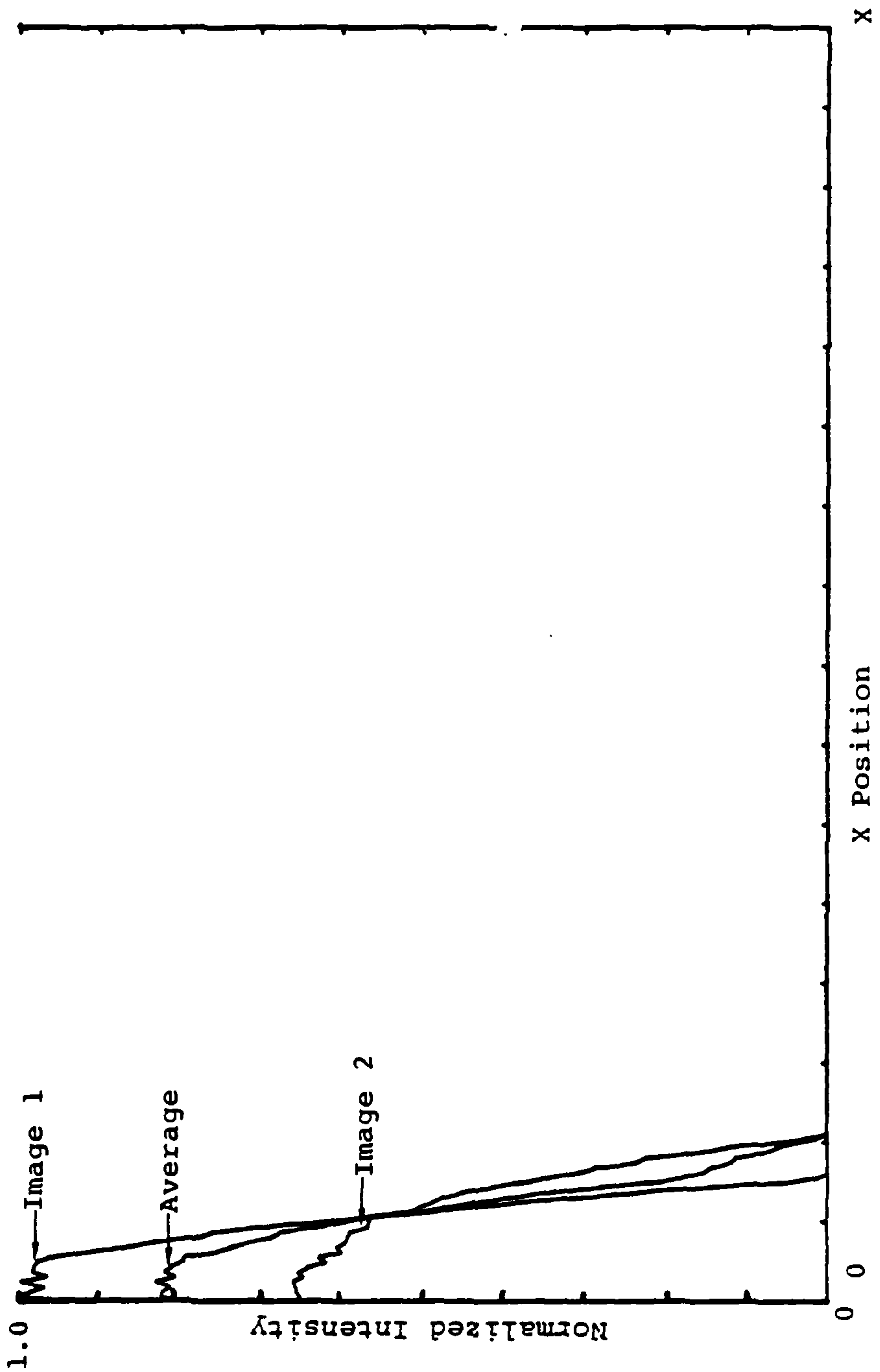

FIGURE 4. AVERAGING EXAMPLE

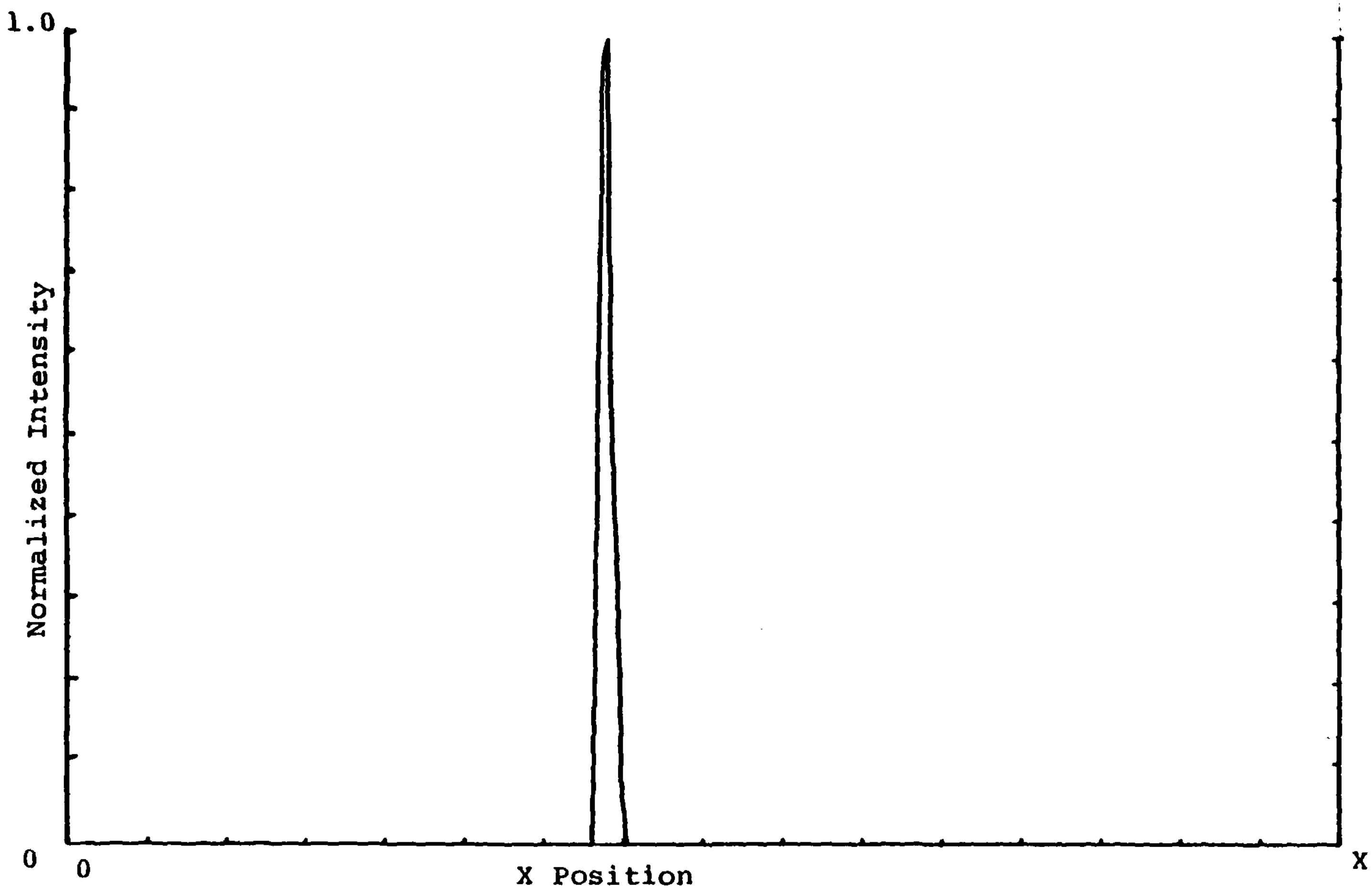

FIGURE 5. LASER SPOT LSF

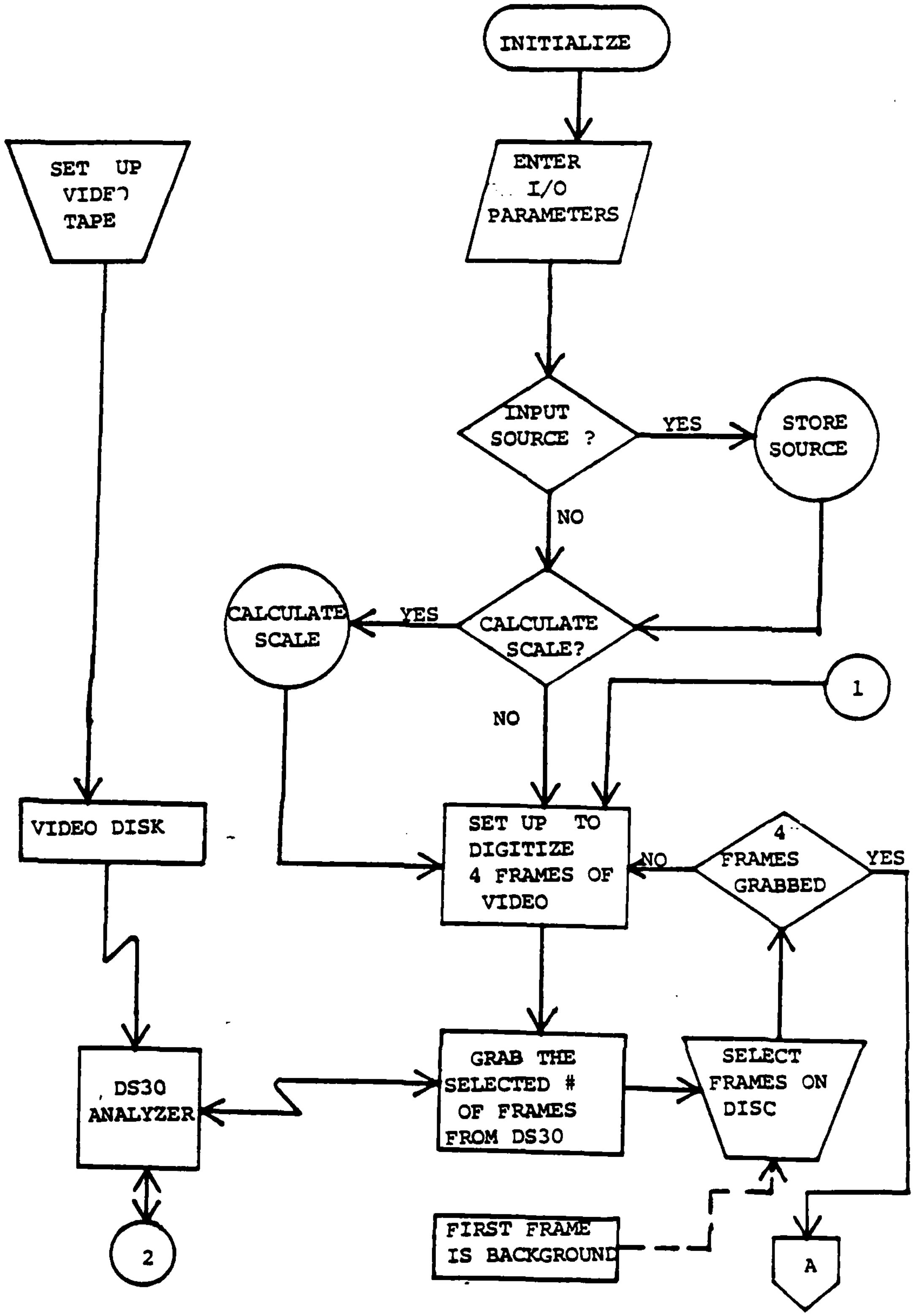

FIGURE 6A. MEASUREMENT PHASE FLOWCHART

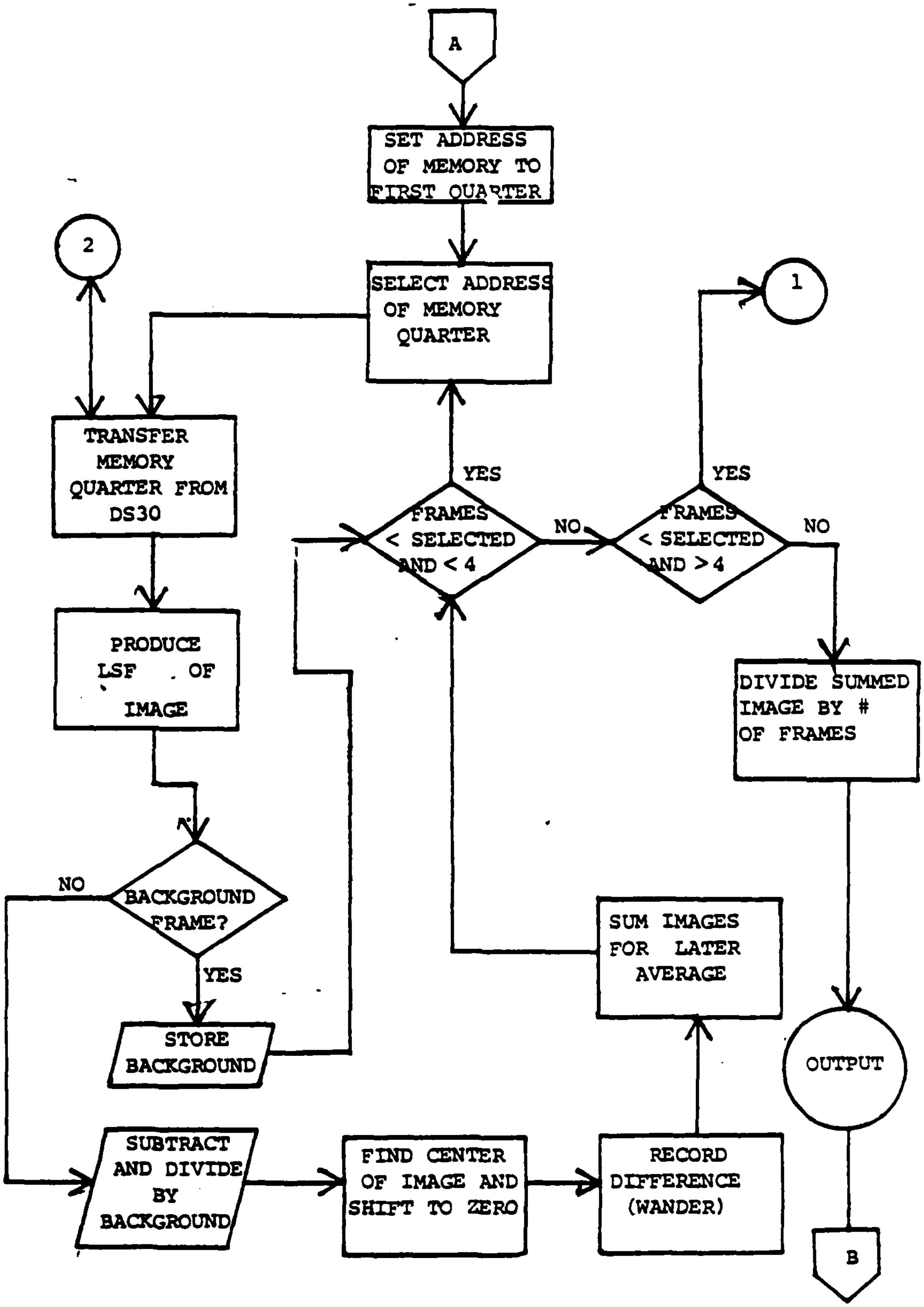

FIGURE 6B. MEASUREMENT PHASE FLOWCHART

II. PREDICTION PHASE

Section IV (steps 119 - 139) enters the parameters of the atmosphere and optics needed to model and predict the laser spot pattern on the target. This section also yields the calculated Gaussian laser intensity output if that data is not measured in the next section. The output of this section is shown in Figure 7.

Section V (steps 140 - 172) consists mainly of branching, data reading, and subroutine action. These subroutines, branching and data input will be verified with proper operation of the program as a whole.

Section VI (steps 173 - 183) calculates the diffraction limited optics effect on the laser output and produces a radial point spread function of the intensity. The output for a point source should be an airy function as results show in Figure 8.

Section VII (steps 184 - 204) again consists mainly of subprograms and also calculates the product of the calculated optics and laser output transforms. The output is in Figure 9.

Section VIII (steps 205 - 220) computes the MTF of the atmosphere based on the inputs from Section IV. The output is in Figure 10.

Section IX (steps 221 to the end of the main program) is mainly subprogram action in computing the final LSF predicted on the target using the source, optics and atmospheric MTF's. It also provides a link to re-enter the program for changed parameters. The output of this section is listed under the subprograms used.

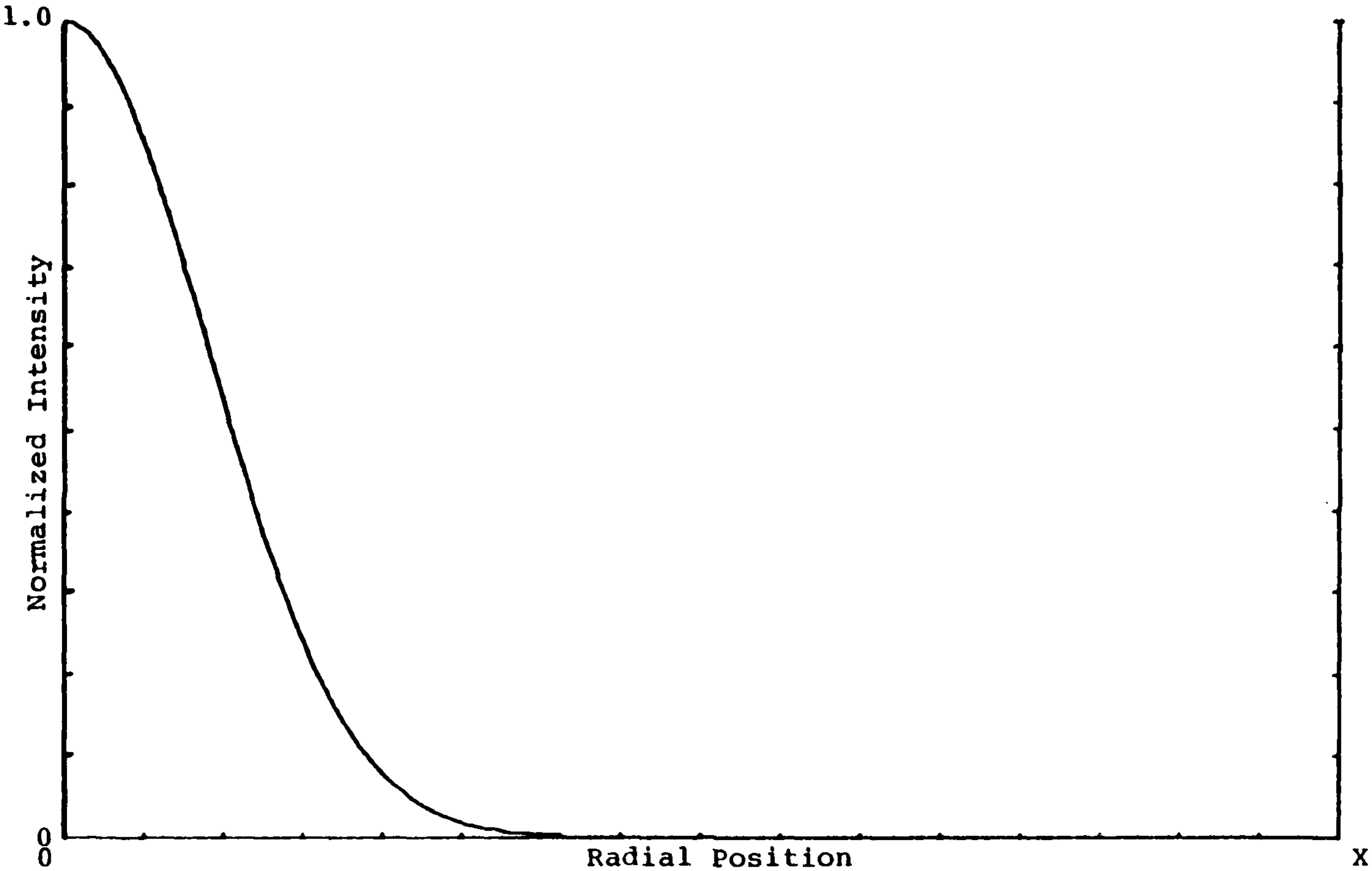

FIGURE 7. EXAMPLE OF CALCULATED LASER OUTPUT

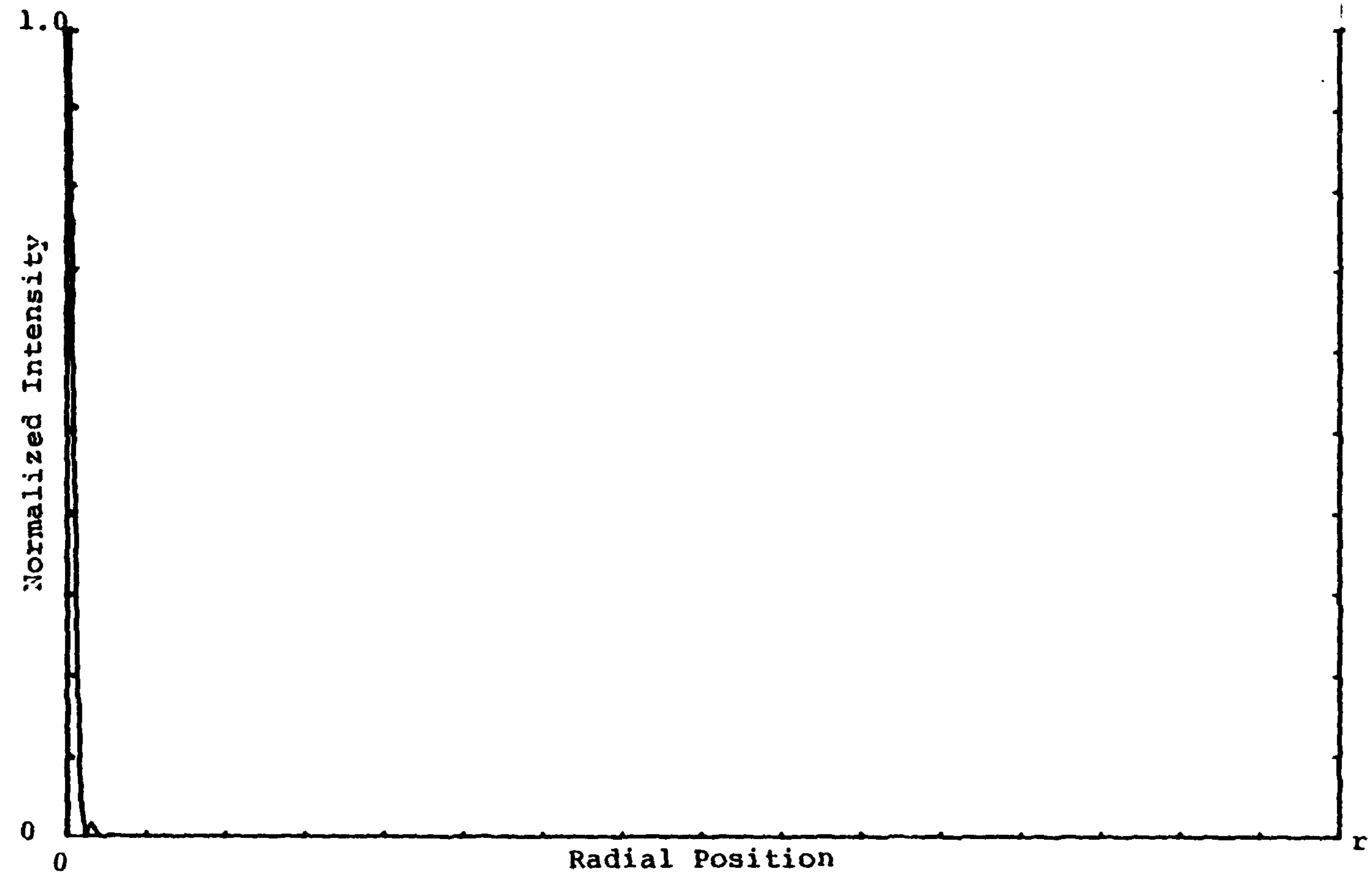

FIGURE 8. OPTICS OUTPUT

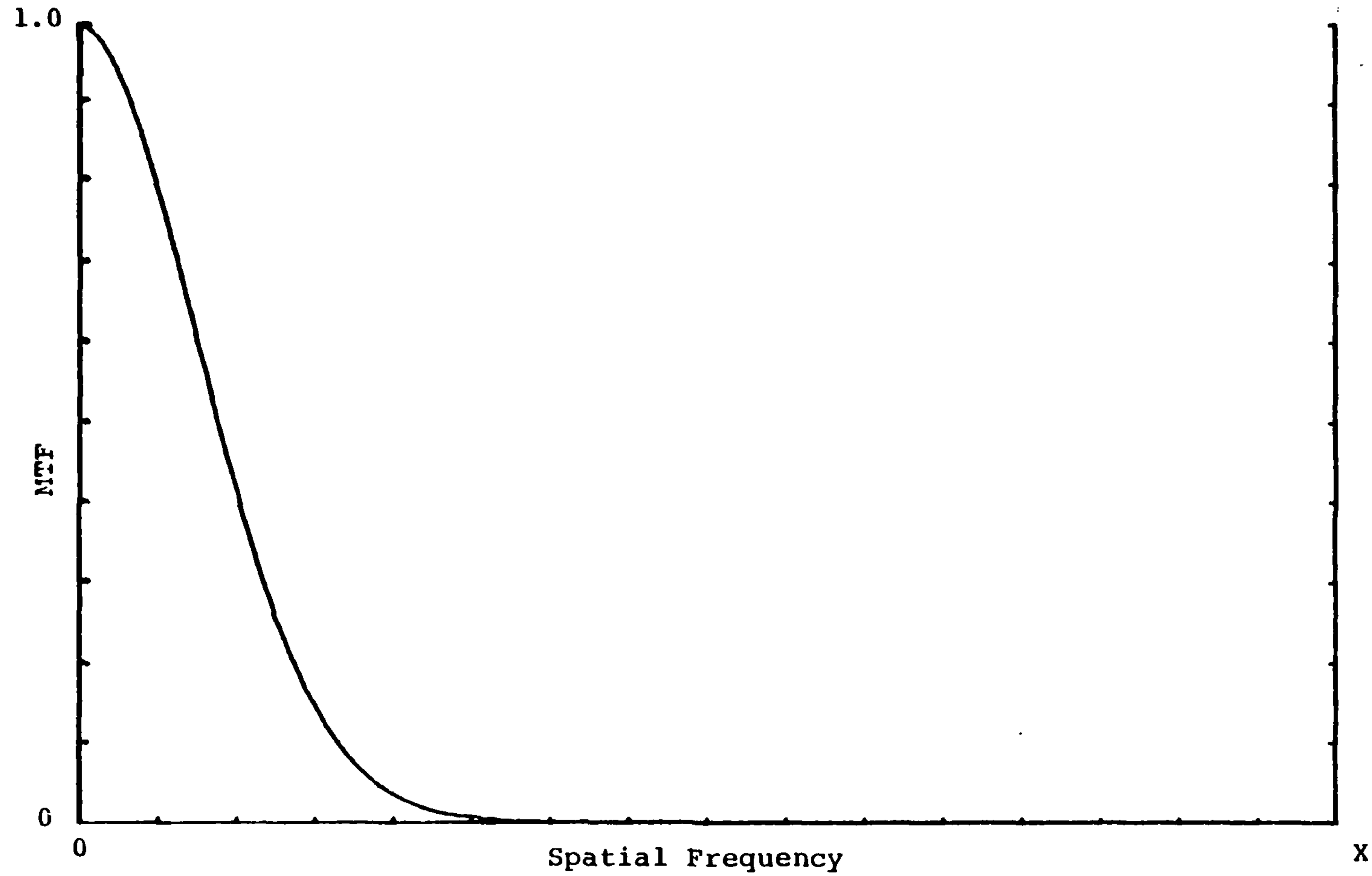

FIGURE 9. LASER AND OPTICS MTF

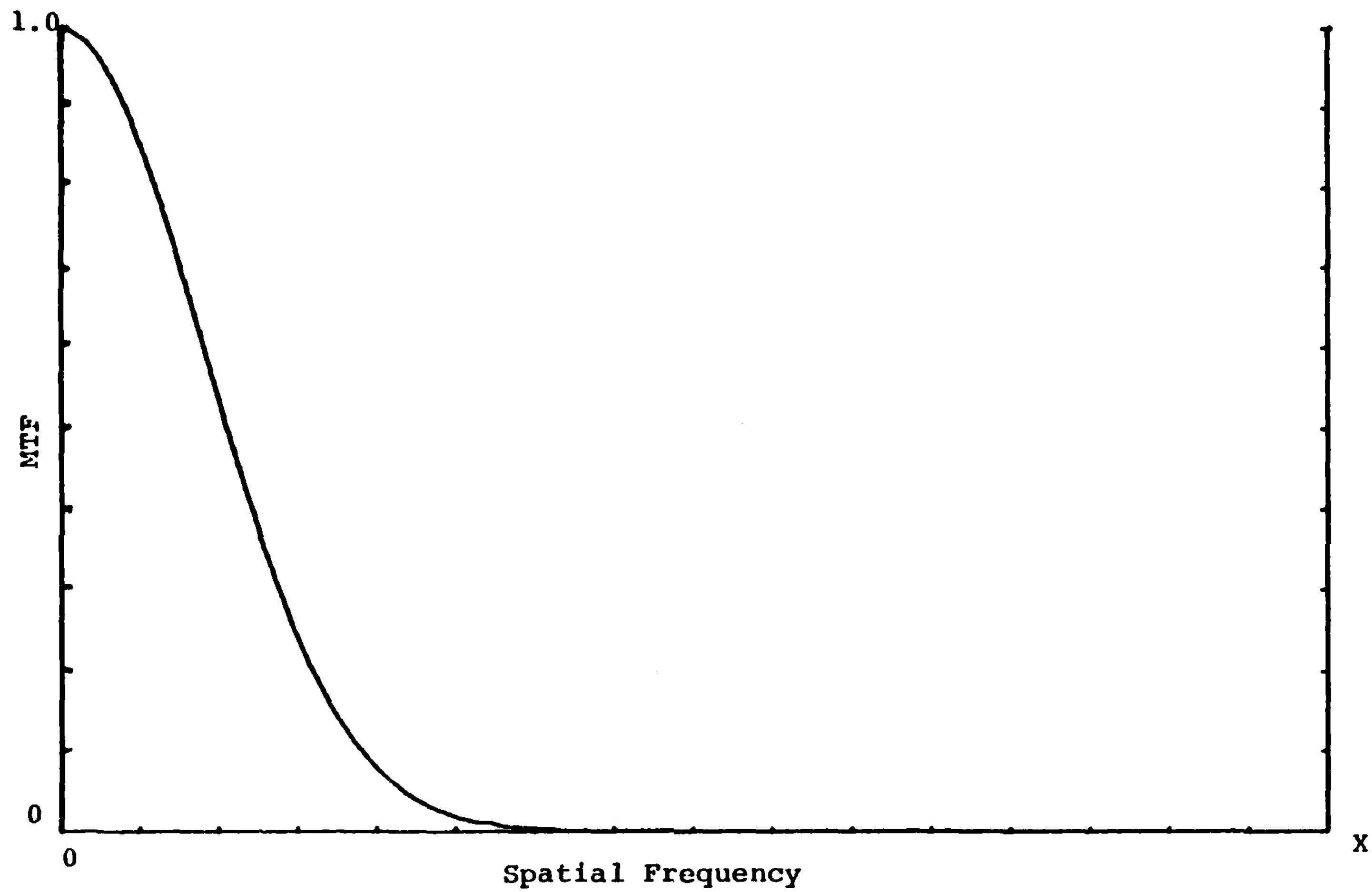

FIGURE 10. MTF OF THE ATMOSPHERE (SHORT TERM)

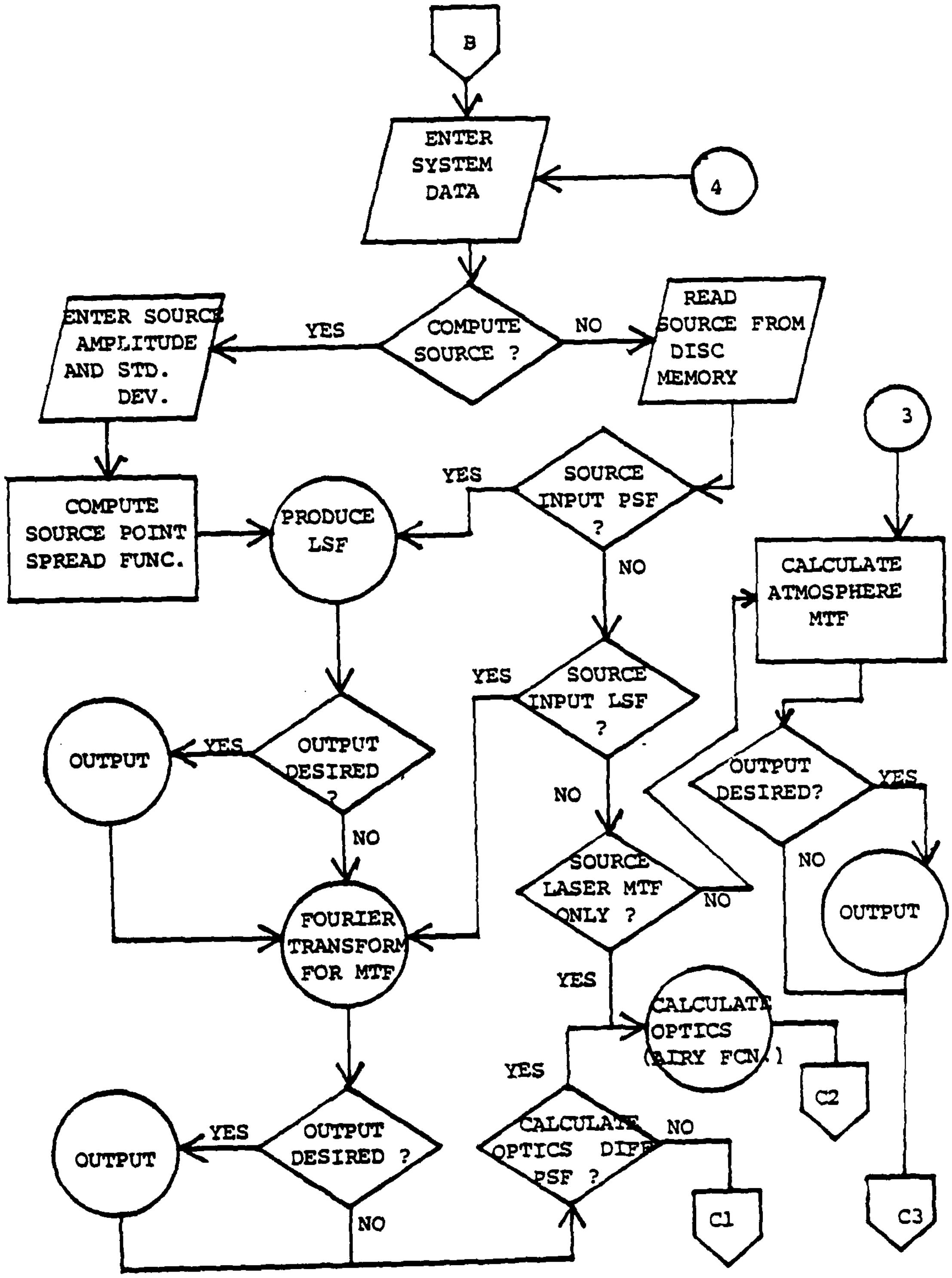

FIGURE 11A. PREDICTION PHASE FLOWCHART

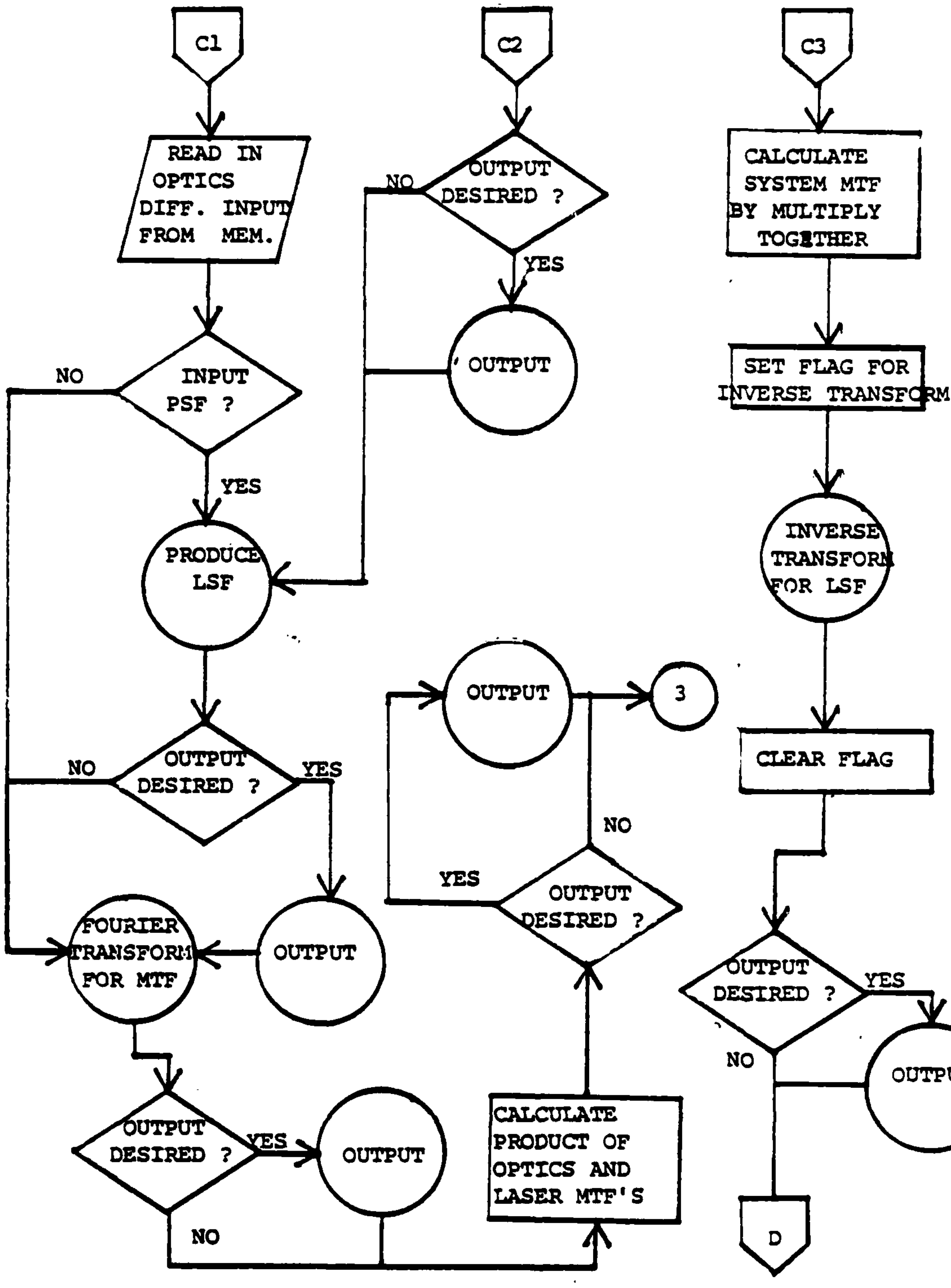

FIGURE 113. PREDICTION PHASE FLOWCHART

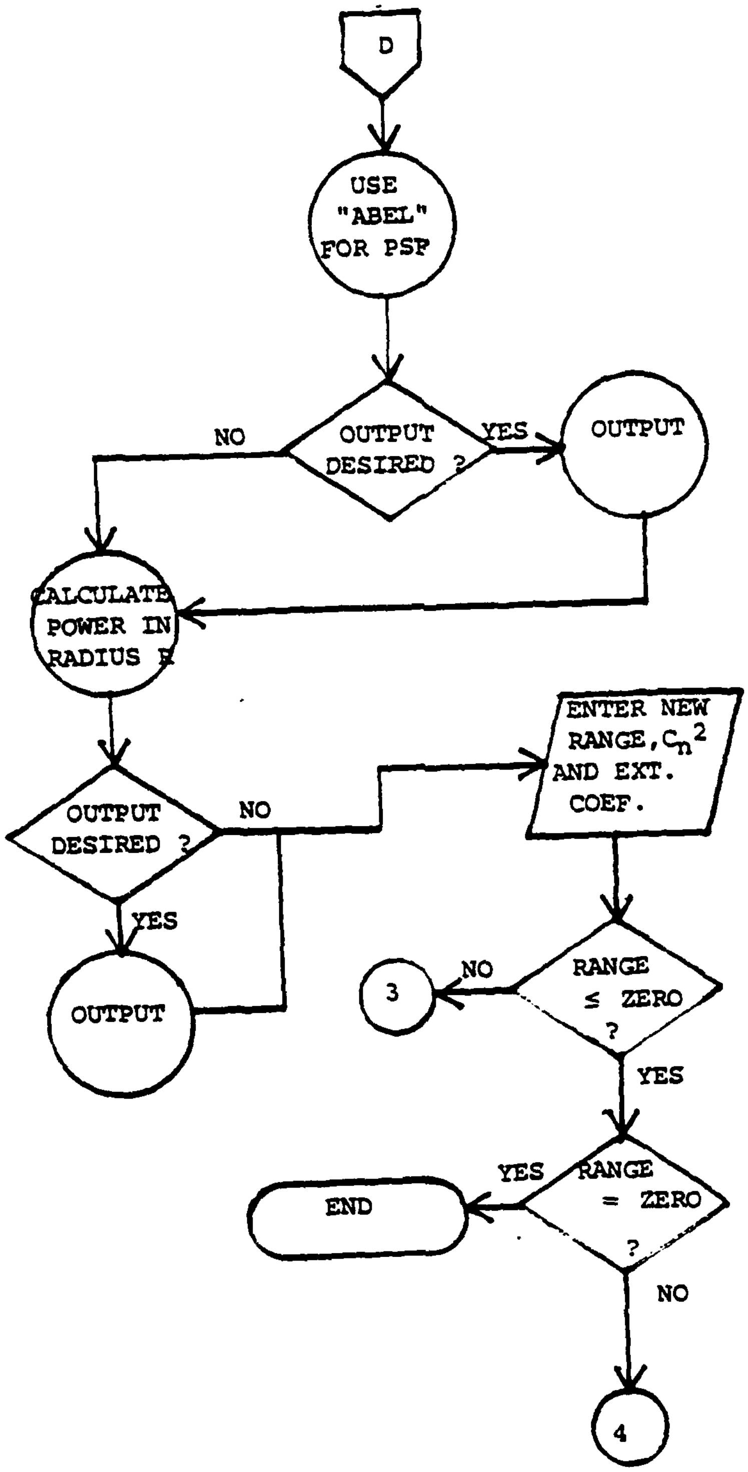

FIGURE 11C. PREDICTION PHASE FLOWCHART

III. SUBPROGRAMS

Section X (subprogram ABEL) produces a point spread function (PSF) from the LSF computed for the target laser spot. The input and resulting output is shown in Figures 12 and 13.

Section XI (subprogram LSF) enables the program to compute a line spread function for later conversion to a MTF when the input is calculated by Sections IV and VI as point spread functions or when the data is input in Section V in the point spread function format. Sample input and output is in Figures 14 and 15.

Section XII (subprogram B) calculates the fraction of the power inside a circle of a chosen radius about the center of the laser spot. This is helpful in determining if the spot is intense enough on the target. The input and output are Figures 16 and 17.

Section XIII (subprogram FXFORM) is a discrete Fourier transform program that functions both as direct and inverse depending on the flag set in the main programs. Several Fourier pairs were checked to ensure correct calculations, Figures 18 through 21.

Section XIV (subprogram SOURCE) digitizes an image of the laser source for inclusion in the prediction calculations. It is a storage of DS-30 video from the Vidicon camera input.

Section XV (subprogram SCALE) digitizes an image with a standard diffraction grating for calculating the scale of the data. Figure 22 is an example of this image.

Section XVI (subprogram OUTPUT) yields in useable form all the data required for analysis. This subprogram was used for all the output in the plot format. Functions "MIN" and "MAX" are used by the "OUTPUT" subprogram.

The program was run as a whole numerous times with different I/O parameters and data in order to exercise the branching combinations and program steps. Table 1 lists the I/O parameters available and their uses. This operation was simply to ensure the program ran as was intended.

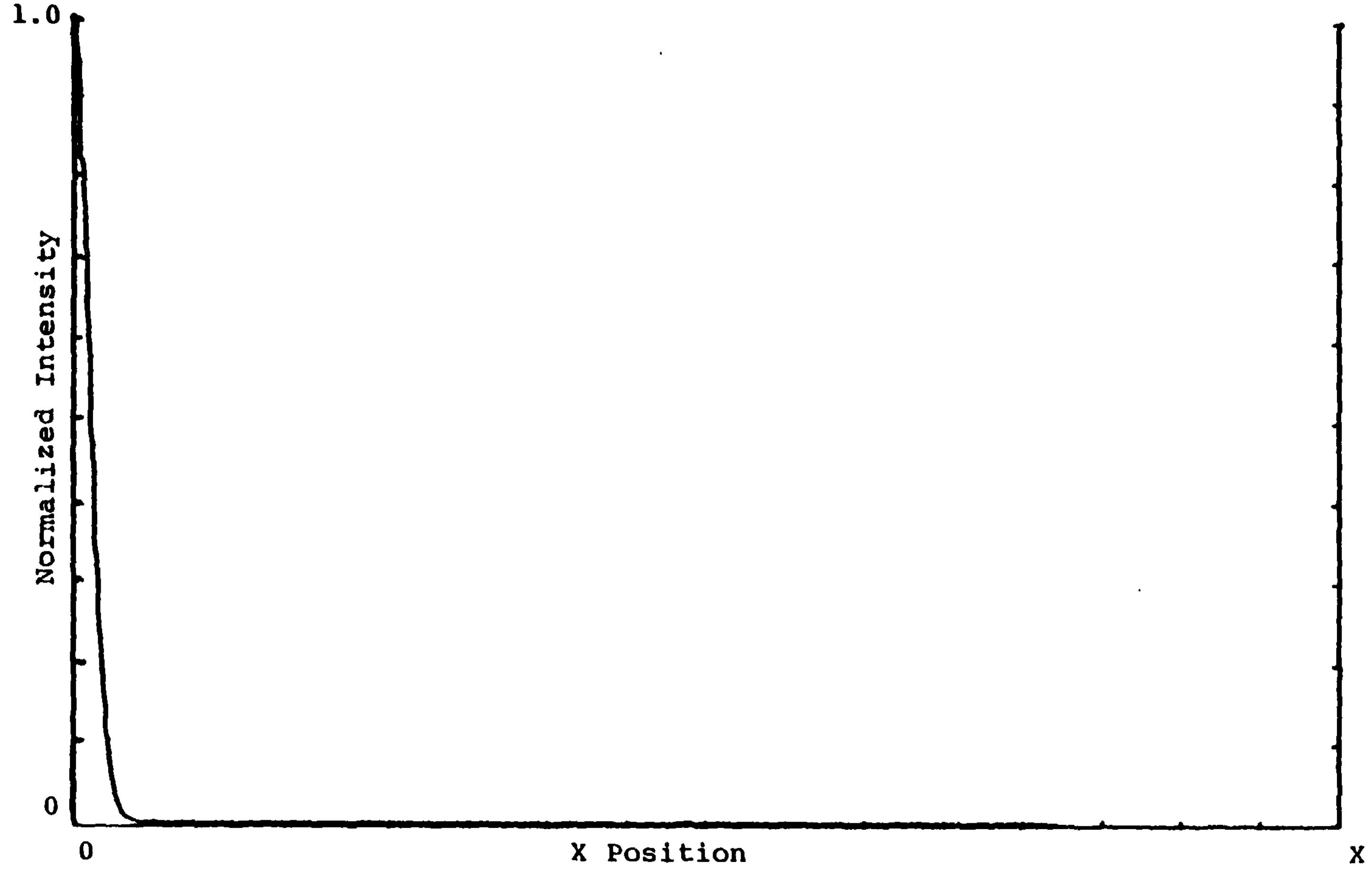

FIGURE 12. "ABEL" INPUT (LSF)

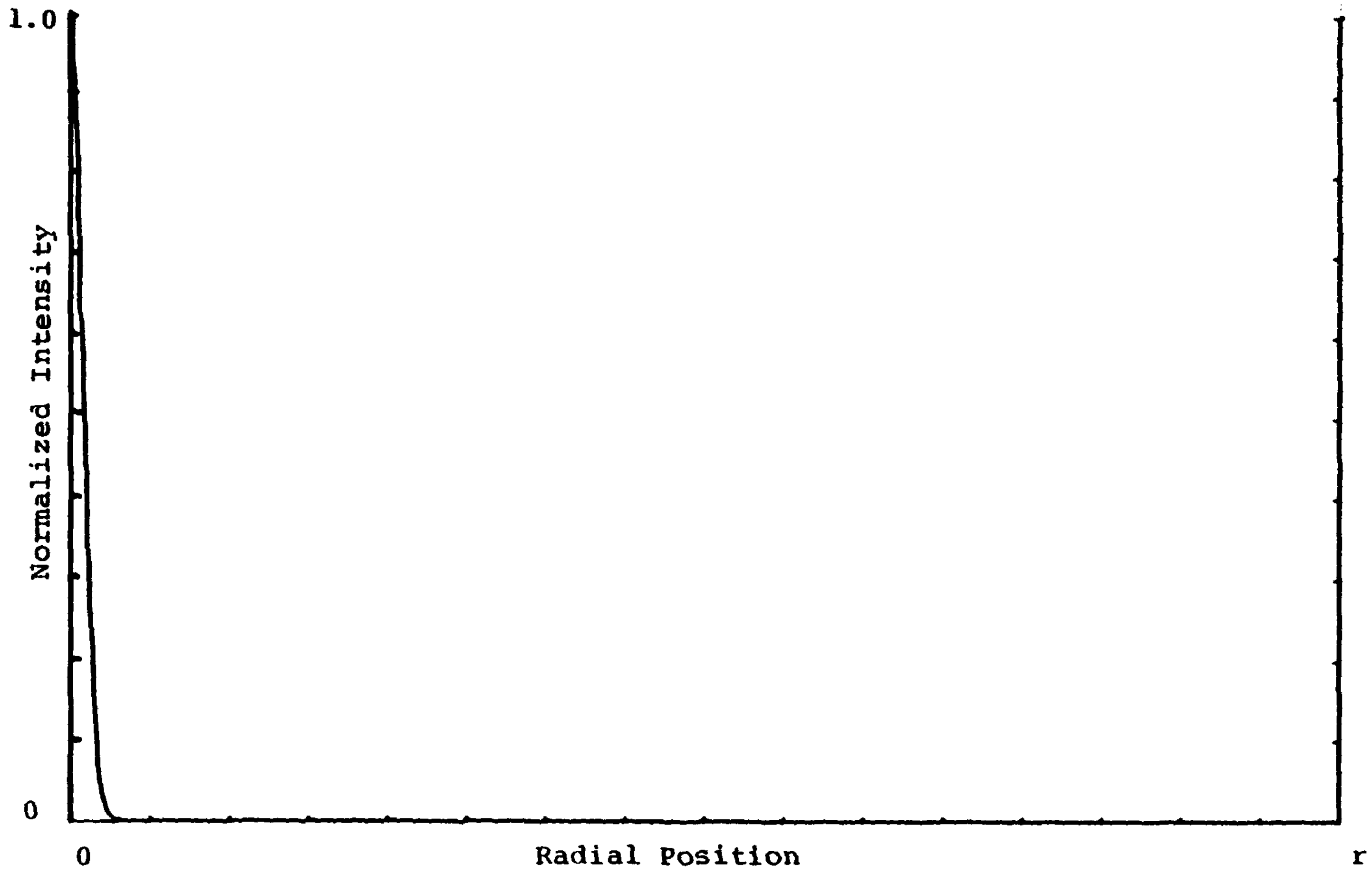

FIGURE 13. "ABEL" OUTPUT (PSF)

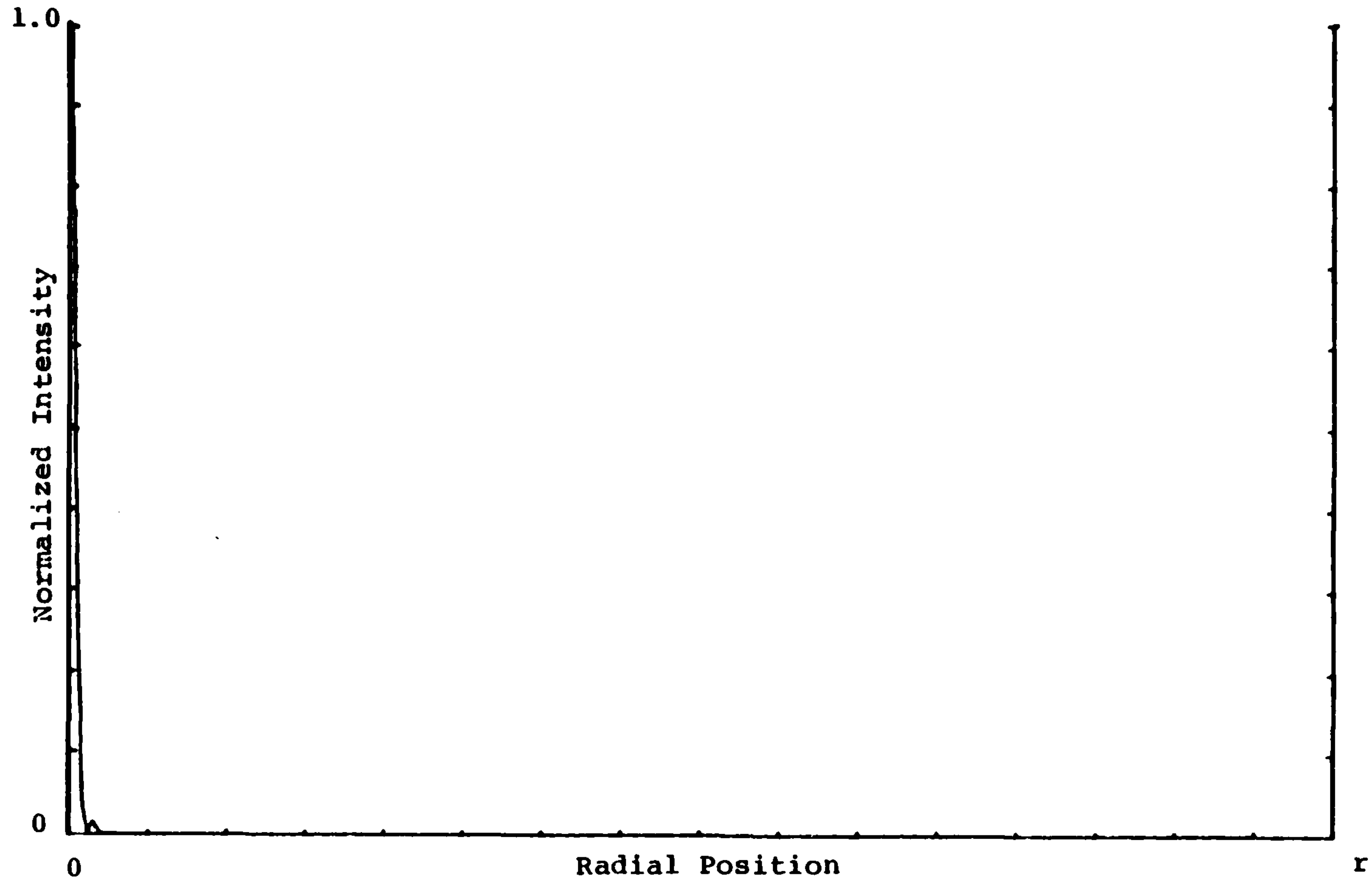

FIGURE 14. "LSF" INPUT EXAMPLE

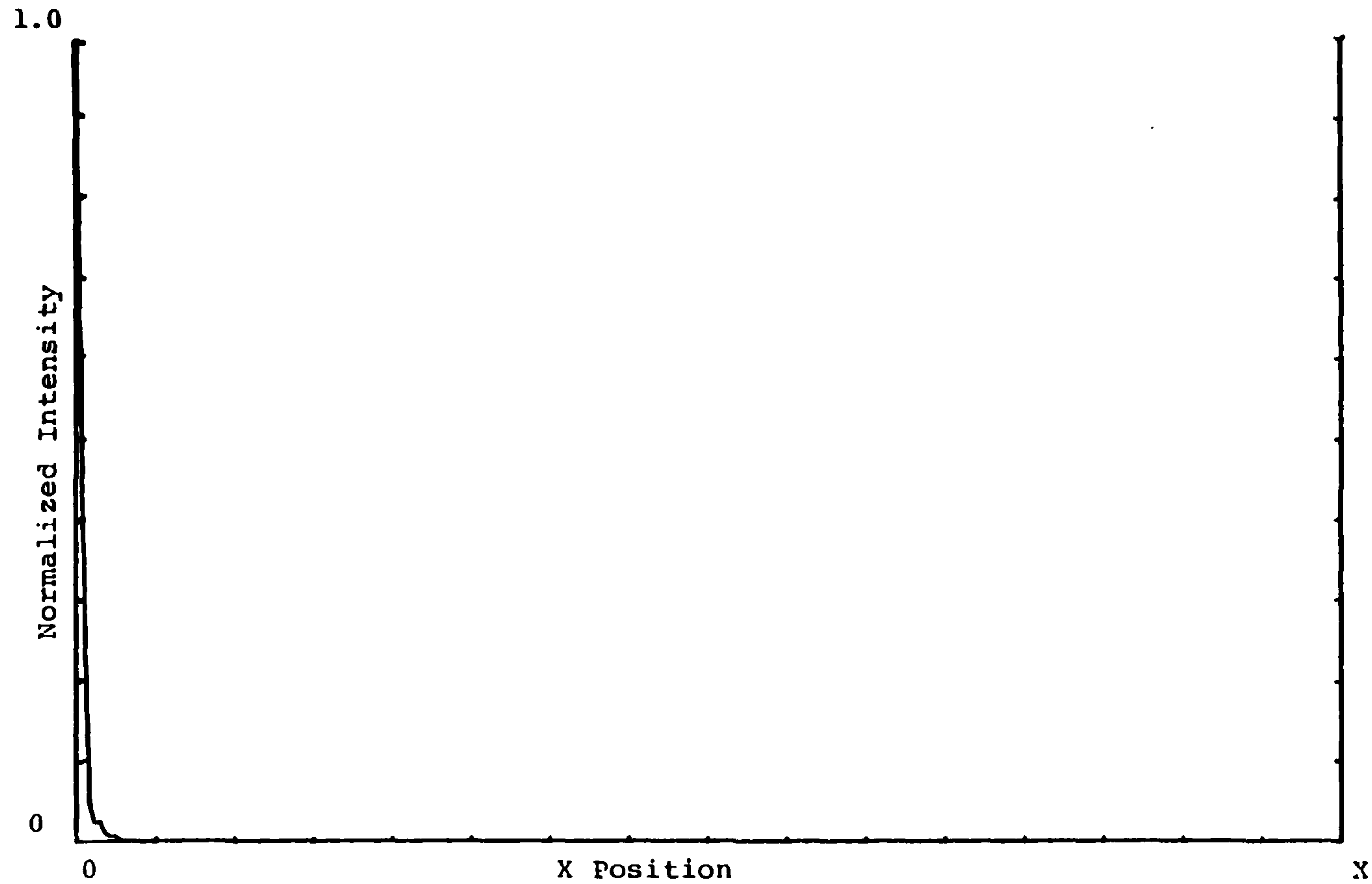

FIGURE 15. "LSF" OUTPUT

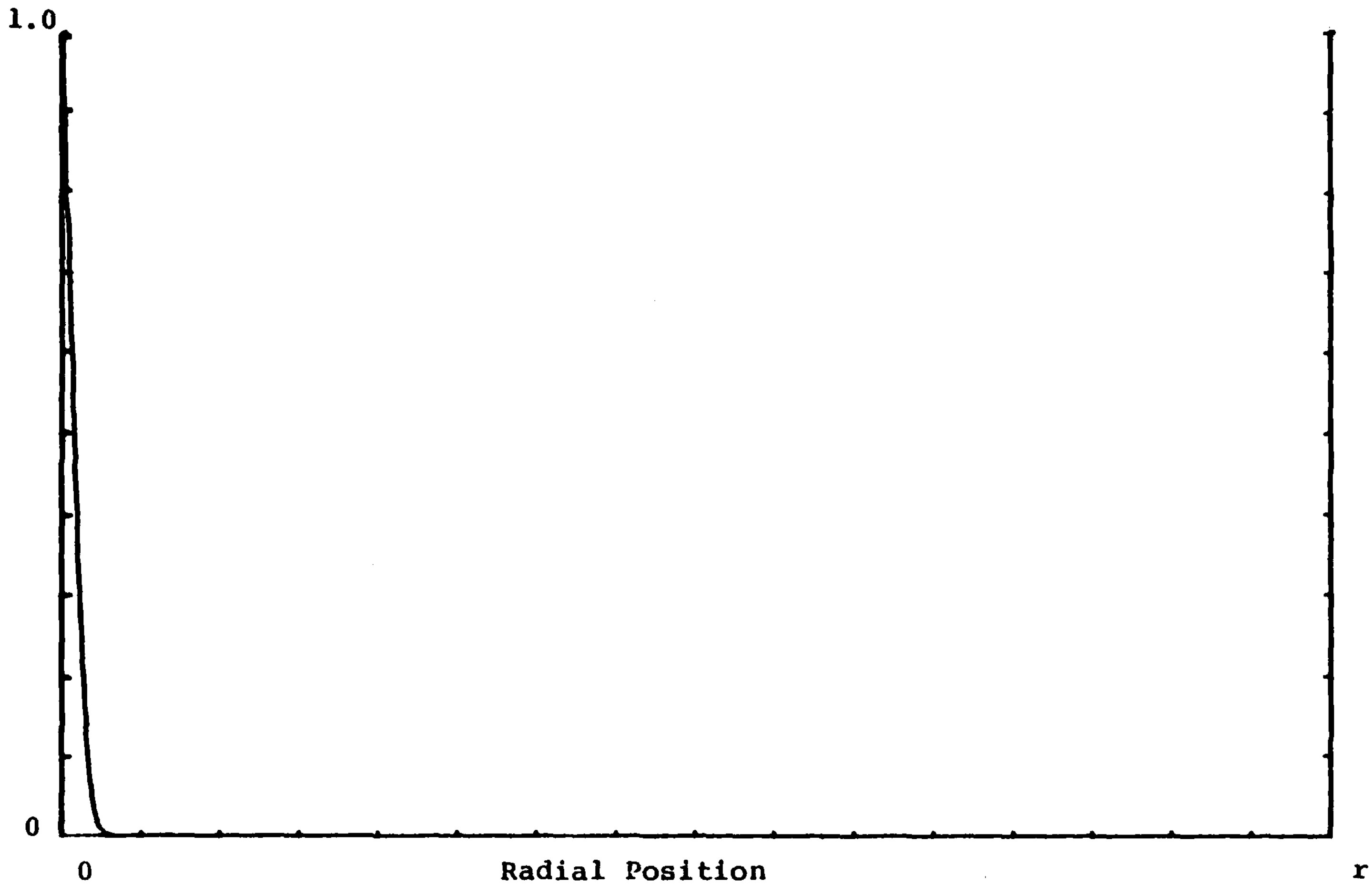

FIGURE 16. "B" INPUT

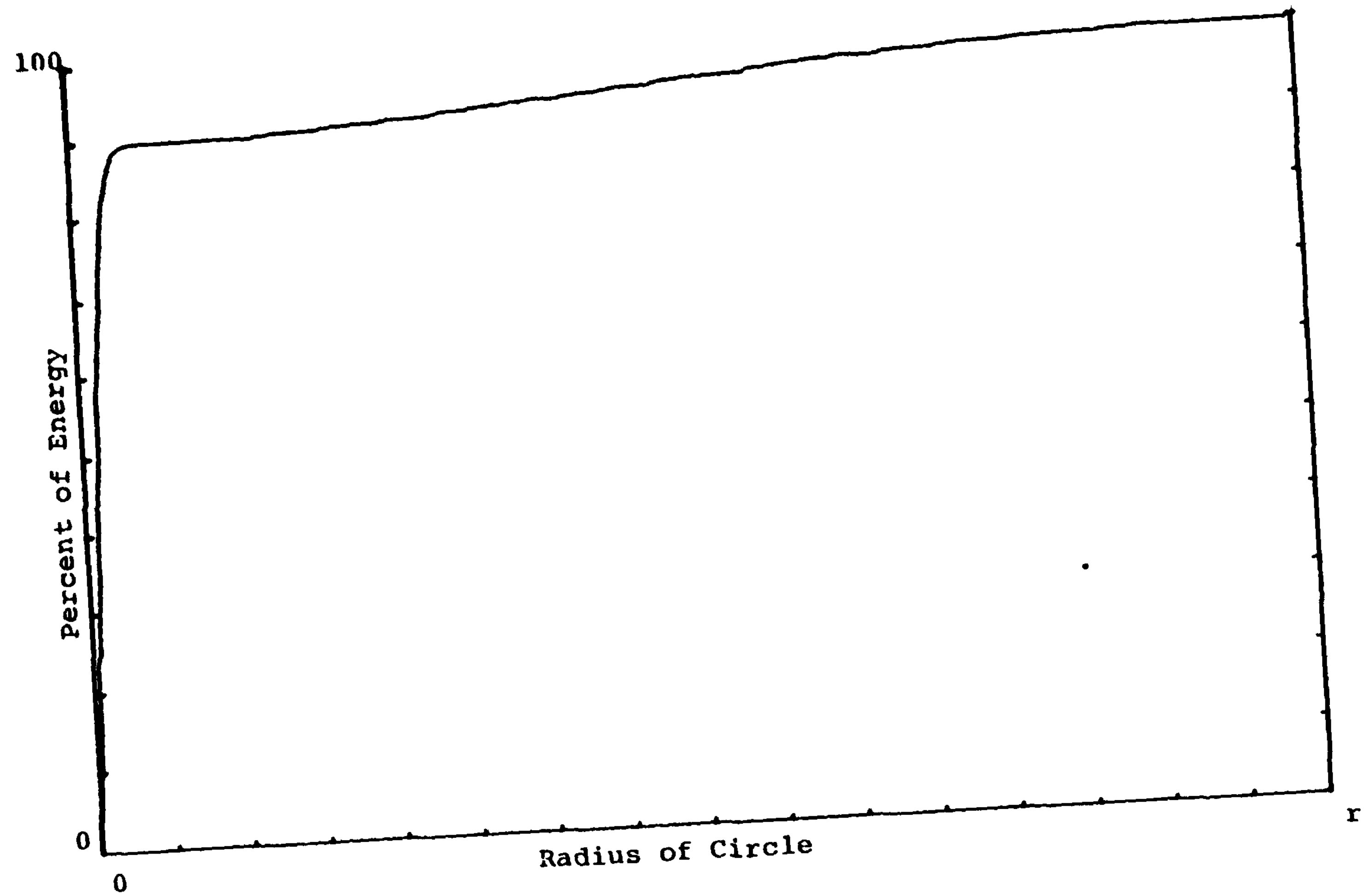

FIGURE 17. "B" OUTPUT

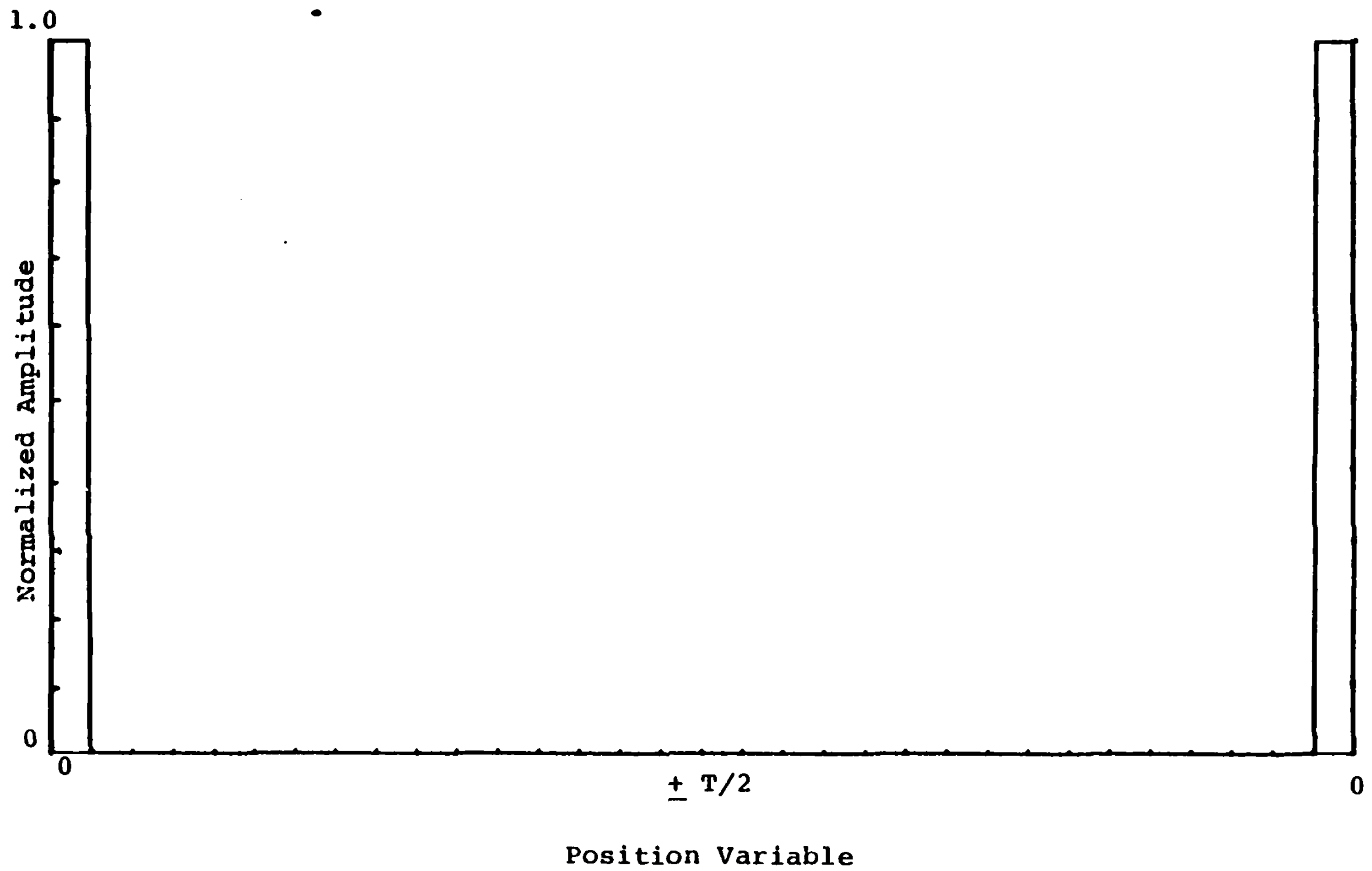

FIGURE 18. FOURIER TRANSFORM INPUT EXAMPLE

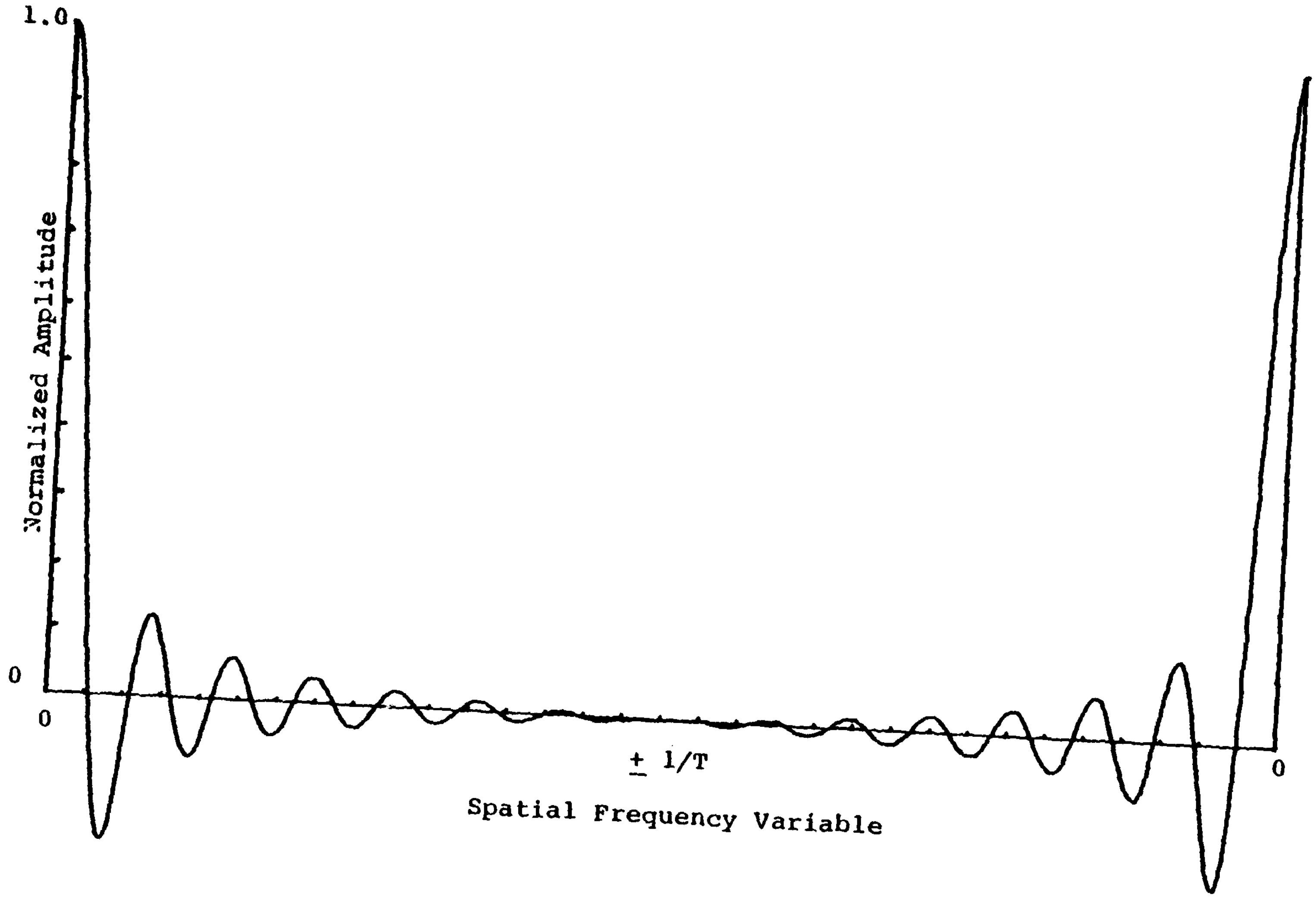

FIGURE 19. FOURIER TRANSFORM OUTPUT EXAMPLE

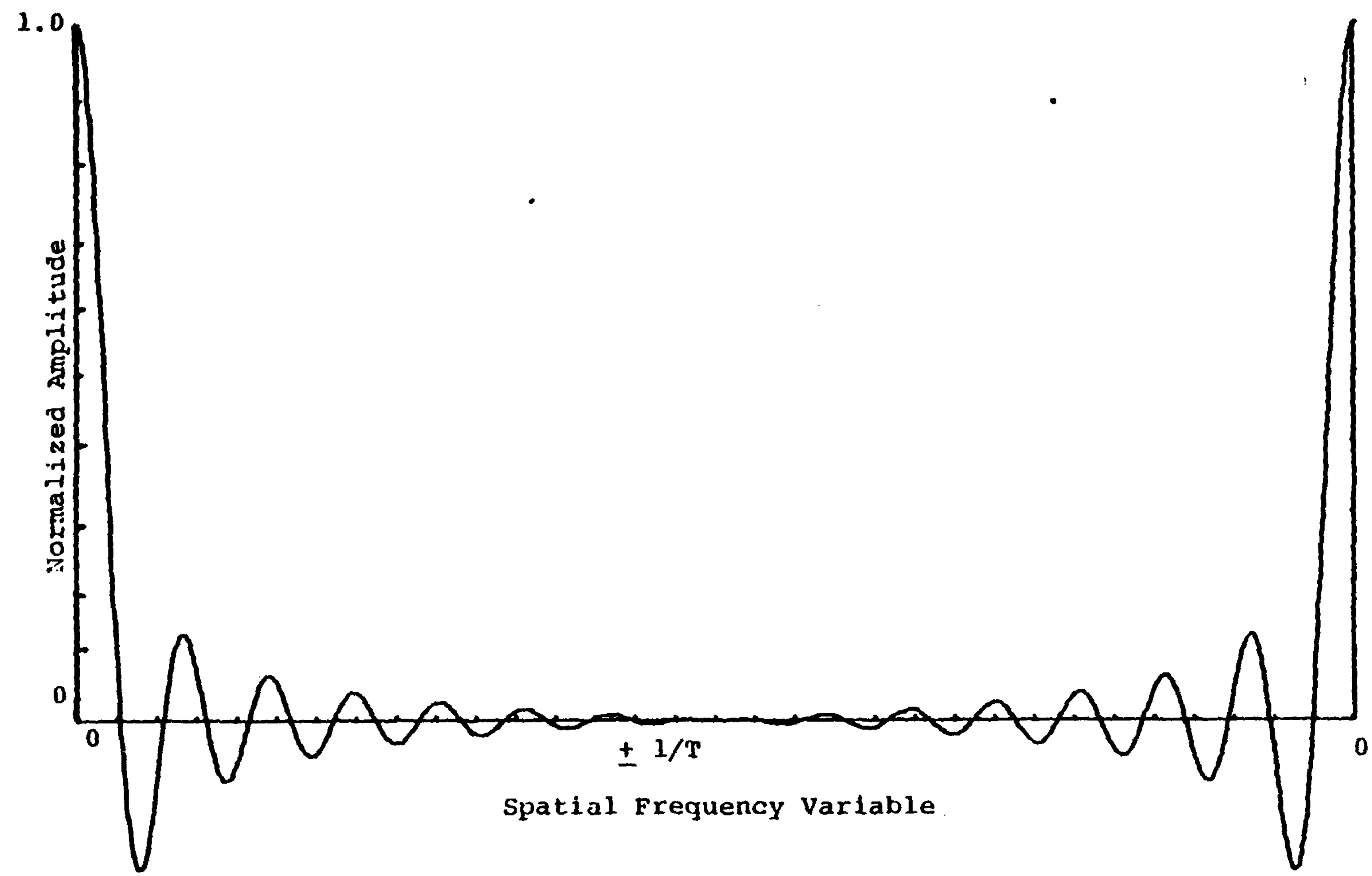

FIGURE 20. INVERSE TRANSFORM INPUT EXAMPLE

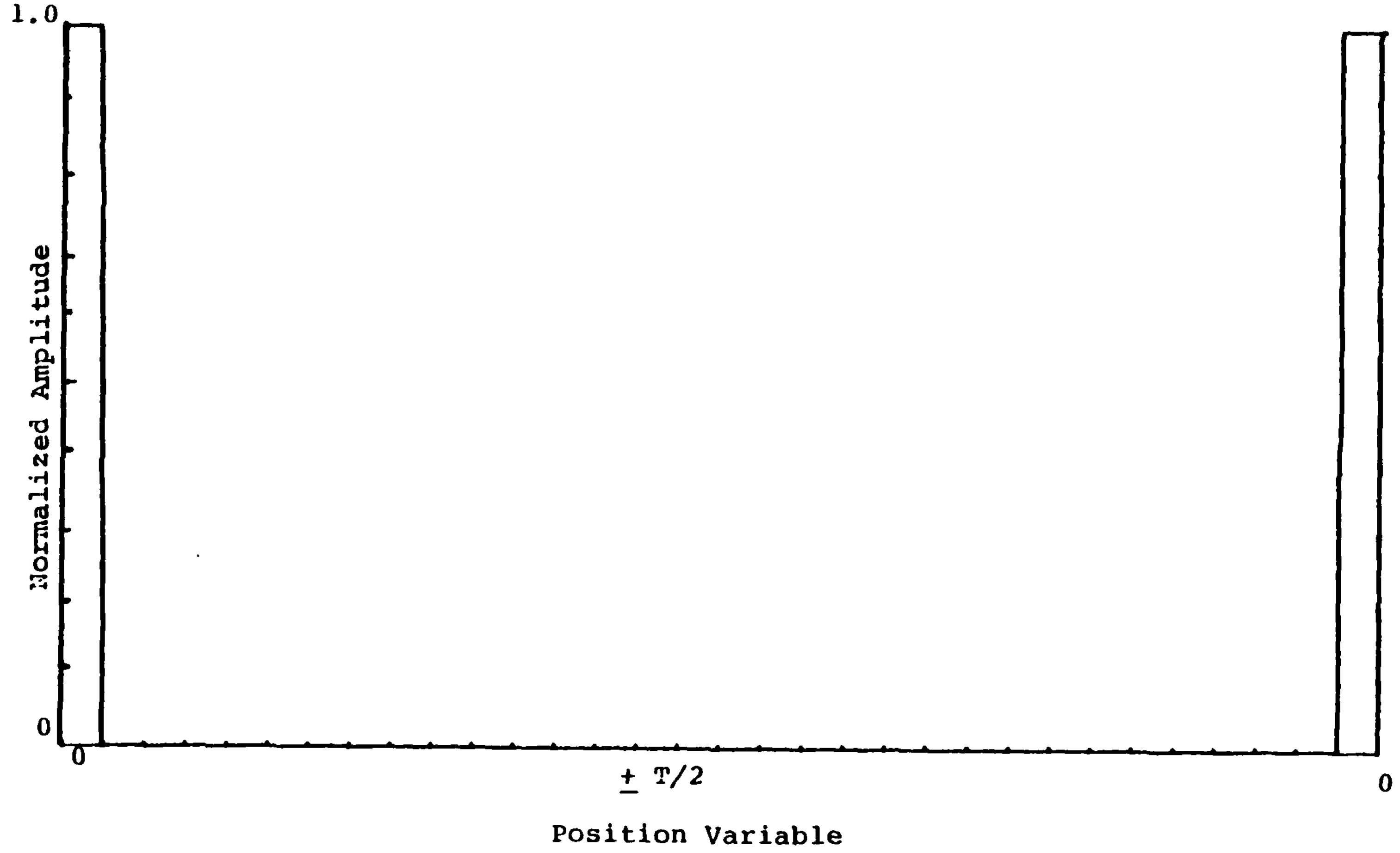

FIGURE 21. INVERSE TRANSFORM OUTPUT EXAMPLE

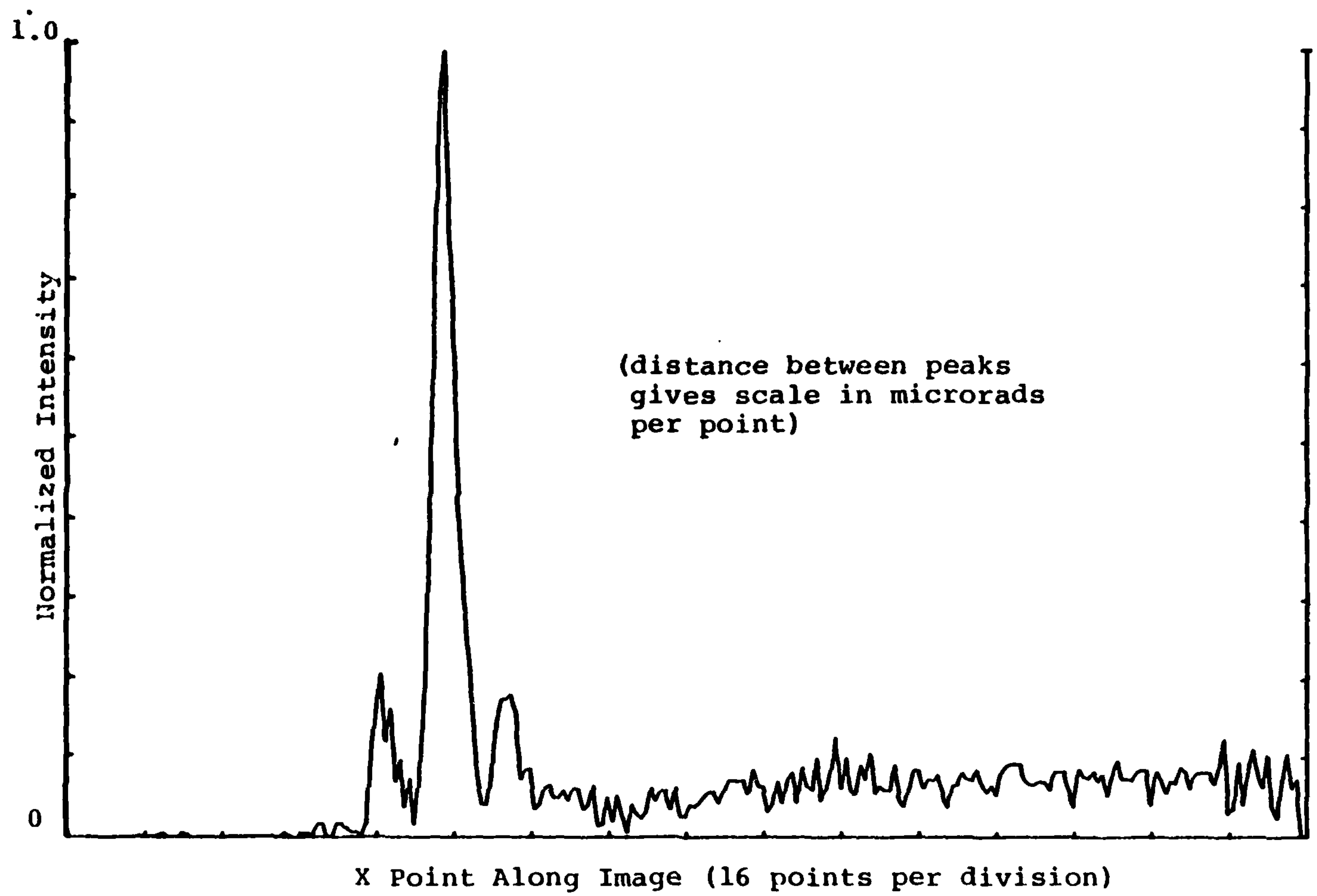

FIGURE 22. SCALE IMAGE EXAMPLE

TABLE 1

INPUT/OUTPUT PARAMETERS

ARRAY VARIABLE	VALUES	USE
O(1)	0	Same as 1 except program after one time through ends, not allowing for computations with new range, C_n^2, ext. coeff.
	1	Source pattern input is point spread function.
	2	Source pattern input is line spread function.
	3	Source pattern input is modulation transfer function of laser only.
	4	Source pattern input is modulation transfer function of source and optics.
	5	Source pattern is to be calculated with amplitude and sigma of intensity distribution as factors.
O(2)	0	Optics diffraction input as PSF.
	1	Optics diffraction input as LSF.
	2	Optics diffraction pattern to be calculated as PSF.
O(3)	0	No plot of source line spread function is required.
	>0	Plots source line spread function (available only if O(1)=0,1 or 5).
O(4)	0	No plot of source MTF required.
	>0	Plots source MTF (available only if O(1) does not equal 3 or 4).
O(5)	0	No plot of product of source and optics MTF required.
	>0	Plots product of source and optics MTF's (available only if O(1) does not equal 4).

TABLE 1 (CONT'D)

ARRAY VARIABLE	VALUE	USE
0(6)	0	No plot of optics diffraction PSF required.
	>0	Plots optics diffraction PSF (available only if 0(1) does not equal 4 and 0(2)=2).
0(7)	0	No plot of optics LSF required.
	>0	Plots optics LSF (available only if 0(1) does not equal 4 and 0(2) does not equal 1).
0(8)	0	No plot of optics MTF required.
	>0	Plots optics MTF (available only if 0(1) does not equal 4).
0(9)	0	No plot of atmosphere MTF required.
	>0	Plots atmosphere MTF.
0(10)	0	No plot of system MTF.
	>0	Plots total system MTF.
0(11)	0	No plot of LSF of predicted target spot.
	>0	Plots LSF of target spot.
0(12)	0	No plot of target PSF required.
	>0	Plots target PSF.
0(13)	0	No plot of the fraction of power inside circle required.
	>0	Plots fraction of power inside a circle of radius r.
0(14)	0	No plot of calculated source PSF required.
	any other value	Plots calculated source PSF.

TABLE 1 (CONT'D)

ARRAY VARIABLE	VALUES	USE
0(15)	0	Plots measured LSF of target spot.
	>0	Used as indicators of output branching only, entry value not significant.
0(16)	1	Inputs source with diffraction grating from DS-30 for scale computations from output. No output plotted.
	2	Same as 1 except plots the above.
	any other value	Does not do above input

ANNEX C

PROGRAM LISTING

```
0: dim B$[23],C$[5],D$[7],I$[272],O$[5],P$[5],Q$[5],X$[40],R[
512],I[512]
1: dim O[16],A$[13],Y$[40],Z$[40]
2: files O,T,E,R,G,V,W,C,I,F
3: fmt 1,z,c
4: time 150
5: cfg 3;cfg 2;cfg 1
6: rread 7,1;sprt 7,R[*];rread 7,1
7: buf "DATA",I$,3
8: rread 4,1;sprt 4,R[*]
9: beep
10: "INPUT I/O CONTROL O[I]":
11: for I=1 to 16;ent O[I];next I
12: if O[1]=2;gsb "SOURCE"
13: clr 704
14: if O[16]=1 or O[16]=2;gsb "SCALE"
15: beep;dsp "ENSURE VIDEODISC ON THEN PRESS CONTINUE"
16: stp
17: beep;ent "# OF FRAMES TO AVERAGE",H
18: ent "WINDOW WIDTH ,FIRST PIXEL",r9,"LAST PIXEL",r10
19: H+1→H
20: 0→r3
21: for O=1 to H by 4
22: for I=2 to 9
23: char(47)&char(55)&char(64)&char(80)&char(96)→C$
24: if I=2;"930 020"→D$
25: if I=3;"020"→D$
26: if I=4;"930 120"→D$
27: if I=5;"020"→D$
28: if I=6;"930 220"→D$
29: if I=7;"020"→D$
30: if I=8;"930 320"→D$
31: if I=9;"020"→D$
32: if len(D$)<4;gto 38
33: char(1)&"2"&char(2)&C$&char(15)&D$[5,7]→B$
34: cli 7
35: wait 100
36: wrt 704,B$
37: cli 7
38: char(46)→C$[1,1]
39: char(1)&"2 "&char(2)&C$&char(15)&D$[1,3]→A$
40: cli 7
41: wait 100
42: wrt 704,A$
43: cli 7
44: if I#3 or O>1;gto 47
```

```
45: dsp "BACKGROUND RECORDED"
46: wait 500;dsp "CONTINUE WHEN NXT FRAME READY";stp
47: if D$#"020" or I=3 or I=9 and O<5;gto 49
48: dsp "CONT. WHEN NXT FRAME SELECTED";stp
49: next I
50: if H-O+1<4;gto 53
51: for X=1 to 4
52: gto 54
53: for X=1 to H-O+1
54: "!"&"O"&"A"&"P"&char(96)→P$
55: if X#1;gto 57
56: 1→J;0→Y;gto 62
57: if X#2;gto 59
58: sfg 3;256→J;0→Y;gto 62
59: if X#3;gto 61
60: 1→J;255→Y;gto 62
61: 256→J;255→Y
62: for L=1 to 256
63: dsp L
64: 0→D;""→O$;Y+1→Y
65: Y*512+J→S
66: for I=2 to 6
67: int(S/16)→T
68: T→U
69: S-T*16+I*16→T
70: U→S
71: O$&char(T)→O$
72: next I
73: char(1)&"="&char(34)&char(2)&O$&char(3)&P$&char(15)→B$
74: fmt 1,z,c
75: cli 7
76: wrt 704.1,B$
77: buf "DATA"
78: tfr 704,"DATA",256
79: rds("DATA")→E;if E=-1;jmp 0
80: for I=r9 to r10
81: num(I$[I,I])→Z
82: D+Z→D
83: next I
84: D/(r10-r9)→R[L]
85: next L
86: if flg3=0;gto 91
87: "TAKE DIFFERENCE OF IMAGE AND BACKGROUND":
88: rread 3,1;sread 3,I[*];for I=1 to 256
89: abs(R[I]-I[I])→R[I];next I
90: gto 93
91: rread 3,1;sprt 3,R[*]
92: gto 113
93: 0→G;0→F
94: for I=30 to 226
```

```
95: R[I]+G→G;next I
96: for I=30 to 226;R[I]+F→F
97: if F>=G/2;gto 99
98: next I
99: I→A
100: if O=1 and X=2;1→r1
101: r1-A→r2
102: for J=1 to 256+r2
103: R[J-r2]→R[J]
104: if J<256+r2;next J
105: for K=256+r2 to 256
106: 0→R[K]
107: next K
108: sprt 7,r2
109: rread 4,1;sread 4,I[*]
110: for I=1 to 256
111: I[I]+R[I]→R[I];next I
112: rread 4,1;sprt 4,R[*]
113: next X;next O
114: "TAKE AVERAGE OF ALL FRAMES":
115: for I=1 to 256;R[I]/(H-1)→R[I];R[I]→R[513-I];next I
116: rread 4,1;sprt 4,R[*]
117: if O[15]<1;gsb "OUTPUT"
118: beep
119: ent "RANGE",R,"SQCN",Q,"EXT COEF",E,"WAVLNGTH",W,"OBJ LE
NS",O
120: ent "OBS/OBJ",B,"SCALE",r11;sprt 6,R,Q,E,W,O,B,r11
121: "SYSTEM DATA-W=WAVLNTH IN METERS O=DIA OF OBJ LENS IN ME
TERS":
122: "B=DIA OF OBSUR/DIA OF OBJ LENS r11=SCALE OF DATA IN MIC
RORADS/PT":
123: "R=DISTANCE TO TGT IN METERS":
124: "Q=SQUARE OF ATMOS TURB INDEX IN METERS^-2/3":
125: "E=EXTINCTION COEFF (1/METERS)":
126: if O[1]#5;gto 140
127: beep
128: ent "AMPLITUDE",A,"SIGMA",C
129: for I=1 to 256
130: r11*(I-1)→F
131: F^2/(2*C^2)→G
132: if G>13;gto 134
133: A*exp(-G)→I[I];I→K;gto 135
134: 0→I[I]
135: next I
136: rread 5,1;sprt 5,I[*];rread 5,1;sread 5,R[*]
137: 1→O[15];if O[14]#0;gsb "OUTPUT"
138: gto 149
139: "SOURCE PATTERN DATA INPUT":
140: rread 2,1;sread 2,R[*]
141: for I=1 to 256
142: I→K
```

```
143: if R[I]<-500;gto 146
144: next I
145: gto 149
146: for J=I to 256
147: 0→R[J]
148: next J
149: O[1]→I
150: "BRANCH ACCORDING TO TYPE OF SOURCE PATTERN DATA":
151: gto 152;if I>1;gto 155;if I>2;gto 161;if I>3;gto 206;if
I>4;gto 152
152: "CONVERTS SOURCE POINT SPREAD FUNCTION TO LINE SPREAD FC
N":
153: gsb "LSF"
154: 2→O[15];if O[3]>0;gsb "OUTPUT"
155: "CALCULATION OF FOURIER TRANSFORM OF LINE SPREAD FCN OF
SOURCE":
156: for I=1 to 256
157: R[I]→R[513-I];next I
158: gsb "FXFORM"
159: rread 5,1;sprt 5,R[*]
160: 3→O[15];if O[4]>0;gsb "OUTPUT"
161: if O[2]=2;gto 173
162: "OPTICS DIFFRACTION INPUT IF NOT CALCULATED":
163: rread 8,1;sread 8,R[*]
164: for I=1 to 256
165: I→K
166: if R[I]<-500;gto 169
167: next I
168: gto 182
169: for J=I to 256
170: 0→R[J];next J
171: gto 182
172: "CALCULATION OF DIFFRACTION LIMIT POINT SPREAD FCN":
173: B^2→D;1-D→H;3.14159e-6*r11*O/W→Z
174: for I=1 to 256
175: Z*(I-1)→Y;if Y>30;gto 178
176: ('AIRY'(Y)-D*'AIRY'(Y*B))^2/H^2→R[I]
177: I→K;gto 179
178: 0→R[I]
179: next I
180: rread 8,1;sprt 8,R[*]
181: 4→O[15];if O[6]>0;gsb "OUTPUT"
182: if O[2]=1;gto 188
183: "CONVERTS OPTICS POINT SPREAD FCN TO LINE SPREAD FCN":
184: rread 8,1;sread 8,R[*]
185: gsb "LSF"
186: rread 8,1;sprt 8,R[*]
187: 5→O[15];if O[7]>0;gsb "OUTPUT"
188: "TAKES FOURIER TRANSFORM TO GET OPTICS MODULATION TRANSF
ER FCN":
```

```
189: rread 8,1;sread 8,R[*]
190: for I=1 to 256
191: R[I]→R[513-I];next I
192: gsb "FXFORM"
193: for I=1 to 256
194: if R[1]=0;gto 196
195: R[I]/R[1]→R[I];next I
196: rread 8,1;sprt 8,R[*]
197: 6→O[15];if O[8]>0;gsb "OUTPUT"
198: "CALCULATION OF THE PRODUCT OF TWO FOURIER TRANSFORMS":
199: rread 8,1;sread 8,R[*];rread 5,1;sread 5,I[*]
200: for I=1 to 256
201: R[I]*I[I]→R[I];next I
202: rread 10,1;sprt 10,R[*]
203: 7→O[15];if O[5]>0;gsb "OUTPUT"
204: exp(-E*R)→X
205: "ATMOS MODULATION TRANSFER FCN CALC-SHORT TERM":
206: Q*R*21.6→A;W^(-.3333333)→B;0→V;0→L;X→R[1]
207: for I=2 to 256
208: gto 214;if L<=0;gto 215;if L=0;gto 209
209: 976.5625*(I-1)/r11→T;A*T^1.666667*(B-(T/O)^.3333333)→G
210: sfg 14
211: if G>13;1→L
212: if G-V<0;-1→L
213: G→V;X*exp(-G)→R[I];I→K;cfg 14;gto 218
214: 0→R[I];gto 218
215: R[K]*cos((I-K)*3.14159/K)^2→R[I]
216: gto 217;if I-3*K/2<0;gto 218
217: I→K;1→L
218: next I
219: rread 9,1;sprt 9,R[*]
220: 8→O[15];if O[9]>0;gsb "OUTPUT"
221: "TRANSFER FCN OF SOURCE*OPTICS*ATMOSPHERE":
222: rread 10,1;sread 10,R[*];rread 9,1;sread 9,I[*]
223: for I=1 to 256
224: I[I]*R[I]→I[I]
225: I[I]→R[I]
226: R[I]→R[513-I]
227: next I
228: 9→O[15];if O[10]>0;gsb "OUTPUT"
229: "INVERSE FOURIER TRANSFORM GIVES TARGET LINE SPREAD FCN"
:
230: sfg 1;gsb "FXFORM";I→K;cfg 1
231: 10→O[15];if O[11]>0;gsb "OUTPUT"
232: "CONVERTS LINE SPREAD FCN TO POINT SPREAD FCN BY ABEL TR
ANSFORM":
233: gsb "ABEL"
234: 11→O[15];if O[12]>0;gsb "OUTPUT"
235: "CALCULATES THE FRACTION OF THE POWER INSIDE A CIRCLE OF
 RADIUS R":
```

```
236: gsb "B"
237: 12→O[15];if O[13]>0;gsb "OUTPUT"
238: "READ IN NEW RANGE AND Q IF RANGE NEG. READ IN ALL NEW D
ATA":
239: "STARTING WITH I/O CONTROL CARD,IF RANGE=0 PROGRAM STOPS
":
240: "IF RANGE IS POS. THE PROGRAM CARRIES OUT CALC'S WITH TH
E NEW":
241: "RANGE AND Q":
242: if O[1]=0;gto 245
243: ent "RANGE",R,"SQCN",Q,"EXT COEF",E
244: gto 206;if R<=0;gto 119;if R=0;gto 245
245: end
246: "ABEL":R[1]→N;1.4R[1]-1.8R[2]+.4R[3]→R[1];for I=2 to K
247: R[I]→M
248: .4N+.2M-.6R[I+1]→R[I];M→N;next I
249: for I=1 to K
250: R[I]/(2*√((I+.1)^2-II))→R[I]
251: for J=I+1 to K
252: R[I]+R[J]/√((J+.1)^2-II)→R[I]
253: next J;R[I]/π→R[I];dsp I;next I
254: ret
255: "LSF":for I=1 to K
256: 1→J;dsp I;R[I]→Z
257: √(I*I+J*J)→Y
258: 2*((1-frc(Y))*R[int(Y)]+frc(Y)*R[int(Y)+1])+Z→Z
259: J+1→J;if Y<K;jmp -2
260: Z→R[I];next I;ret
261: "B":.25πR[1]→R[1]
262: for I=2 to K
263: 2πIR[I]+R[I-1]→R[I]
264: next I
265: if R[K]=0;ret
266: for I=1 to K;R[I]/R[K]→R[I];next I;ret
267: "AIRY":if pl<0;beep;dsp "ERROR pl<0";stp
268: if pl=0;1→r4;ret r4
269: 0→r5;if pl>15;jmp 2
270: 20+10pl-pl^(2/3)→r6;jmp 2
271: 90+pl/2→r6
272: if pl<5;6+pl→r12;jmp 2
273: 1.4*pl+60/pl→r12
274: max(int(r12),int(3+pl/4))→r12
275: for M=r12 to r6 by 3;1e-28→r8;0→r13→r14
276: sfg 10;if M/2=int(M/2);cfg 10
277: for J=1 to M-2;2*(M-J)*r8/pl-r13→r15;r8→r13
278: r15→r8;if M-J-2=0;r15→r4
279: cmf 10;r14+2*r8*flg10→r14;next J
280: 2*r8/pl-r13→r15
281: r14+r15→r14;r4/r14→r4
282: if abs(r4-r5)-abs(r4*1e-6)<=0;2*r4/pl→r4;ret r4
283: r4→r5;next M
```

```
284: beep;dsp "Accuracy not obtained";wait 1000;ret r4
285: "FXFORM":rad;9→N;ina I
286: π/2^(N-1)→T
287: for M=1 to N;2^(N-M)→r16
288: for J=0 to 2^(M-1)-1;cll 'BI'(J,P,N-1)
289: cos(PT)→C;sin(PT)(1-2flg1)→P
290: for I=2r16J+1 to 2r16J+r16
291: R[I]→r0;R[I+r16]→r1
292: I[I]→r2;I[I+r16]→r3
293: r0+r1*C+r3*P→R[I];r2+r3*C-r1*P→I[I]
294: r0-r1*C-r3*P→R[I+r16]
295: r2-r3*C+r1*P→I[I+r16]
296: next I;next J;next M
297: for I=0 to 2^N-1;cll 'BI'(I,J,N);if I-J>0;jmp 8
298: if I=J;jmp 5
299: R[I+1]/√(2^N)→P
300: I[I+1]/√(2^N)→Z
301: R[J+1]→R[I+1];I[J+1]→I[I+1]
302: P→R[J+1];Z→I[J+1]
303: R[I+1]/√(2^N)→R[I+1]
304: I[I+1]/√(2^N)→I[I+1]
305: next I;deg;ret
306: "BI":0→p2;p1→p4
307: for Z=1 to p3
308: p4/2→p4;2p2→p2
309: if frc(p4)#0;p2+1→p2
310: int(p4)→p4;next Z;ret
311: "SOURCE":sfg 2
312: beep;dsp "DISPLAY SOURCE IMAGE ON VID DISC";wait 3000
313: cll 'SCALE'
314: rread 2,1;sprt 2,R[*]
315: cfg 2;ret
316: "SCALE":if flg2;gto 318
317: beep;dsp "DISPLAY SCALE IMAGE ON VID DISC";wait 3000
318: dsp "THEN PRESS CONTINUE";stp
319: ent "WINDOW WIDTH, FIRST PIXEL",r9,"LAST PIXEL",r10
320: for I=2 to 3
321: char(47)&char(55)&char(64)&char(80)&char(96)→C$
322: if I=2;"930 020"→D$
323: if I=3;"020"→D$
324: if len(D$)<4;jmp 5
325: char(1)&"2"&char(2)&C$&char(15)&D$[5,7]→B$
326: cli 7
327: wait 100
328: wrt 704,B$
329: char(46)→C$[1,1]
330: char(1)&"2 "&char(2)&C$&char(15)&D$[1,3]→A$
331: cli 7
332: wait 100
333: wrt 704,A$
```

```
334: next I
335: "!"&"0"&"A"&"P"&char(96)→P$
336: 1→J;0→Y
337: for L=1 to 256
338: dsp L
339: 0→D;""→O$;Y+1→Y
340: Y*512+J→S
341: for I=2 to 6
342: int(S/16)→T;T→U;S-T*16+I*16→T
343: U→S;O$&char(T)→O$
344: next I
345: char(L)&"="&char(34)&char(2)&O$&char(3)&P$&char(15)→B$
346: cli 7
347: wrt 704.1,B$
348: buf "DATA"
349: tfr 704,"DATA",256
350: rds("DATA")→E;if E=-1;jmp 0
351: for I=r9 to r10
352: num(I$[I,I])→Z;D+Z→D
353: next I
354: D/(r10-r9)→R[L]
355: next L
356: if flg2;gto 358
357: if O[16]=2;gsb "OUTPUT"
358: ret
359: "OUTPUT":
360: beep
361: dsp "STOP IF PLOTTER NOT READY THEN CONTINUE";wait 5000
362: sfg 14;'MIN'(256)/'MAX'(256)→r17;cfg 14
363: if r17<-.1;scl -.75,1.05,-30,264;plt 1,0,1;jmp 2
364: scl -.15,1.05,-30,264;plt 1,0,1
365: for I=10 to 0 by -1
366: plt I/10,0,2;plt I/10,256/150,2
367: plt I/10,0,2;next I
368: for I=0 to 16
369: plt 0,16I,2;plt 1/150,16I,2
370: plt 0,16I,2
371: next I
372: pen;csiz .9,1,1.4
373: fxd 0;for I=16 to 0 by -1;plt -.1,16I-1,1
374: lbl 16(16-I);next I
375: fxd 1;for I=0 to 10;plt I/10-.06,-5,1
376: lbl I/10;next I
377: if O[15]=10 or O[15]=0;"TARGET LINE NUMBER"→Y$
378: if O[15]=1 or O[15]=11;"POSITION VALUE"→Y$
379: if O[15]=10;"PREDICTED NORMALIZED LINE VALUE"→X$
380: if O[15]=0;"MEASURED NORMALIZED LINE VALUE"→X$
381: plt -.12,51,1;csiz 1.2,1,1.4,90;lbl Y$
382: plt 0,-13,1;csiz 1.2,1,1.4;lbl X$
383: csiz .5,1,.7,0
```

```
384: 'MAX'(256)→r7
385: if r7=0;1→r7
386: for J=1 to 256
387: plt R[J]/r7,257-J;next J
388: pen;ret
389: "MIN":R[1]→p2
390: for I=2 to p1;if R[I]>p2;jmp 2
391: R[I]→p2
392: next I;ret p2
393: "MAX":R[1]→p2
394: for I=2 to p1;if R[I]<p2;jmp 2
395: R[I]→p2
396: next I;ret p2
*21194
```

LIST OF REFERENCES

1. U.S. Army Yuma Proving Ground 416, _Instrumentation Development Final Report of Image Analyzer Systems_, by Scott, E.A., November 1980.

2. Fried, D.L., "Statistics of a Geometric Representation of a Wavefront Distortion," _Journal of the Optical Society of America_, v. 56, 1966.

3. Tatarski, V.I., _Wave Propogation in a Turbulent Medium_, McGraw-Hill, 1961.

4. Ochs, G.R., Bergmann, R.R., and Snyder, J.R., "Laser Beam Scintillation Over Horizontal Paths From 5.5 to 145 Kilometers," _Journal of the Optical Society of America_, v. 59, 1969.

5. Naval Postgraduate School Report 61-78-003, _Optical Resolution in the Turbulent Atmosphere of the Marine Boundary Layer_, by E.C. Crittenden, Jr. and others, February 1978.

6. Griem, H., _Plasma Spectroscopy_, McGraw-Hill, 1964.

7. Crittenden, E.C., Milne, E.A., Rodeback, G.W., _Systems For Analysis of Laser Designator Spot Wander and Profile_, Naval Postgraduate School, Informal Report, 12 February 1982.

APPENDIX D

COMPARATIVE MEASUREMENTS AND VIDEO DATA ANALYSIS USING A DIGITAL STORAGE OSCILLOSCOPE

AD-A144 858 OPTICAL TURBULENCE MEASUREMENT - INVESTIGATIONS FOR ANALYSIS OF LASER DES..(U) ARMY ELECTRONIC PROVING GROUND FORT HUACHUCA AZ E C CRITTENDEN ET AL. MAY 83 2/3

UNCLASSIFIED USAEPG-FR-1226 F/G 20/6 NL

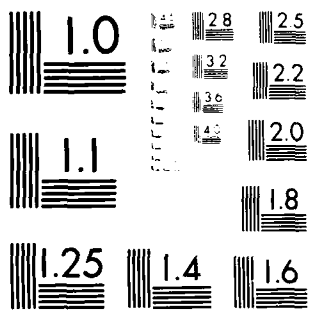

MICROCOPY RESOLUTION TEST CHART

NATIONAL BUREAU [illegible]

ABSTRACT

This appendix presents a comparative analysis of common path (laboratory environment) measurements of C_n2 for a telescope/slit scan system and a video system. Included is a computer program in algorithmic language that uses a digital storage oscilloscope to analyze the video data. Both HeNe and GaAs lasers are used in the comparative measurements.

(THIS PAGE IS INTENTIONALLY BLANK)

(THIS PAGE IS INTENTIONALLY BLANK)

TABLE OF CONTENTS

LIST OF FIGURES

(THIS PAGE IS INTENTIONALLY BLANK)

I. INTRODUCTION

A. BACKGROUND

The increasing use of lasers and laser technology for military applications has brought about a need for analysis of the laser beam in its environment, the turbulent atmosphere. A project at Naval Postgraduate School dealing with this subject is continuing and is the main topic of this thesis.

The patterns produced by lasers on targets have inherent problems that include broadening, beam wander and intensity fluctuations brought about by turbulence in the atmosphere. These effects of atmospheric turbulence on laser propagation have been well determined [Ref. 1]. In terms of the Fried model, [Ref. 2], C_n^2, the refractive index structure constant, has been determined to adequately express the Modulation Transfer Function (MTF), or the Mutual Coherence Function (MCF) for the atmosphere.

A system has been developed that provides a measurement of C_n^2 for atmospheric turbulence along the optical path through which a laser is propagated. The system employs a vidicon and telescope as the detector and a distant laser as the source. This system duplicates the slit scanning system presently in use at Naval Postgraduate School [Ref. 2]. Tests using the vidicon equipment have been previously completed with values for C_n^2 on the order of 10^{-15} $m^{-2/3}$ being obtained [Ref. 3]. Measurements have been made using the same experimental set-up, except that the Tektronix 468 Digital Storage Oscilloscope are used for digitization instead of the Quantex DS-30 Digital Video Processor. These measurements have demonstrated values of C_n^2 of comparable accuracy.

B. PROBLEM

By using the digital storage capability of the Tektronix 468, the previously recorded laser signal is used as an input and is evaluated by modifying the program developed by Crager [Ref. 4]. A brief overview of the procedure is described below. Detailed explantions of the experiment and computer program are contained in Chapters III and IV, respectively.

The approach taken is basically the same as that of Crager, but because of the unavailability of a disk ROM it is necessary to store both raw and processed data on magnetic tape. The data are loaded and recorded as necessary by the HP 9825. The basic assumption permitting analysis is that the horizontal TV scan line through the laser spot is considered to accurately mirror a point spread function of the image. Final analysis using the 468 oscilloscope has shown this to be a valid hypothesis. The digitized data from the 468 oscilloscope agree with the previously measured data which use many pixels of television data digitized by the DS-30 to express the point spread function.

The sequence of analysis is that a video tape recording is made of the TV image of the propagated laser beam. The output of the video recorder is sent to the Tektronix 468, where the derived TV scan line is digitized, averaged, and stored. The HP 9825 records the digitized data and produces a line spread function (LSF), by integrating the point spread function,

$$LSF(x) = \int_{y(min)}^{y(max)} PSF(r)\ dy \qquad (1.1)$$

where

$r = \sqrt{(x^2+y^2)}$

and computes the Fourier transform of the LSF. The diffraction limited Fourier transform of the optics is now computed if the MTF of the optics has not been previously measured experimentally. Next, the program finds the MTF of the atmosphere by dividing the Fourier transform of the LSF by the Fourier transform of the optics. Finally, by curve fitting, the program computes a single value for C_n^2.

The program now predicts the size of a laser spot on a target using the calculated value of C_n^2. This value of C_n^2 is used to calculate an MTF of the atmosphere which is then multiplied by the Fourier transform of a source, and the Fourier transform of the optics. The program then calculates the inverse Fourier transform of the products of the above and uses the Abel transform to give the angular point spread intensity distribution. From this data, the fraction of energy as a function of the total energy within a given radius R is calculated.

II. THEORETICAL CONSIDERATIONS

The theory of laser beam propagation through a turbulent medium has been explained by Crittenden, and others, and is re-emphasized here for continuity purposes [Ref. 2]. Since the effects of turbulence on laser weapons is of major concern, measurement and prediction capability for these effects on laser beams is entirely relevant.

Due to the existence of reciprocity, these ideas apply to either laser designators or imagers [Ref. 5]. In the study of the theoretical model by Fried, the effects of atmospheric turbulence are investigated [Ref. 6]. This model uses the idea of a long term optical transfer function (OTF) when considering atmospheric turbulence. The long term OTF results from simply taking an image of sufficiently long term which sees effectively all possible turbulence configurations.

When observing the effect of diffraction as the result of the finite aperture of a point source, it can be seen that the resulting image is not uniform. Considering the point spread function to have the same shape in the image plane regardless of its position, the image function is the result of the convolution of the source function and the optics diffraction function. The convolution theorem, as described in Fourier transform theory, yields

$$i(v(x),v(y)) = H(v(x),v(y)) * o(v(x),v(y)) * M(v(x),v(y)) \qquad (2.1)$$

where

$i(v(x),v(y))$ = Fourier transform of the image function

$H(v(x),v(y))$ = Fourier transform of the optics diffraction function

$o(v(x),v(y))$ = Fourier transform of the object function

$M(v(x),(v(y))$ = Modulation Transfer Function of the atmosphere

v = spatial frequency

A point source such as a laser can be analyzed in two dimensions using a point spread function. Through Fourier transform theory, the image point spread function is transformed into a two dimensional OTF of the optical signal. This problem may be simplified by scanning the image point spread function using a vidicon or slit-scanning system. In applying the convolution theorem, the Fourier transform of the image point spread function is multiplied with the Fourier transform of the optical system resulting in the Fourier transform of the overall system. The Abel transform described by Griem, is applied to this result to re-transform the one-dimensional image LSF into a two dimensional image PSF [Ref. 7].

As demonstrated by Crittenden, and others, a numerical value for C_n^2 may be obtained by curve fitting using the following:

$$M = \exp(-21.49*C_n^2*Z*f^{5/3}*\lambda^{-1/3}) \qquad (2.2)$$

where

M = MTF of the atmosphere

Z = Range in meters

f = F*v = Angular spatial frequency in cycles/radian

F = focal length of the optical system

v = linear spatial frequency in cycles/meter

λ = wavelength in meters

C_n^2 is obtained by a linear regression of

$$\ln(M) = -21.49*C_n^2*Z*f^{5/3}*\lambda^{-1/3} \qquad (2.3)$$

where C_n^2 is the only parameter.

III. EXPERIMENTAL PROCEDURE

The experiment is performed using two different laser sources, helium-neon (He-Ne) and gallium-arsenide (Ga-As). Figure 3.1 shows a block diagram of the experimental set-up used for both lasers.

The measurement of C_n^2 along the optical path is made by using a vidicon and telescope at the far end of the corridor in the basement of Spanagel Hall. Atmospheric turbulence is produced by nine overhead hot air ventilators. The optical equipment similar to that described in reference 3, consists of a 6 inch diameter Cassegrain telescope with a 90 inch focal length [Ref. 3].

Using neutral density absorption filters to attenuate the intensity of the laser beam, the telescope is illuminated at its input aperture. The light image from the telescope is split by a beam splitter with one beam sent to the vidicon and the other to a slit scanner for comparison of the two systems. The light is then transformed to an analog signal and recorded on a Panasonic (NV-9240) video tape recorder for processing. The data from the slit scanning system are recorded on a precision instrument tape recorder for analysis. After recording the video signal,

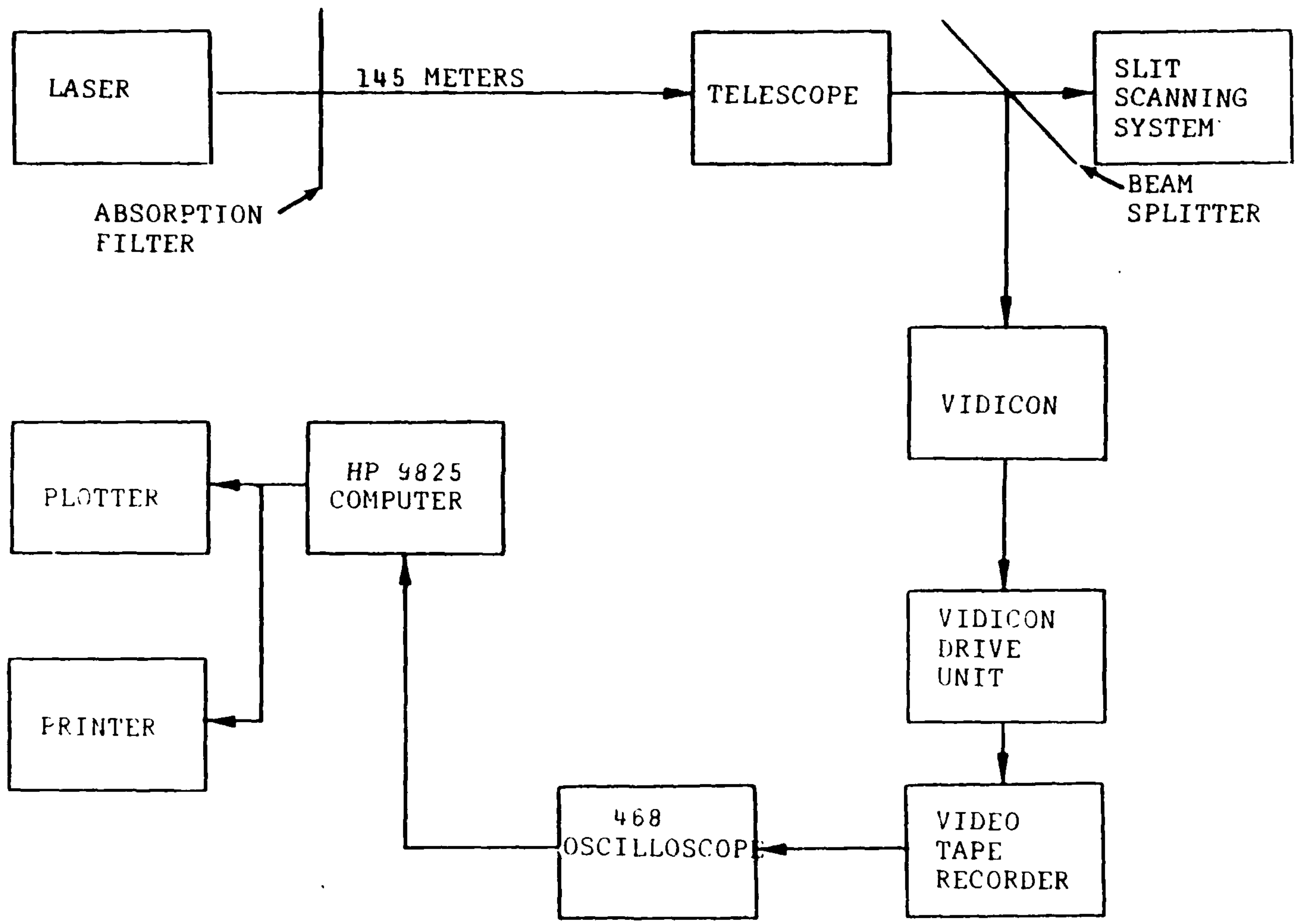

Fig. 3.1 Laser Experimental Set-Up

analysis is accomplished using a Tektronix 468 Digital Storage Oscilloscope and a Hewlett Packard 9825 Computing System. The linearity of the Panasonic tape recorder was demonstrated in Crager's thesis. This is also confirmed by observing the images as real time and recorded displays [Ref. 3].

The 468 oscilloscope is set-up in the following manner. An input signal to channel A is located on the scope using the non-storage mode. The signal is then displayed using the A INTENSITY switch of the horizontal display. This intensified zone is used to position the B sweep (delayed) to the desired location within the A sweep interval to obtain an expanded view of a waveform for examination. Once the waveform is centered on the scope, the horizontal display is switched to B DLY'D. This is done to facilitate the digital storage circuitry time base by using the setting of the B TIME/DIV switch.

The waveform is expanded in time by decreasing the A TIME/DIV switch setting and moving the waveform back to the middle of the scope using the delay time position control dial. When a representative waveform is obtained, the B TIME/DIV switch is then used in conjunction with the delay time position control dial to expand the time scale until the single central maximum of the waveform is centered and one horizontal sweep is displayed.

Once this waveform is satisfactorily obtained, the AVG storage mode is selected. The 468 will average the input signal for a selected number of sweeps and display the accumulated waveform. All data for this thesis use 32 sweeps for each average. The 468 is now ready to transfer data when interrogated by the HP 9825.

The computer is the controller for all interfacing operations with only a minimal amount of operator interaction. The operator interface is mainly to ensure that the equipment is properly set up and to select if data are to be plotted. Digitization of the analog signal is accomplished by the Tektronix 468. Processed waveform data are transferred from the microprocessor memory to the Storage Display RAM [Ref. 8].

The controlling program of the HP 9825 interrogates the 468 via the IEEE 488 interface bus. The 468 receives the data request from the controller and sends the waveform message, both preamble and data. The waveform message is stored in the calculator memory for further processing.

When the message is completed, the 468 concludes with an end of instruction terminator and the controller takes control of the bus again.

Data processing of the digitized signal begins with the data being stored on magnetic tape for further use by the computer. The data are stored, processed and plotted by the main program. Subroutines are called as necessary for their specific uses. The two signal waveforms are recorded and processed. First, the signal from a laser beam incident at the aperture of the telescope is recorded. Figures 3.2 and 3.3 show these recorded data which are referred to as the source data. Second, for calibration, the signal from a laser beam with a diffraction grating in place at the aperture of the telescope is recorded. The entire system is calibrated by using a grating that consists of closely spaced vertical bars in front of the telescope. This produces a diffraction pattern in the image plane and allows for the calculation of the scale factor. These recorded data are referred to as the scale data and are plotted in Figures 3.4 and 3.5.

During the recording process, the signal from the laser beam is recorded on video tape while the signal is observed

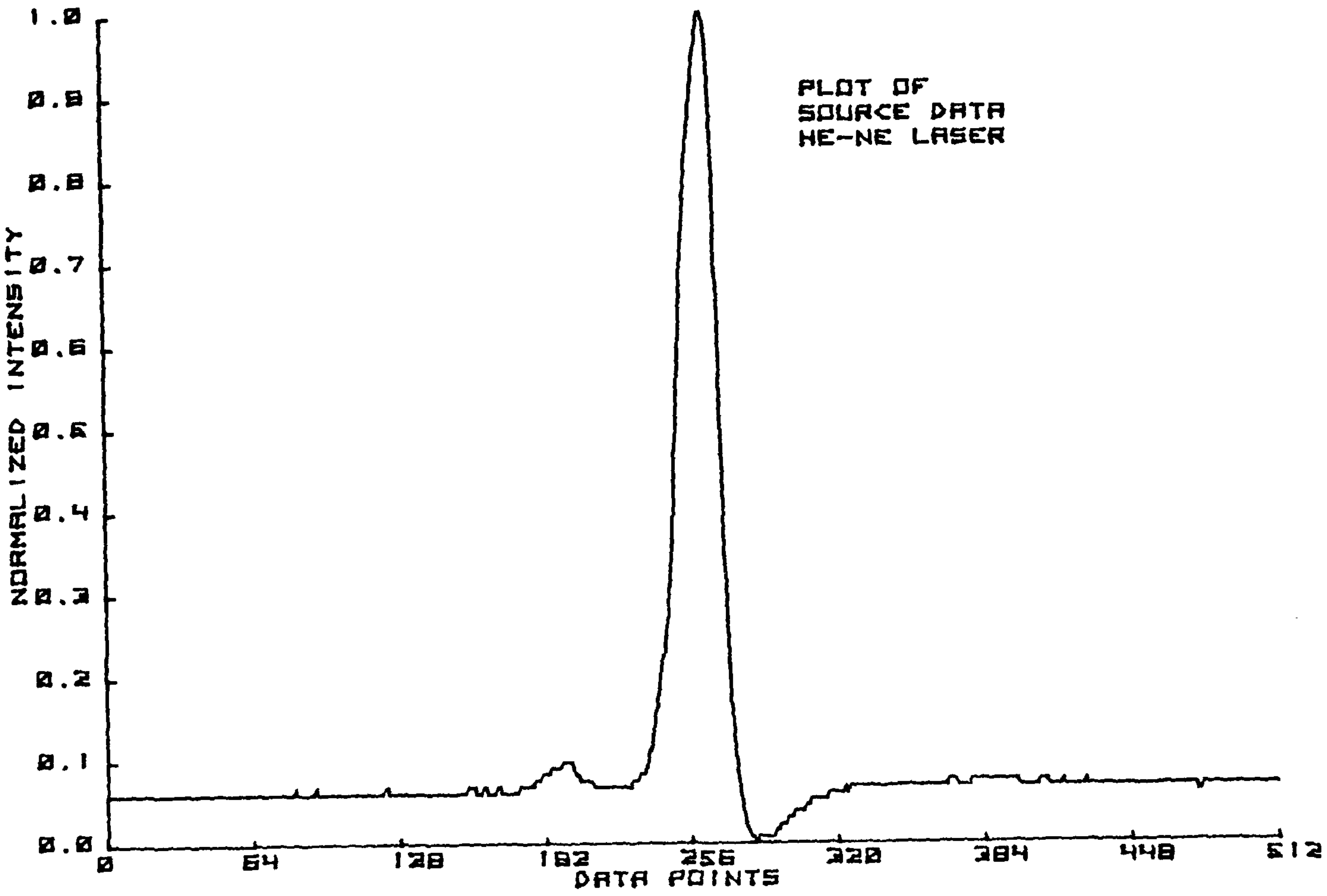

Fig. 3.2 Plot of Source Data for He-Ne Laser

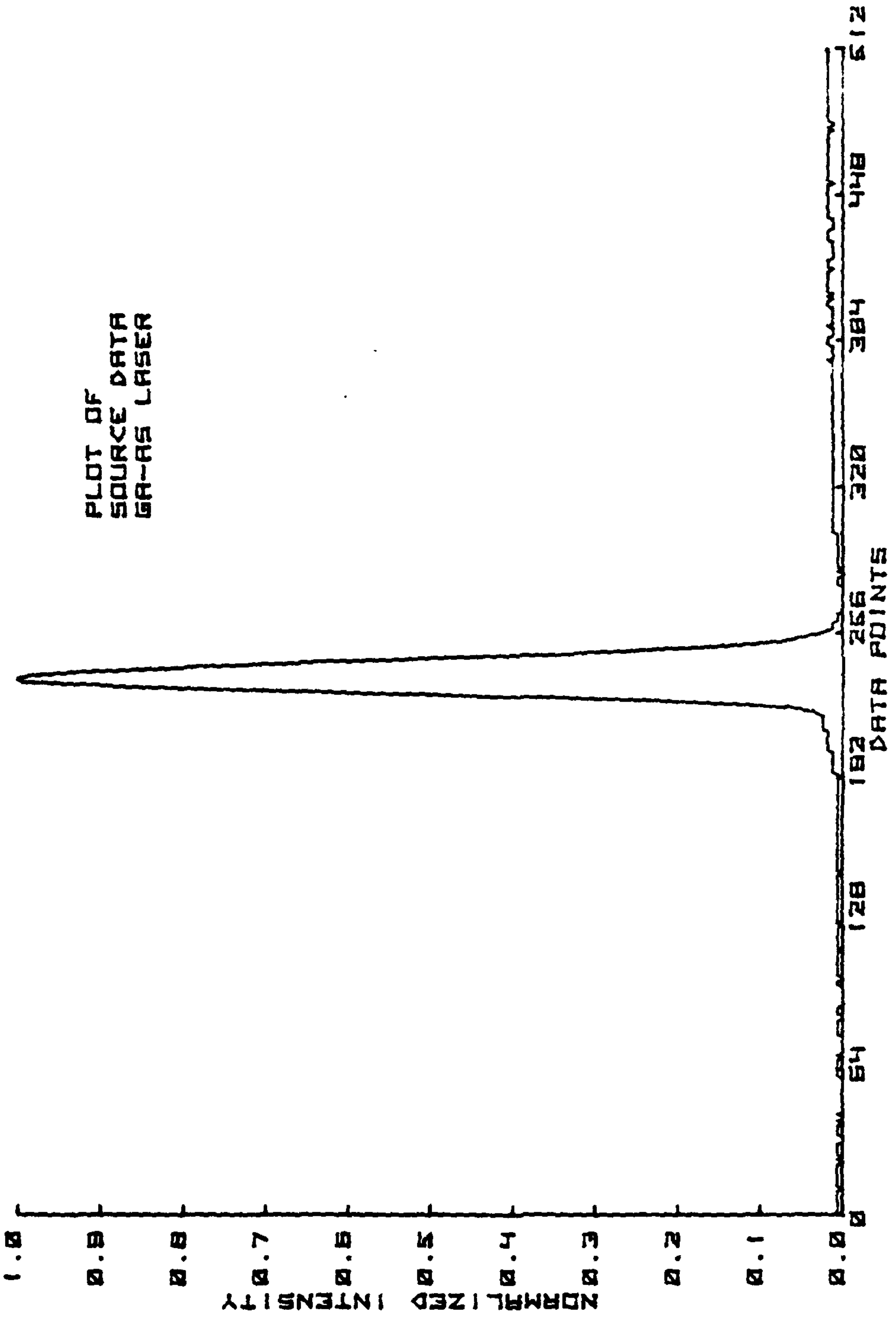

Fig. 3.3 Plot of Source Data for Ga-As Laser

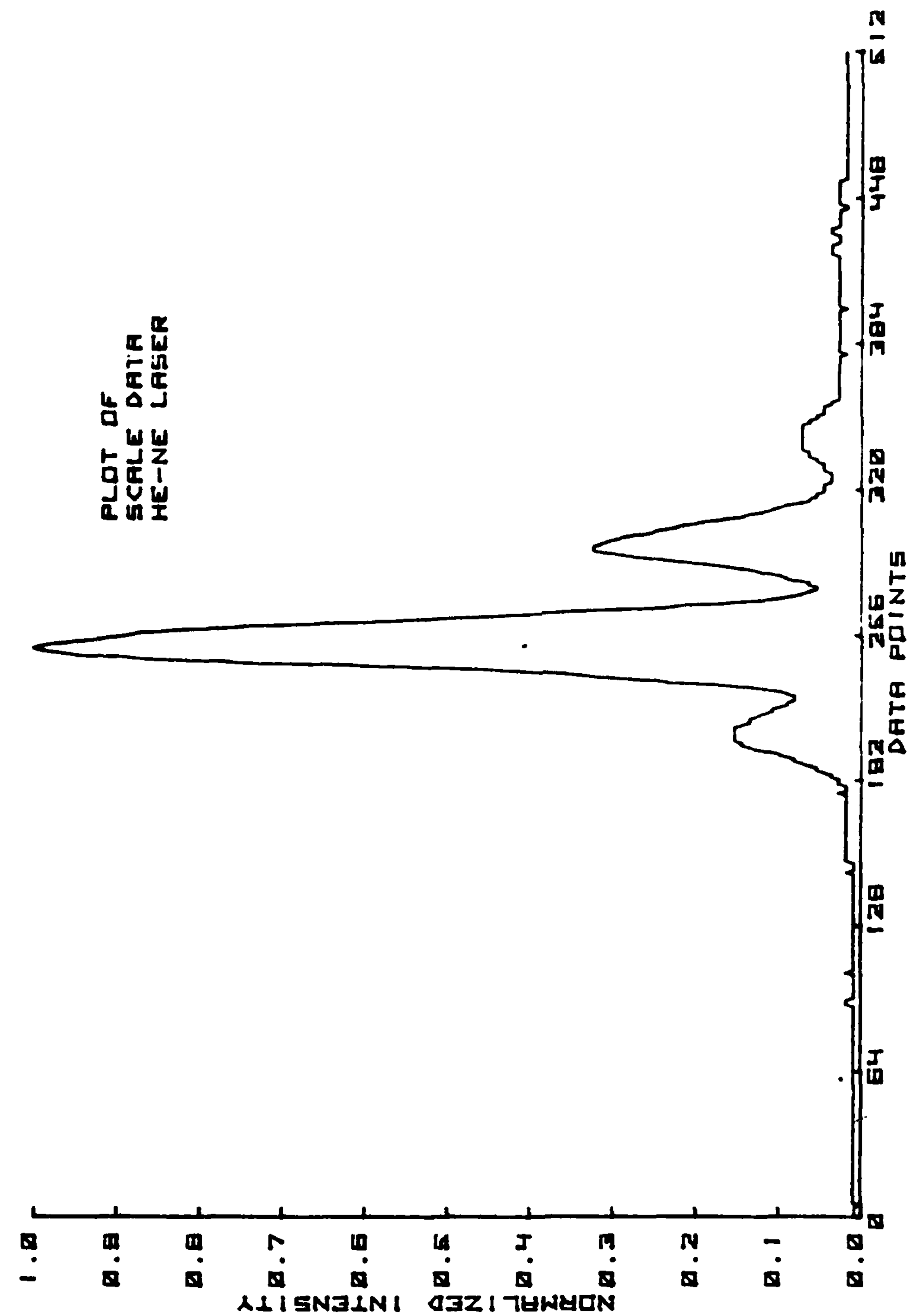

Fig. 3.4 Plot of Scale Data for He-Ne Laser

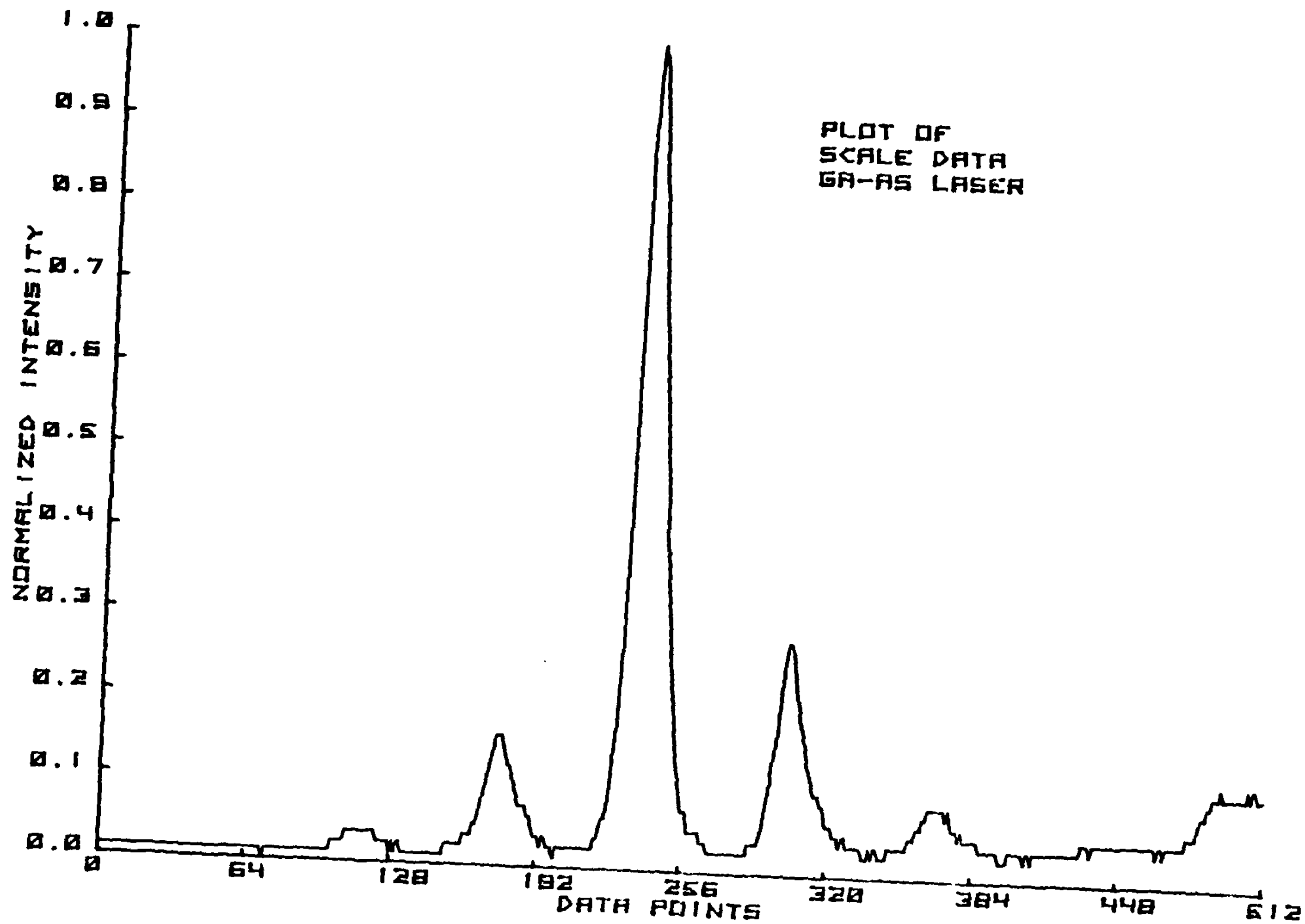

Fig. 3.5 Plot of Scale Data for Ga-As Laser

on the 468 oscilloscope. This procedure is important in data taking since laser alignment and telescope focusing are often very sensitive to minor movements of either. Upon completion of recording the data on video tape, the experiment is concerned with the compilation and analysis of data. The first item to be determined is the scale factor. Once the scale factor has been determined, it will remain constant throughout the calculations, unless the telescope focal length is changed.

The scale factor is calculated in the following manner. The number of points between the peaks in the plot of the scale data (diffraction grating in place in front of the telescope aperture) is measured. When the distance between peaks, the spacing between the bars in the grating, and the wavelength of the laser are known, the scale factor can be calculated from the relation

$$\sin(\text{theta}) = \lambda/d \tag{3.1}$$

$$\sin(\text{theta}) \sim \text{theta} \tag{3.2}$$

(small angle approximation)

$$sf = (\text{theta})/ndp \tag{3.3}$$

$$sf = \lambda/(d*ndp) \tag{3.4}$$

where

sf = scale factor in radians per point

λ = wavelength in meters

d = spacing between lines on grating in meters

ndp = number of points between central maximum and first order diffraction peak

This standardizes the data for the abscissa of the plots in radians per point.

The program now takes the transferred data and computes a point spread function as shown in Figures 3.6 and 3.7. Figures 3.8 and 3.9 represent the point spread function after integration using equation (1.1) to obtain a line spread function. Next, the Fourier transform of the line spread function is calculated. These curves are plotted in Figures 3.10 and 3.11.

The diffraction of the optics is computed and plotted as shown in Figures 3.12 and 3.13. Following the same method as before, the line spread function of the optics function is calculated and plotted in Figures 3.14 and 3.15. The program now takes the Fourier transform of the optics function LSF. These data are plotted in Figures 3.16 and

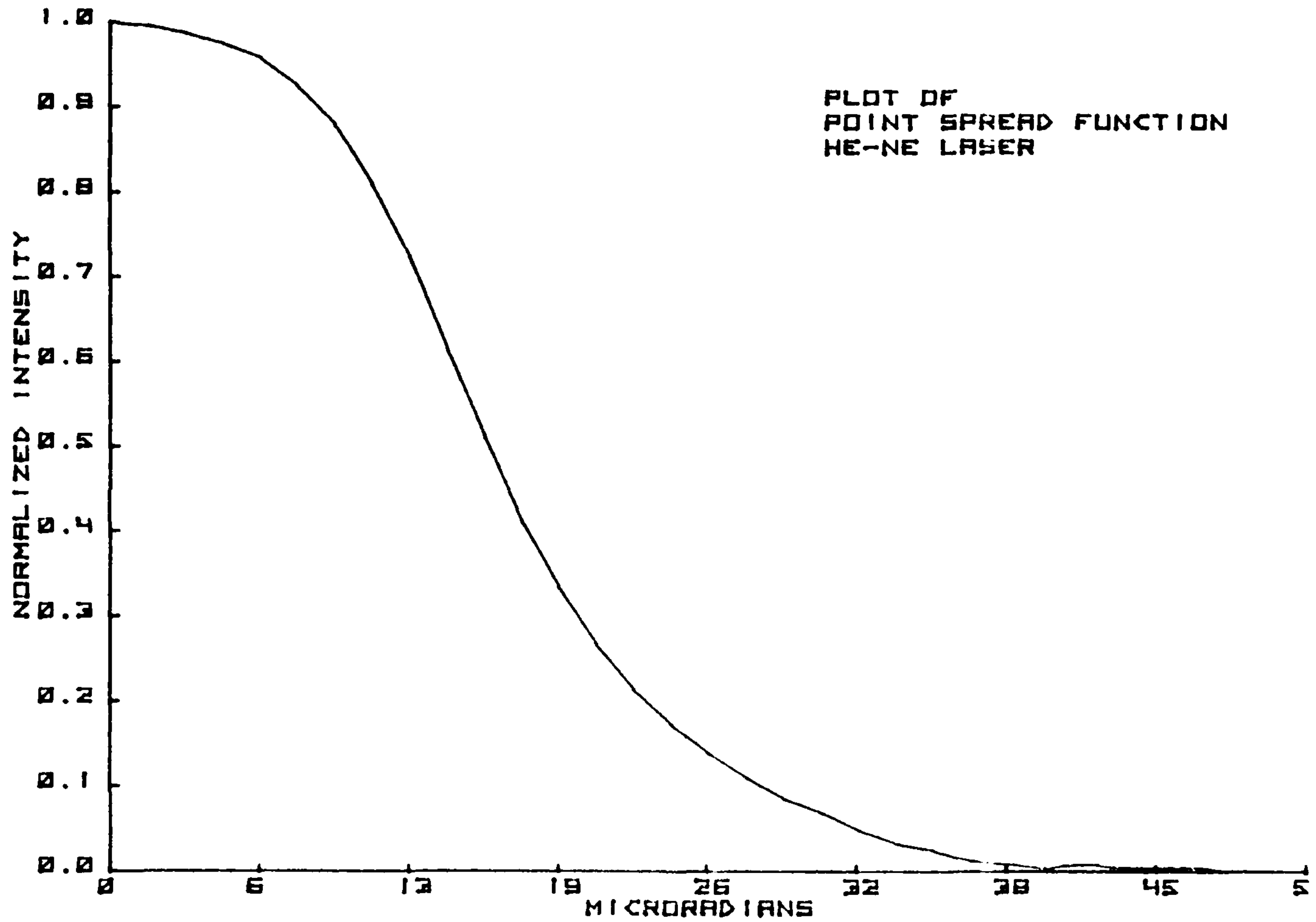

Fig. 3.6 Plot of Point Spread Function for He-Ne Laser

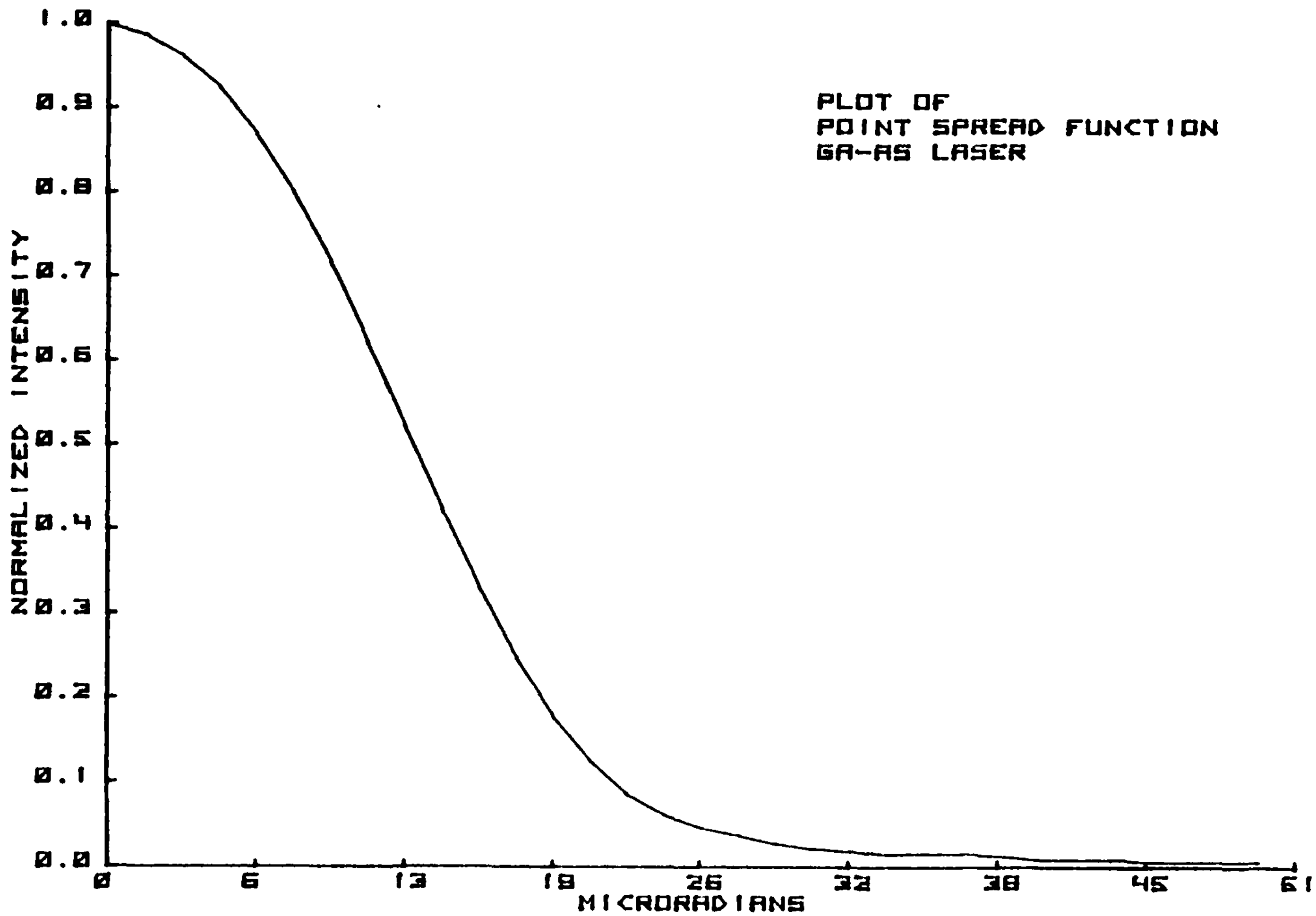

Fig. 3.7 Plot of Point Spread Function for Ga-As Laser

3.17. The Fourier transforms of the system and optics are divided point by point to yield the MTF of the atmosphere, as shown in Figures 3.18 and 3.19. The MTF of the atmosphere will be used to calculate the long-term value of C_n^2.

C_n^2 is calculated by linear regression of ln(MTF) versus $f^{5/3}$. The slope of the regression is proportional to C_n^2. Two simultaneous equations are solved using Cramer's rule and the matrix ROM of the HP 9825. The equations used are

$$a*X + b*I = Y \tag{3.5}$$

$$a*X^2 + b*X = Y*X \tag{3.6}$$

where

a = slope of the curve

b = intercept

X = summation of (I*sf)**(5/3)

X**2 = summation of (I*sf)**(10/3)

I = point number (total number = 256)

Y = summation of natural logarithm of MTF

Y*X = summation of products of two values

C_n^2 is obtained from the above information using equation (2.3). This will yield

$$C_n^2 = a/(-21.49*Z*f**(5/3)* \;**(-1/3)) \qquad (3.7)$$

The program now goes to the prediction phase after calculating C_n^2 for the atmosphere. If a Gaussian distribution for an input source and a value of the standard deviation are assumed or known, the resulting source function can be calculated. A plot of the computed source is shown in Figure 3.20. It can be seen from this plot that the half-width at half-maximum is approximately 4 microradians. As before, the line spread function of the computed source is calculated and plotted. This is shown in Figure 3.21. The Fourier transform of this data is calculated and plotted in Figure 3.22.

The program now multiplies the Fourier transform of the computed source with the transform of the system (including the atmosphere) and plots the result in Figures 3.23 and 3.24. Plots of the inverse Fourier transform are shown in Figures 3.25 and 3.25. Next, the Abel transform is computed and plotted in Figures 3.27 and 3.28. The Abel transform, as described in Chapter II, transforms a one-dimensional line spread function into a two-dimensional point spread function. Finally, the fraction of power inside a circle of radius R is calculated and plotted as shown in Figures 3.29 and 3.30. This is the fraction of power that one would expect to be incident on a target using the measured value of atmospheric turbulence as an input parameter. A detailed analysis of the computer program is the subject of the next chapter.

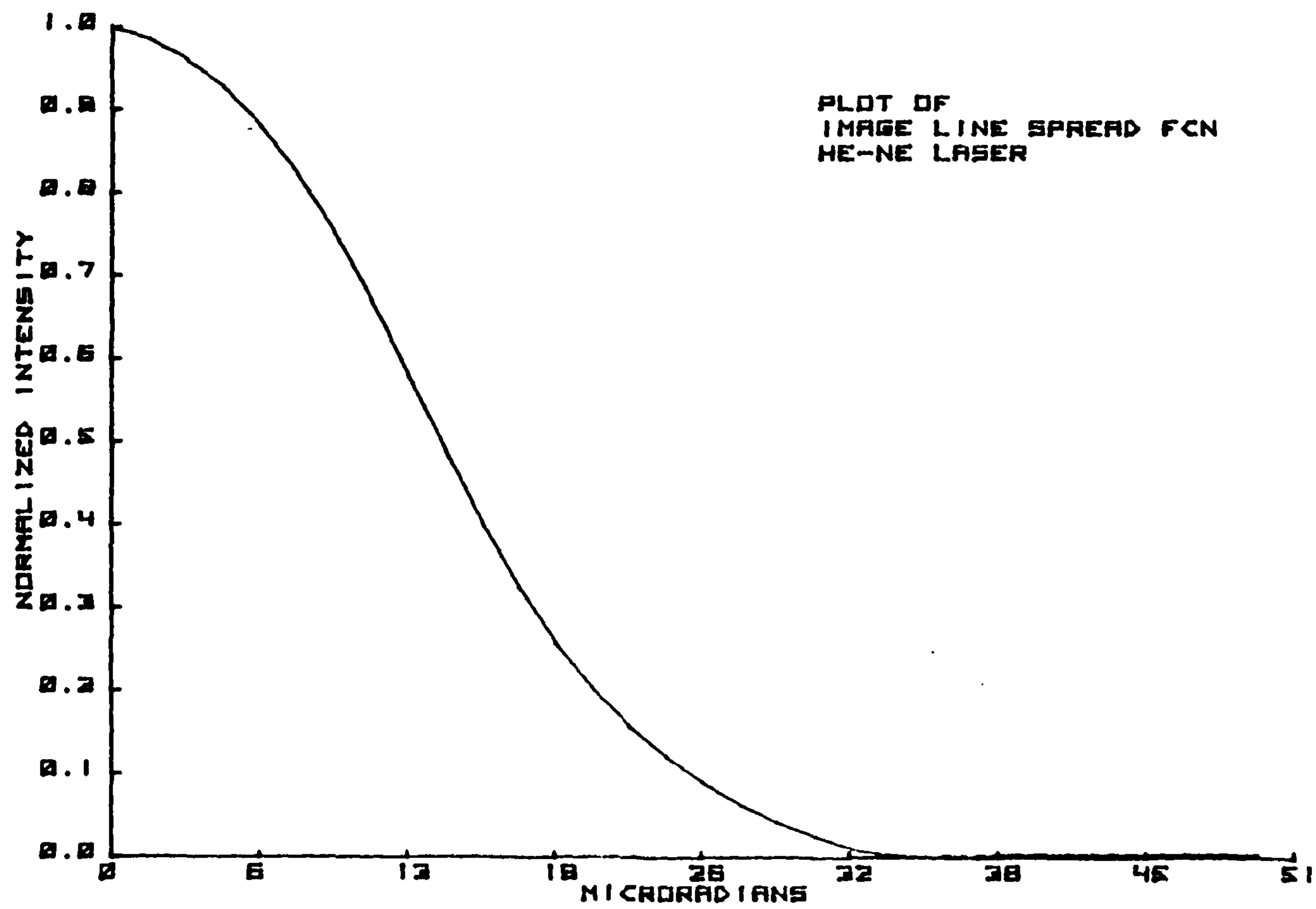

Fig. 3.8 Plot of Line Spread Function for He-Ne Laser

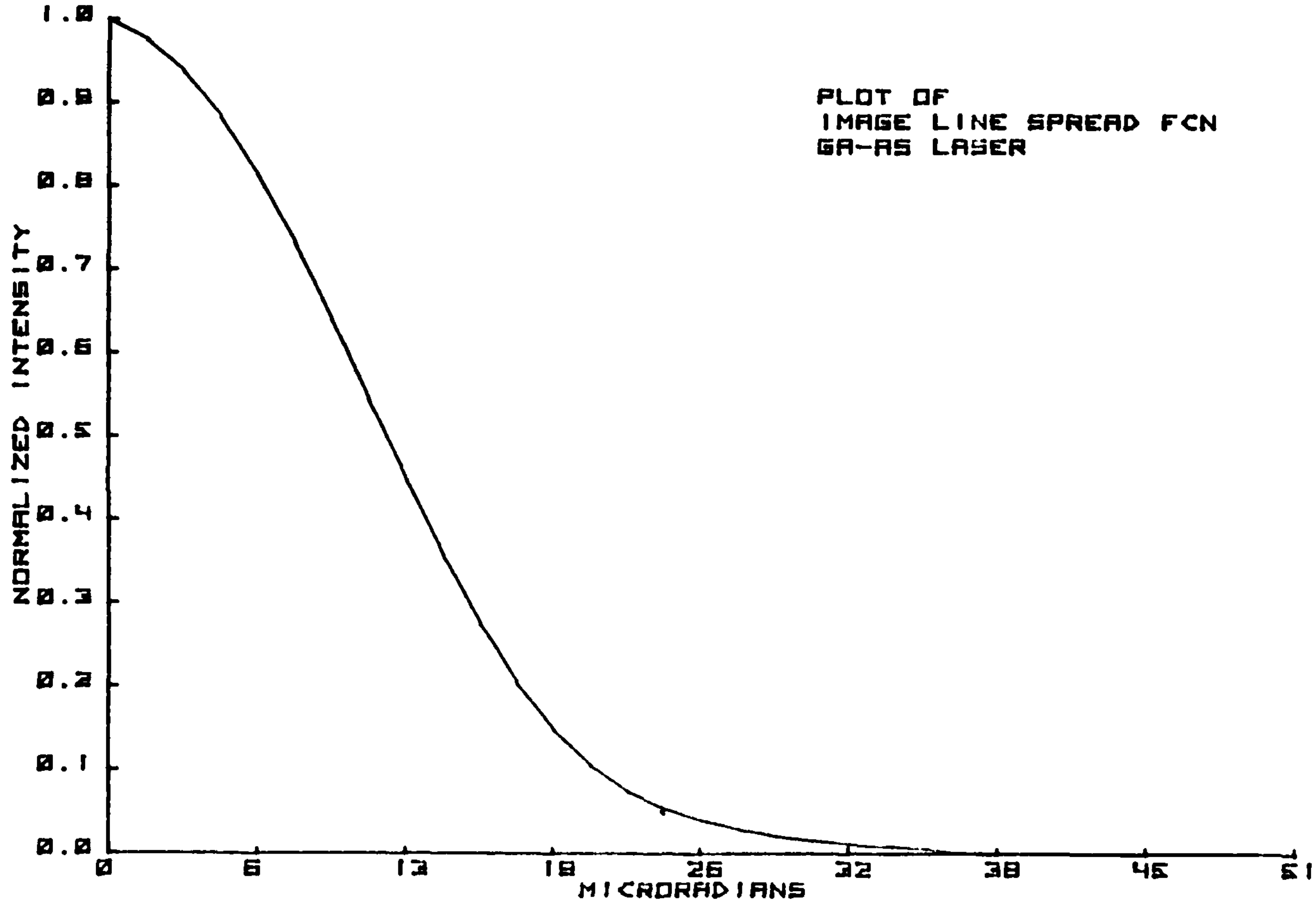

Fig. 3.9 Plot of Line Spread Function for Ga-As Laser

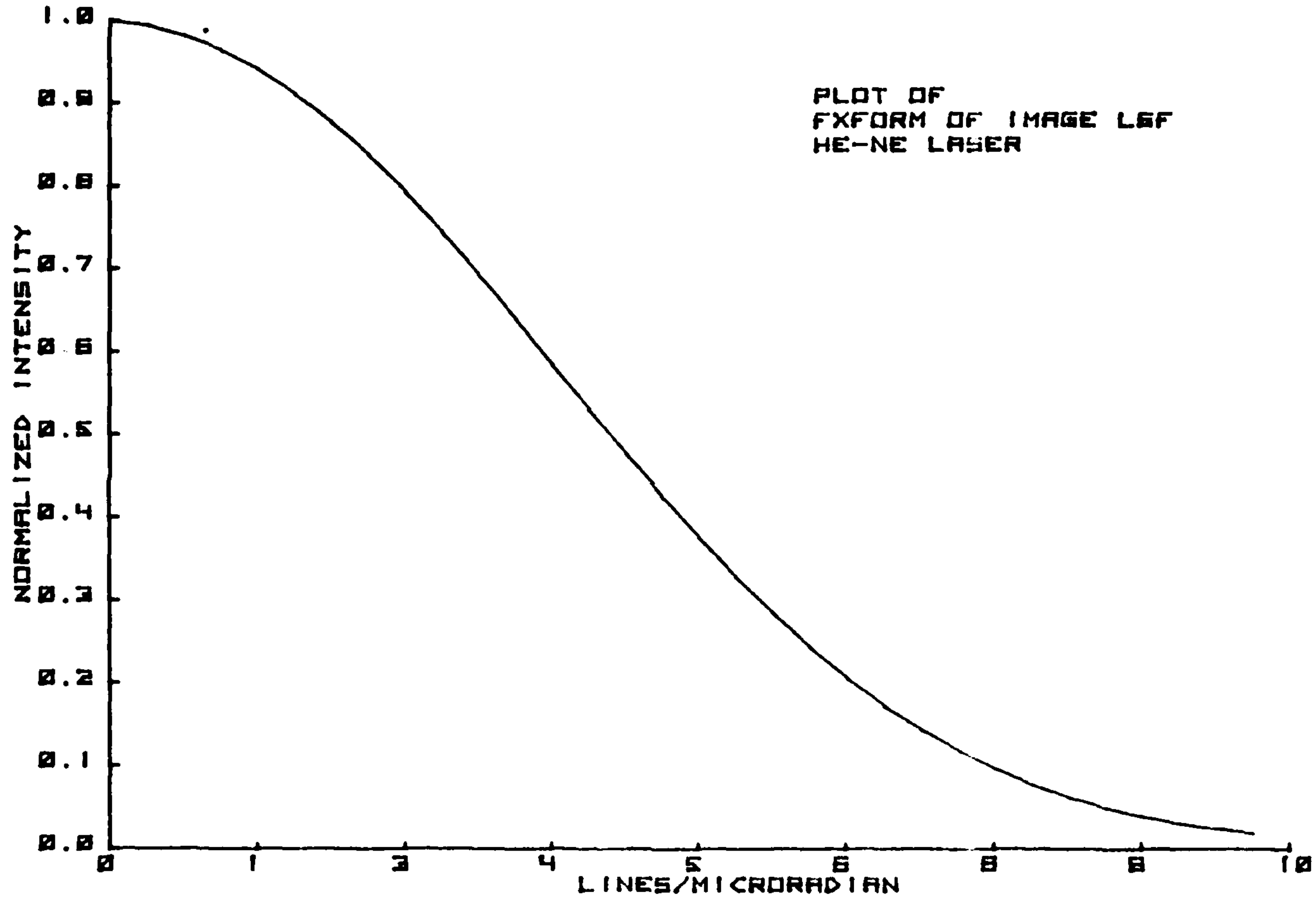

Fig. 3.10 Plot of Fourier Transform of LSF for He-Ne Laser

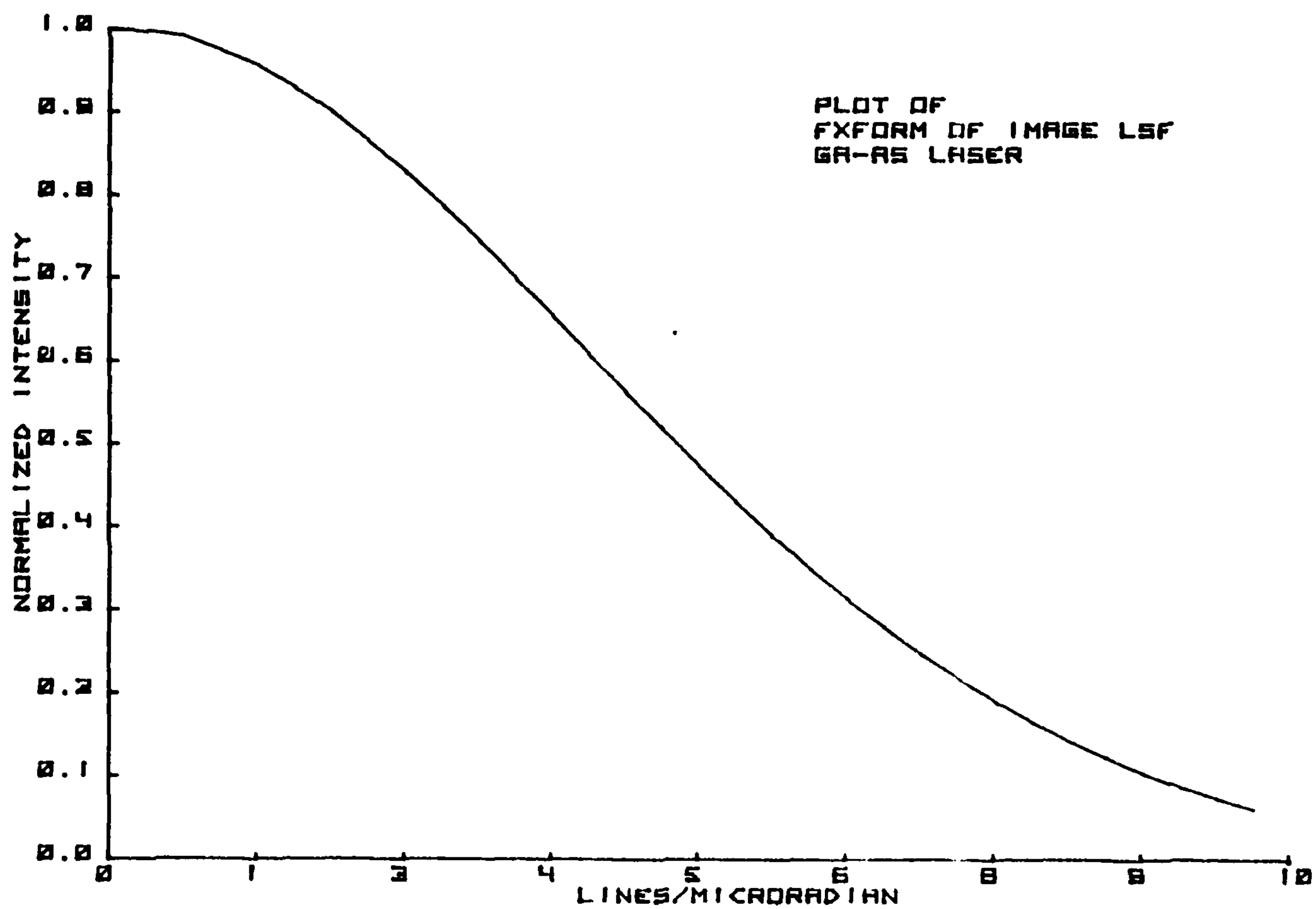

Fig. 3.11 Plot of Fourier Transform of LSF for Ga-As Laser

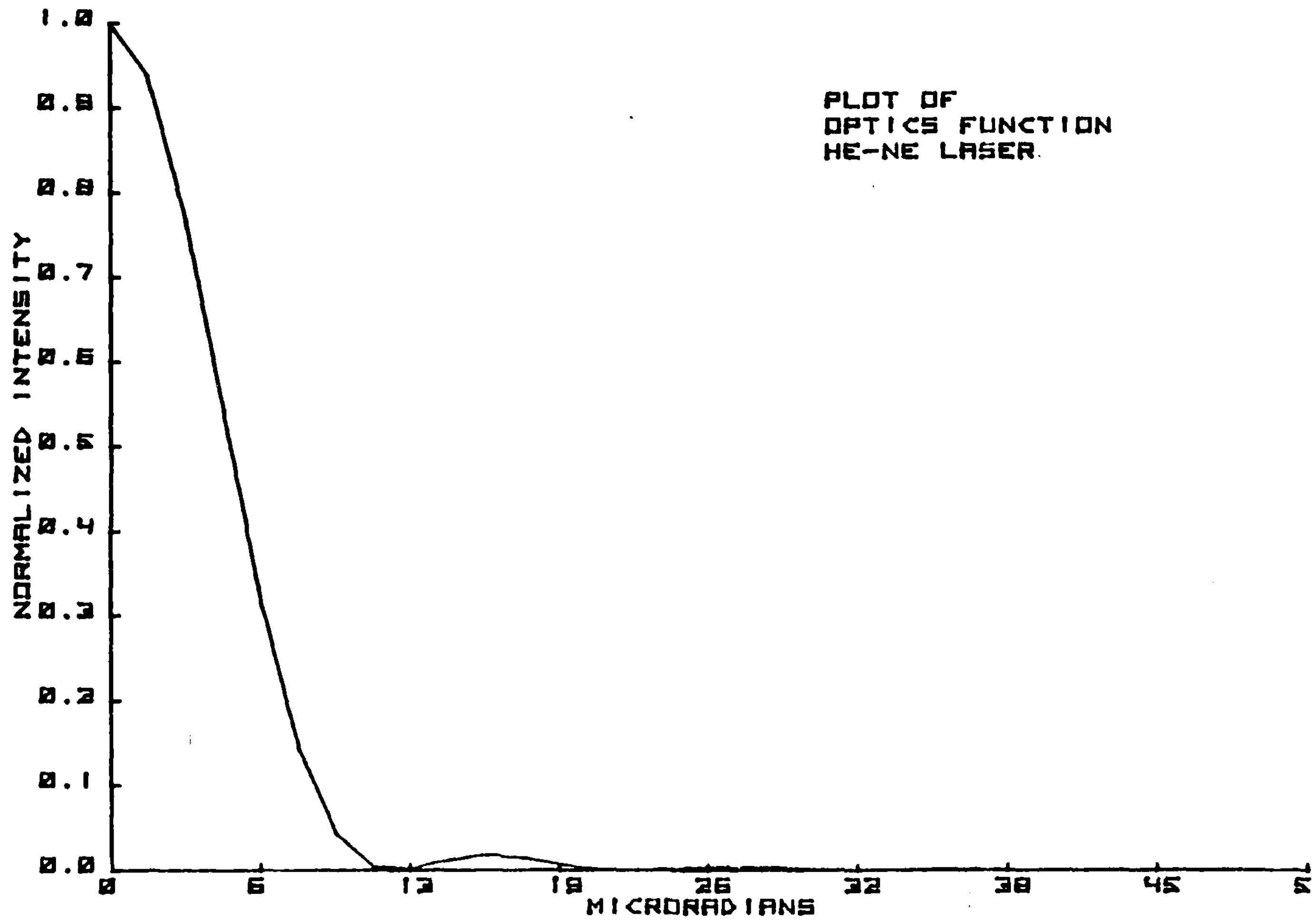

Fig. 3.12 Plot of Optics Diffraction for He-Ne Laser

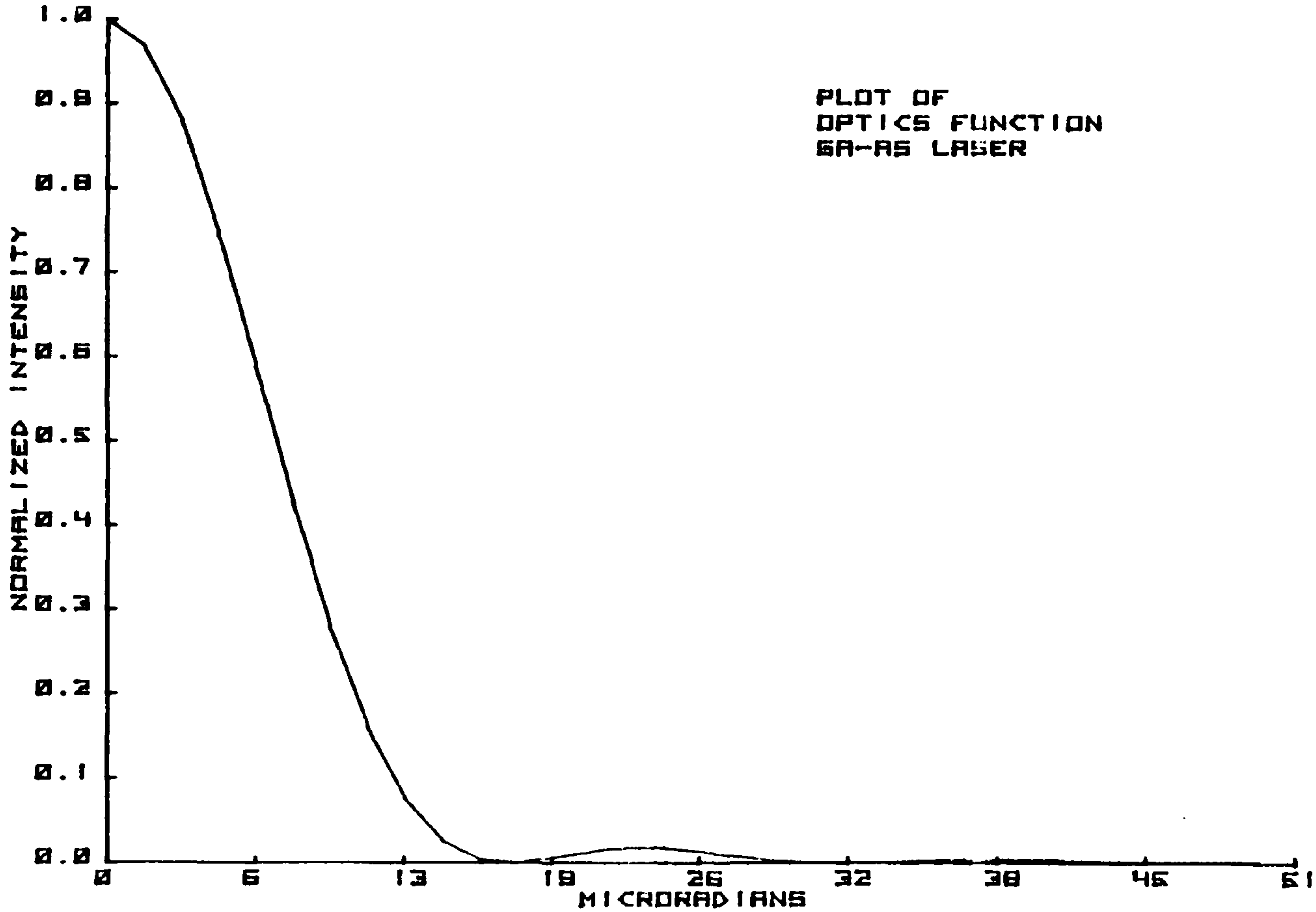

Fig. 3.13 Plot of Optics Diffraction for Ga-As Laser

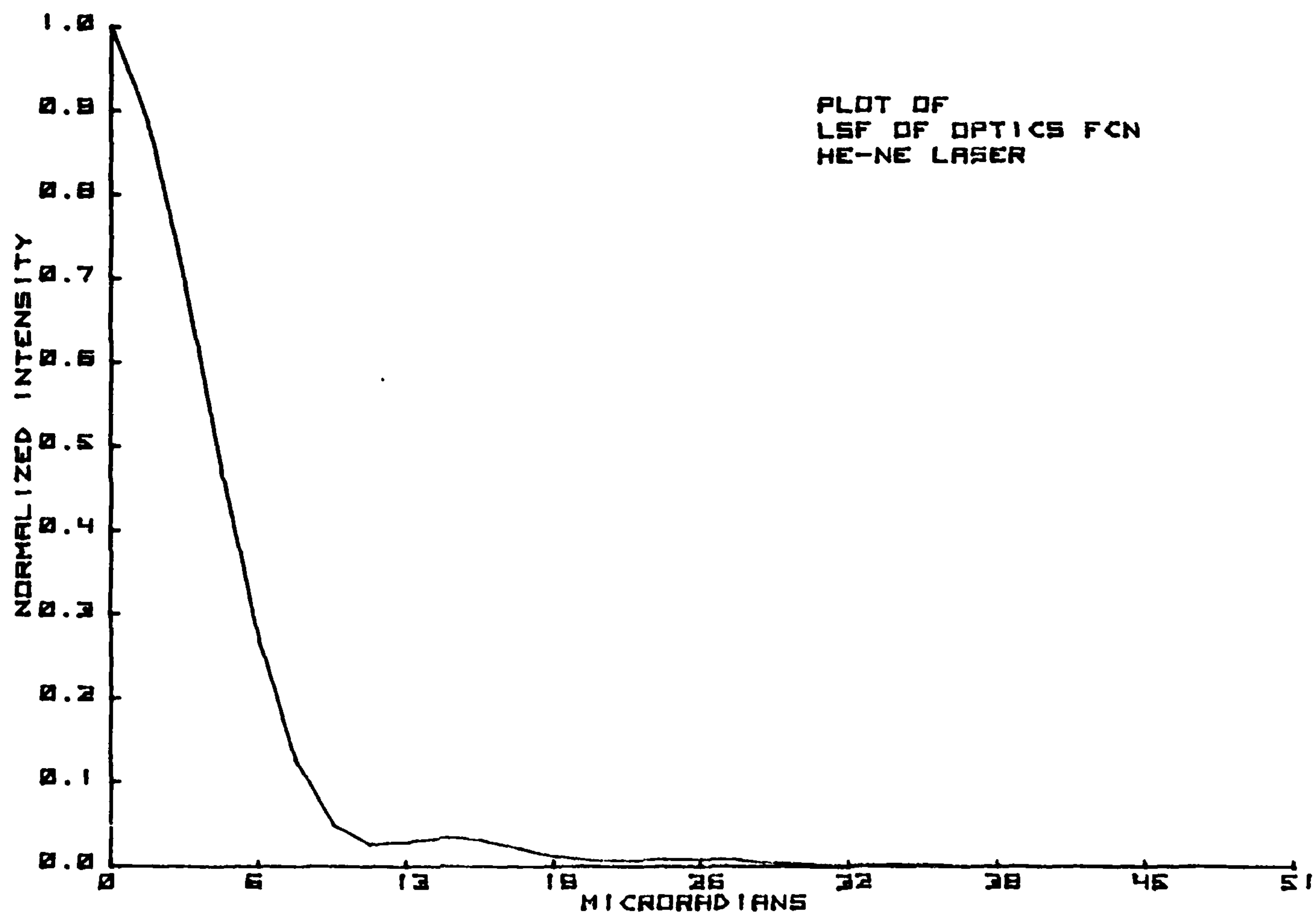

Fig. 3.14 Plot of LSF of Optics Function for He-Ne Laser

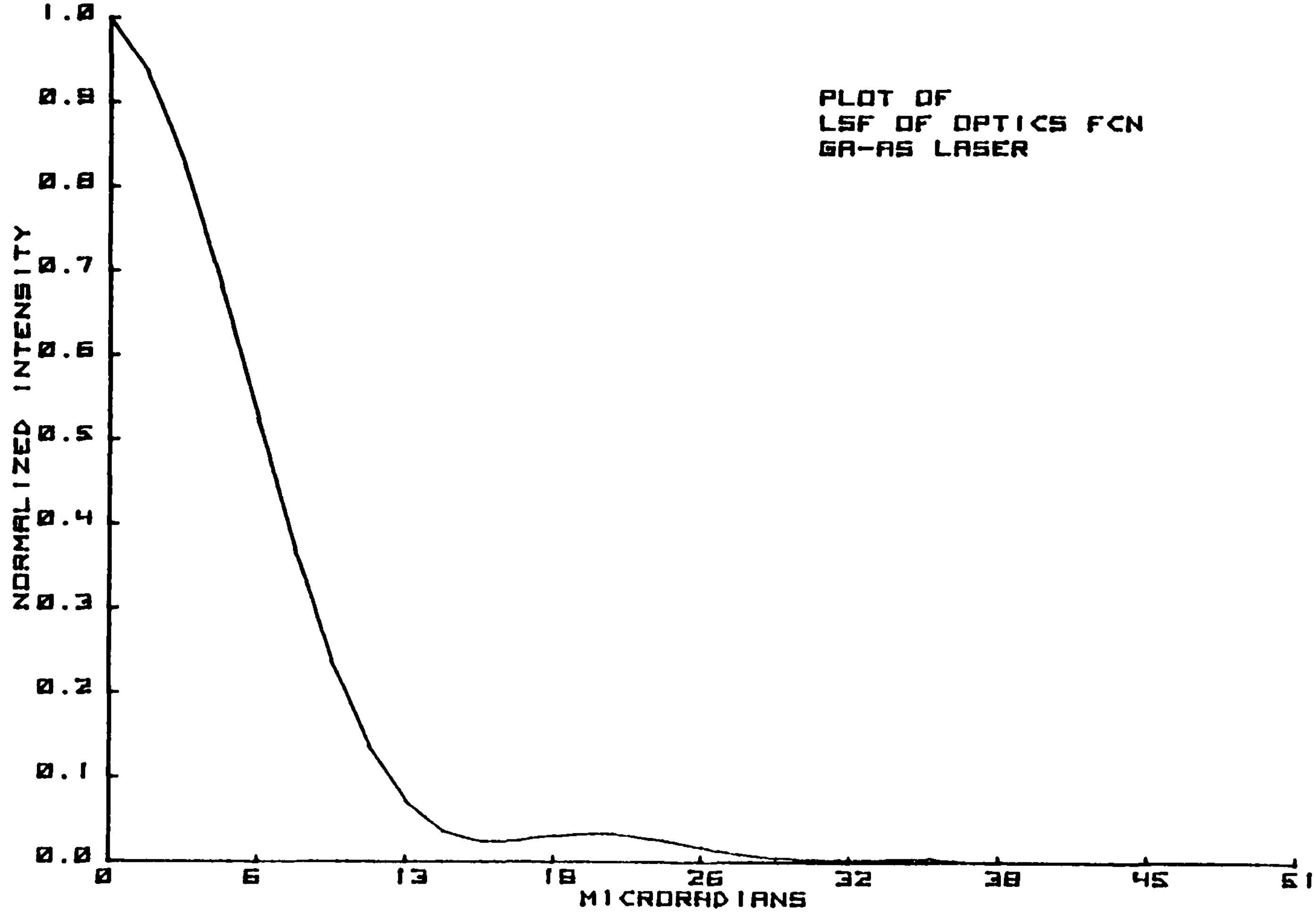

Fig. 3.15 Plot of LSF of Optics Function for Ga-As Laser

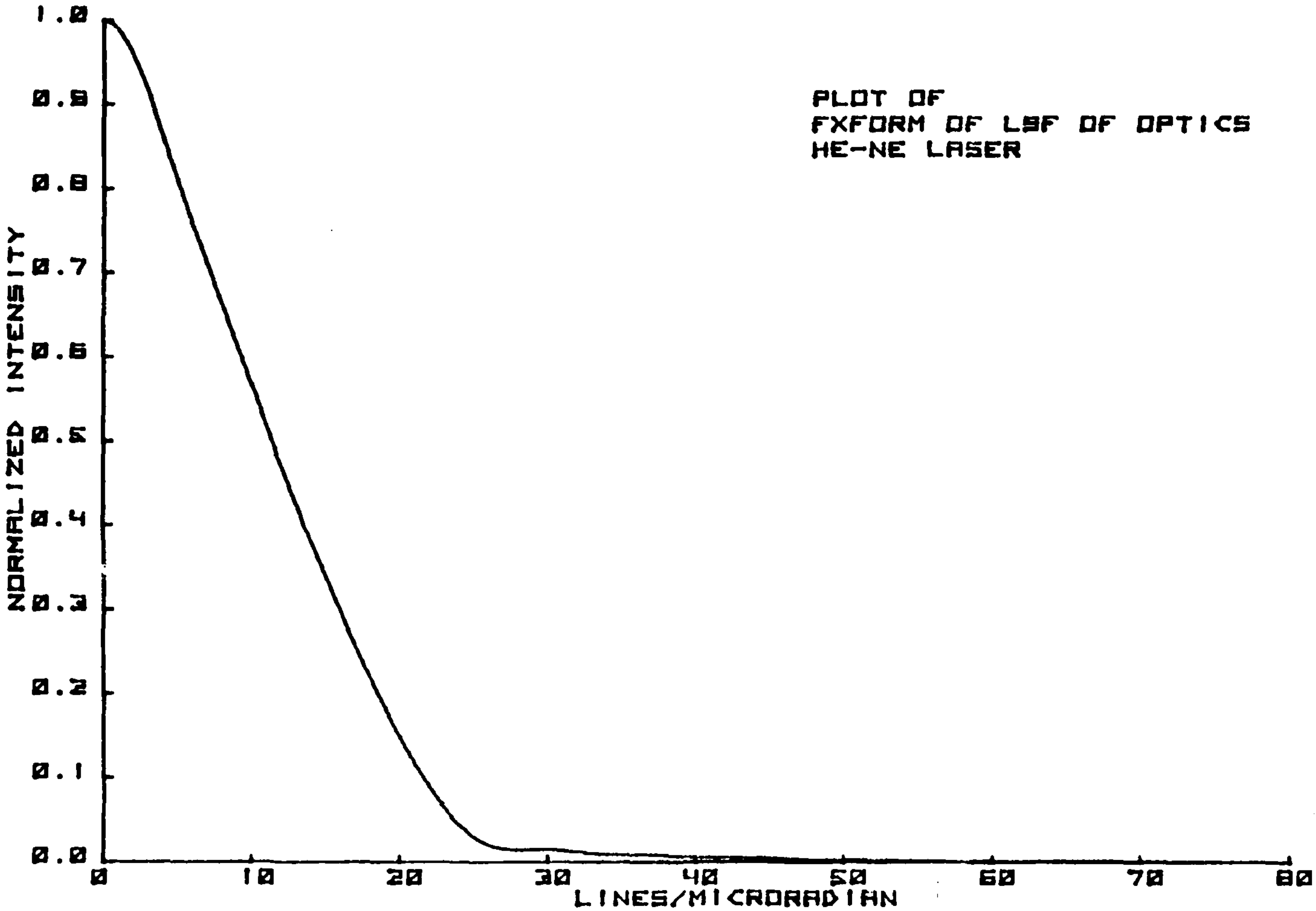

Fig. 3.16 Plot of Fourier Transform of LSF of Optics Function for He-Ne Laser

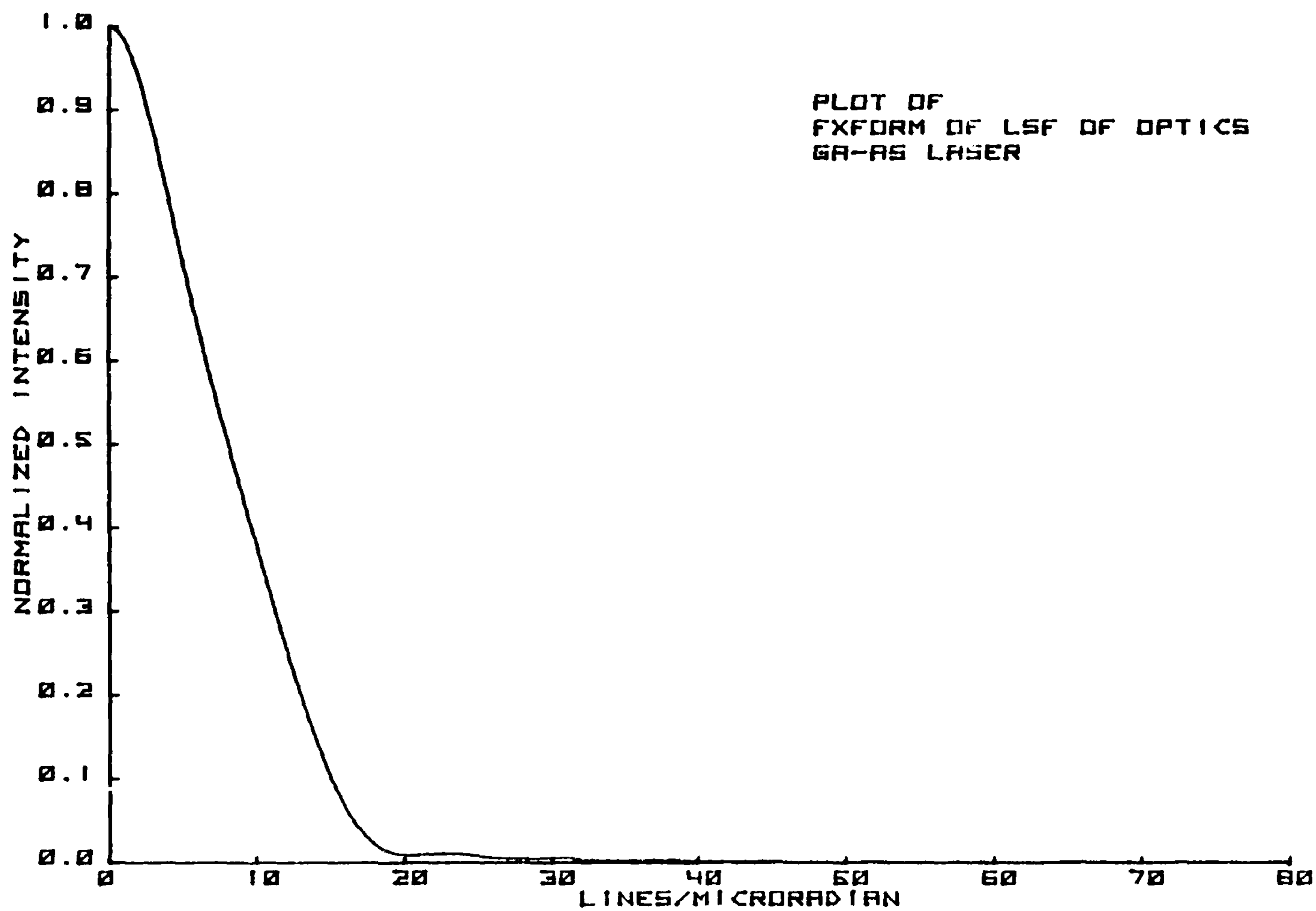

Fig. 3.17 Plot of Fourier Transform of LSF of Optics Function for Ga-As Laser

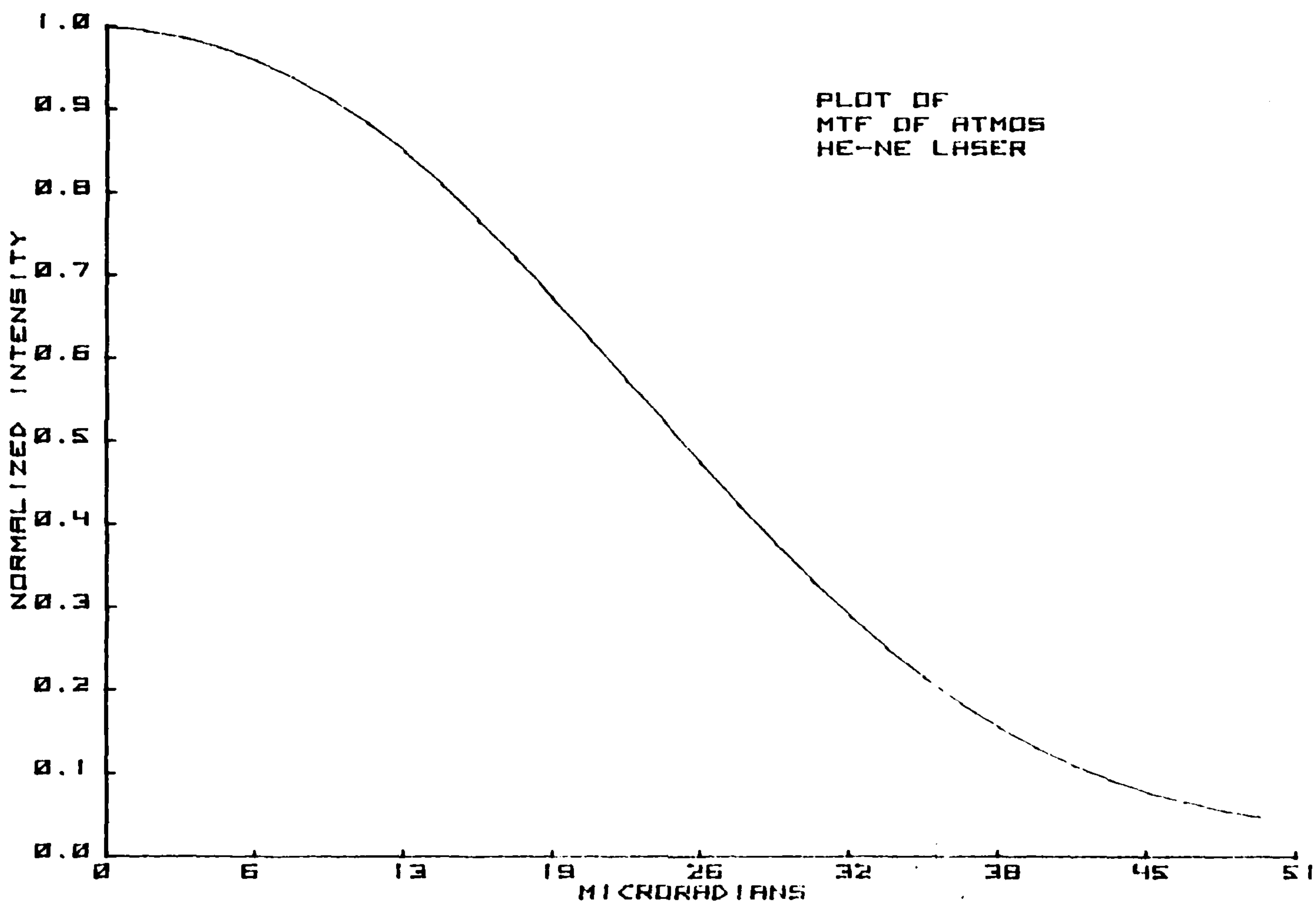

Fig. 3.18 Plot of MTF of Atmosphere for He-Ne Laser

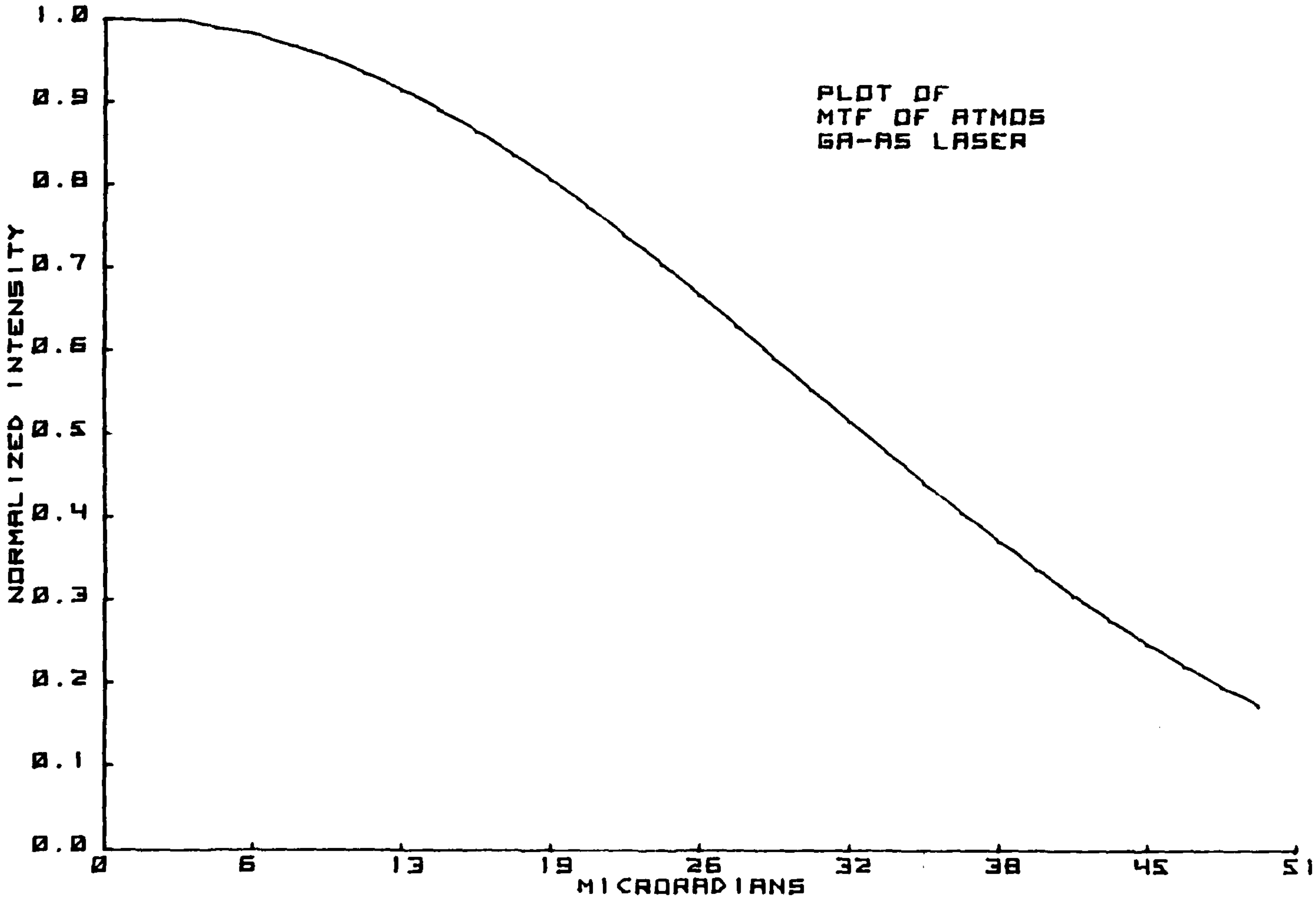

Fig. 3.19 Plot of MTF of Atmosphere for Ga-As Laser

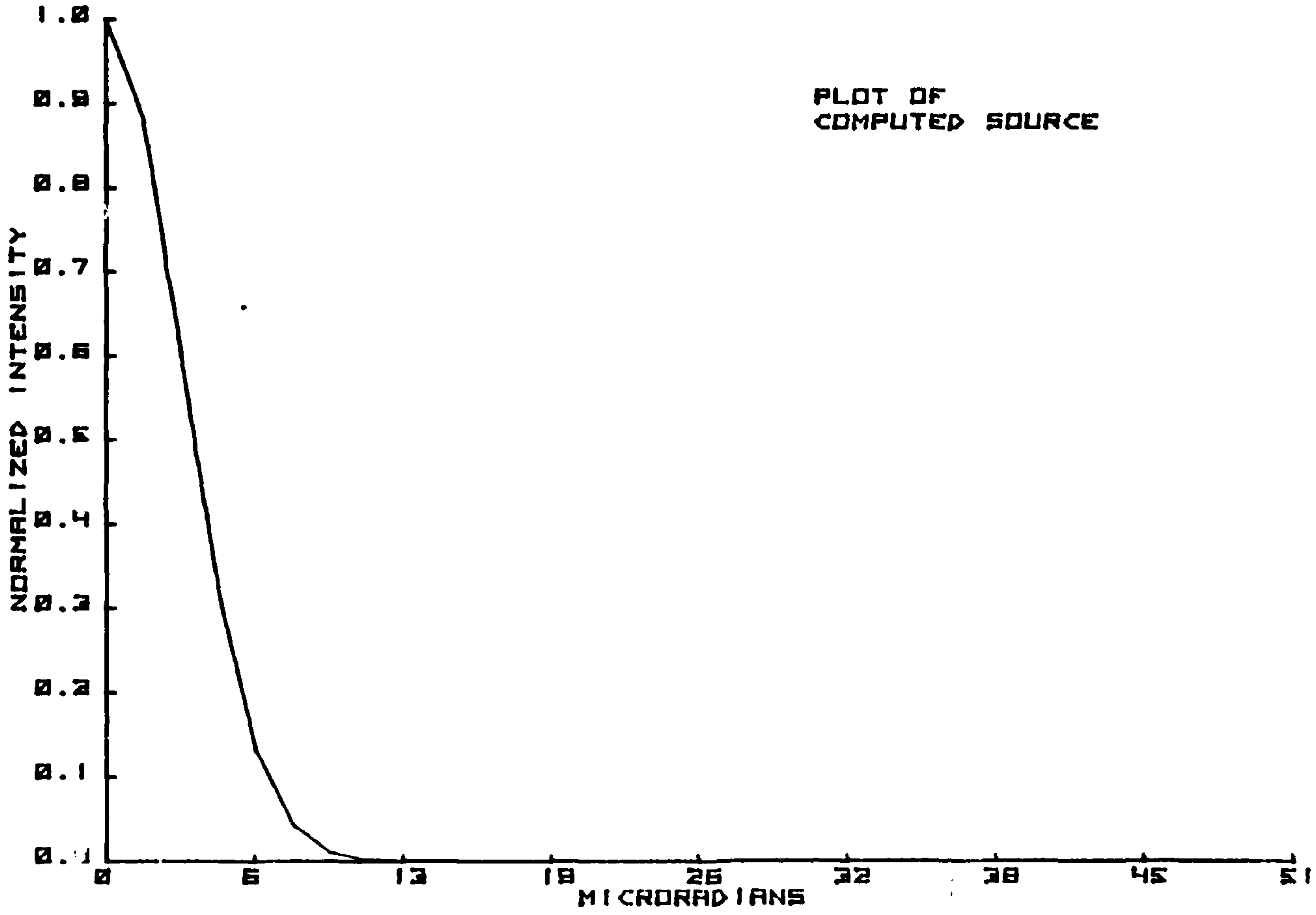

Fig. 3.20 Plot of Computed Source

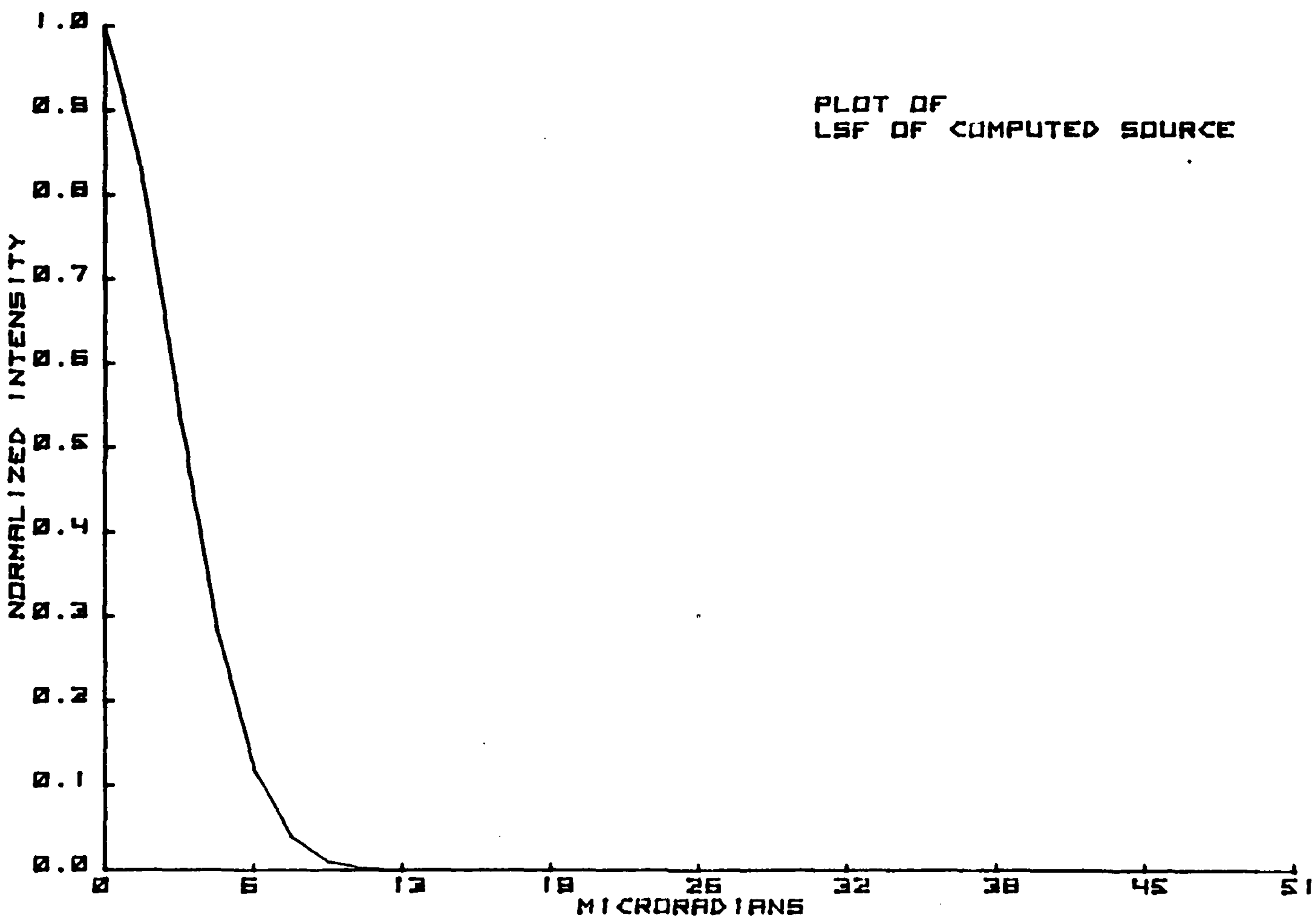

Fig. 3.21 Plot of Line Spread Function of Computed Source

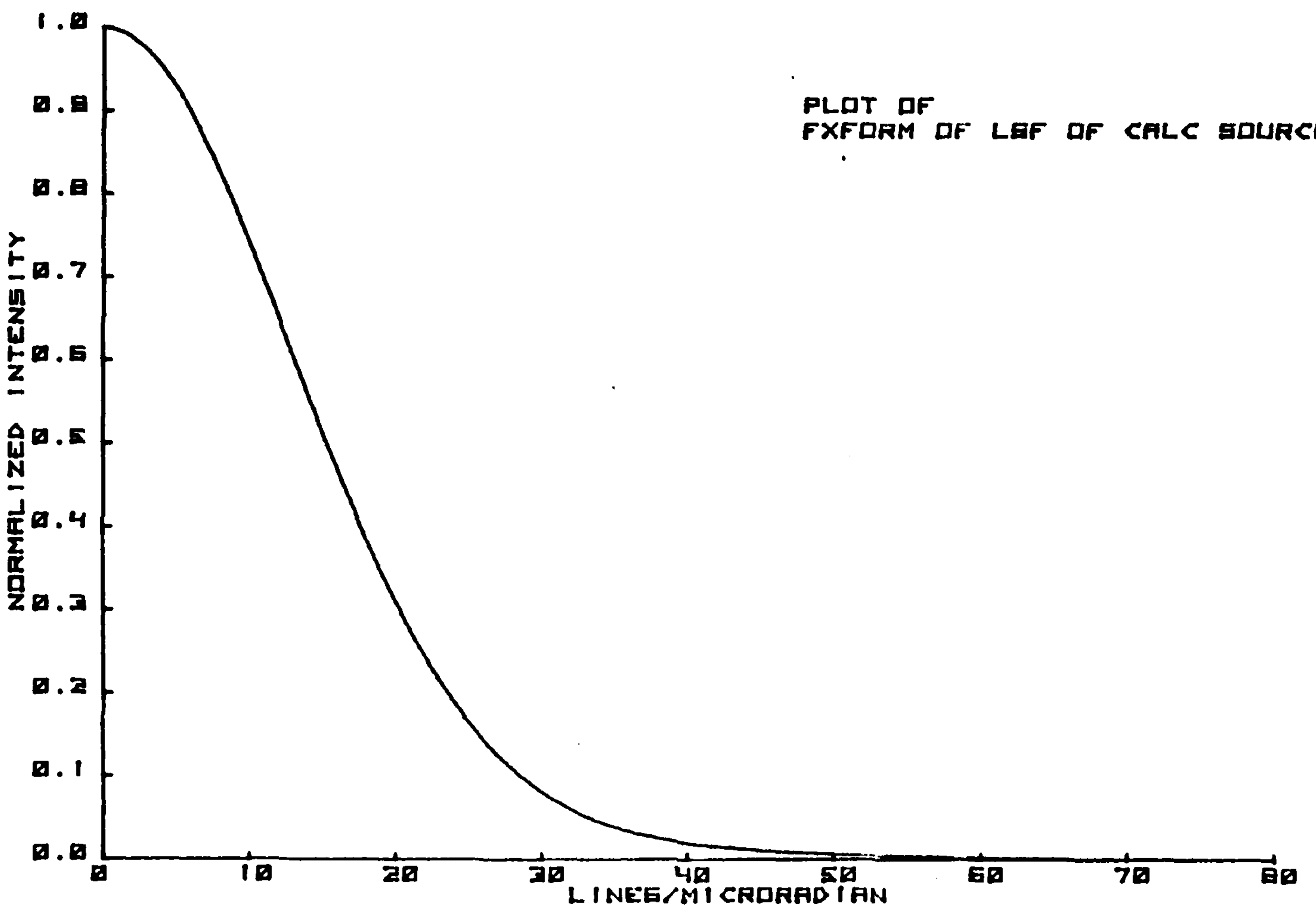

Fig. 3.22 Plot of Fourier Transform of LSF of Computed Source

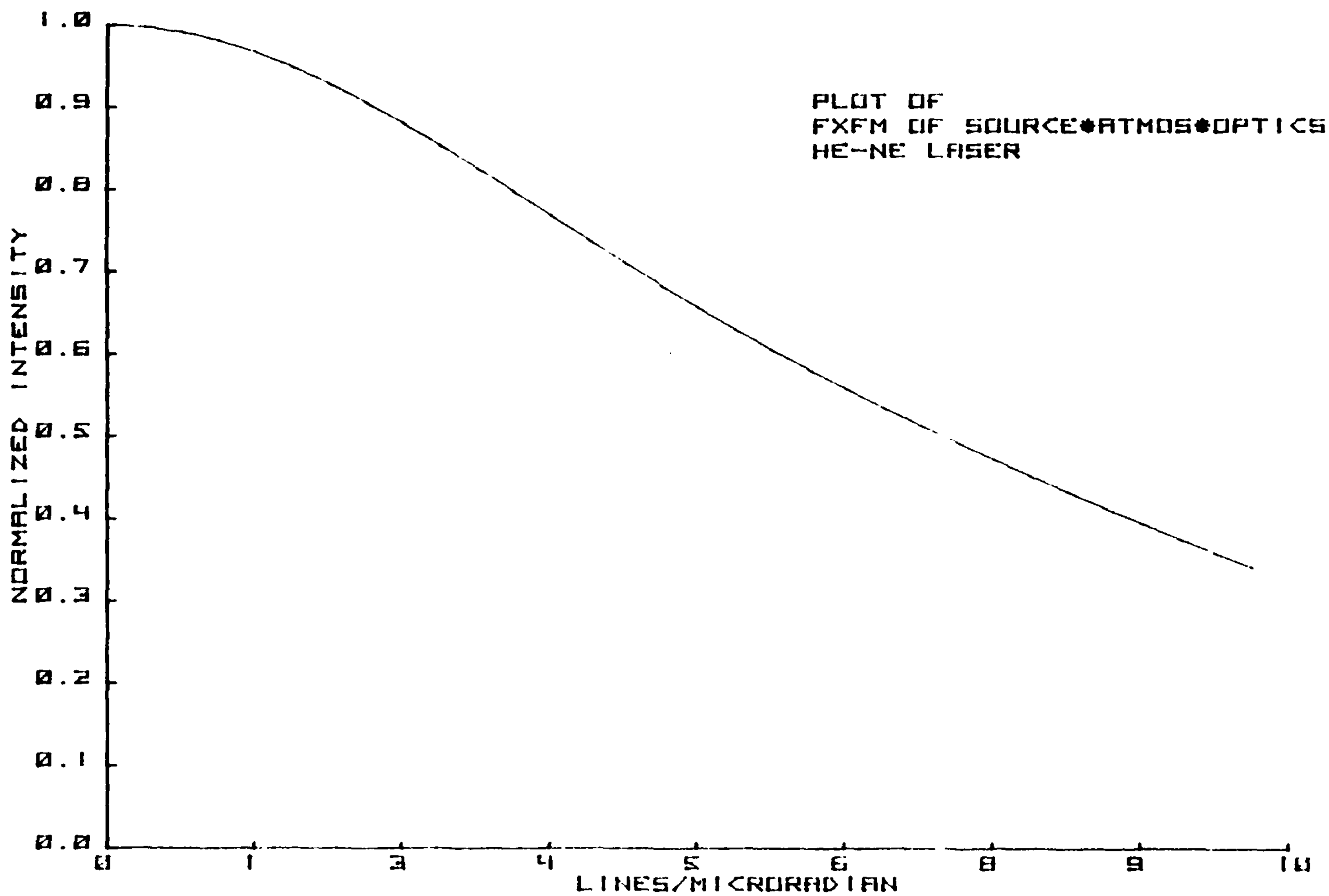

Fig. 3.23 Plot of Products of Fourier Transform of Computed Source, Optics and Atmosphere for He-Ne Laser

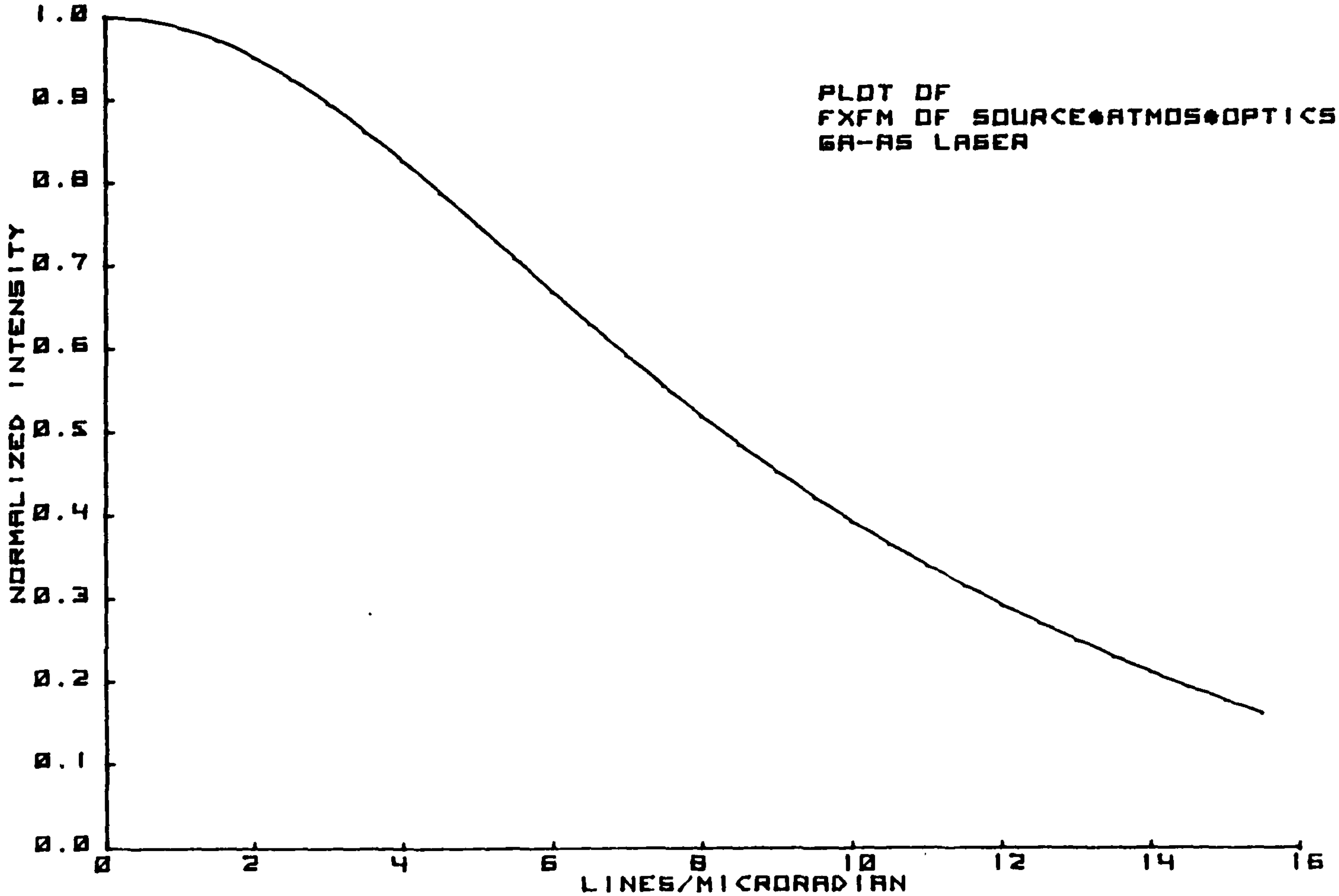

Fig. 3.24 Plot of Products of Fourier Transform of Computed Source, Optics and Atmosphere for Ga-As Laser

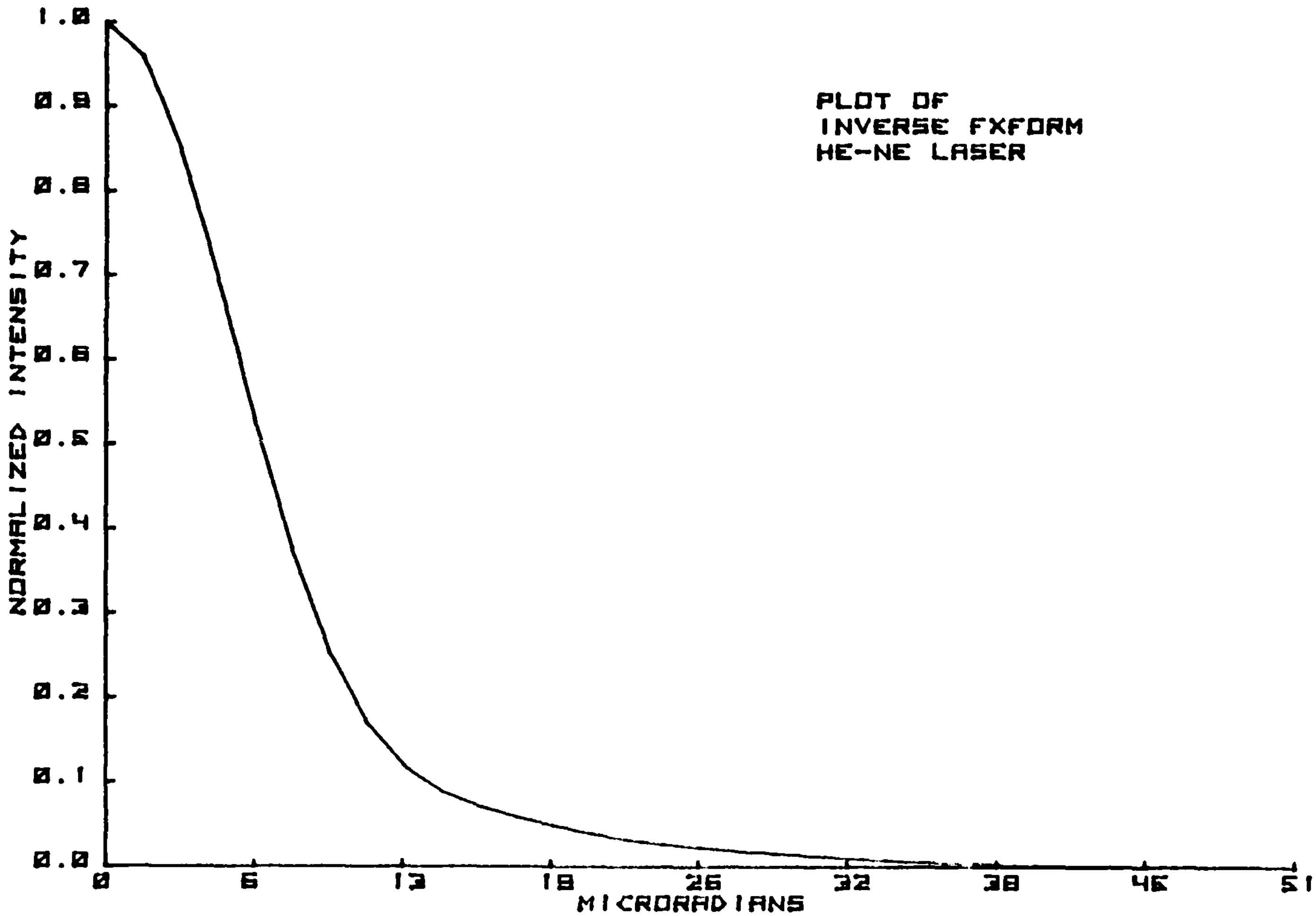

Fig. 3.25 Plot of Inverse Fourier Transform for He-Ne Laser

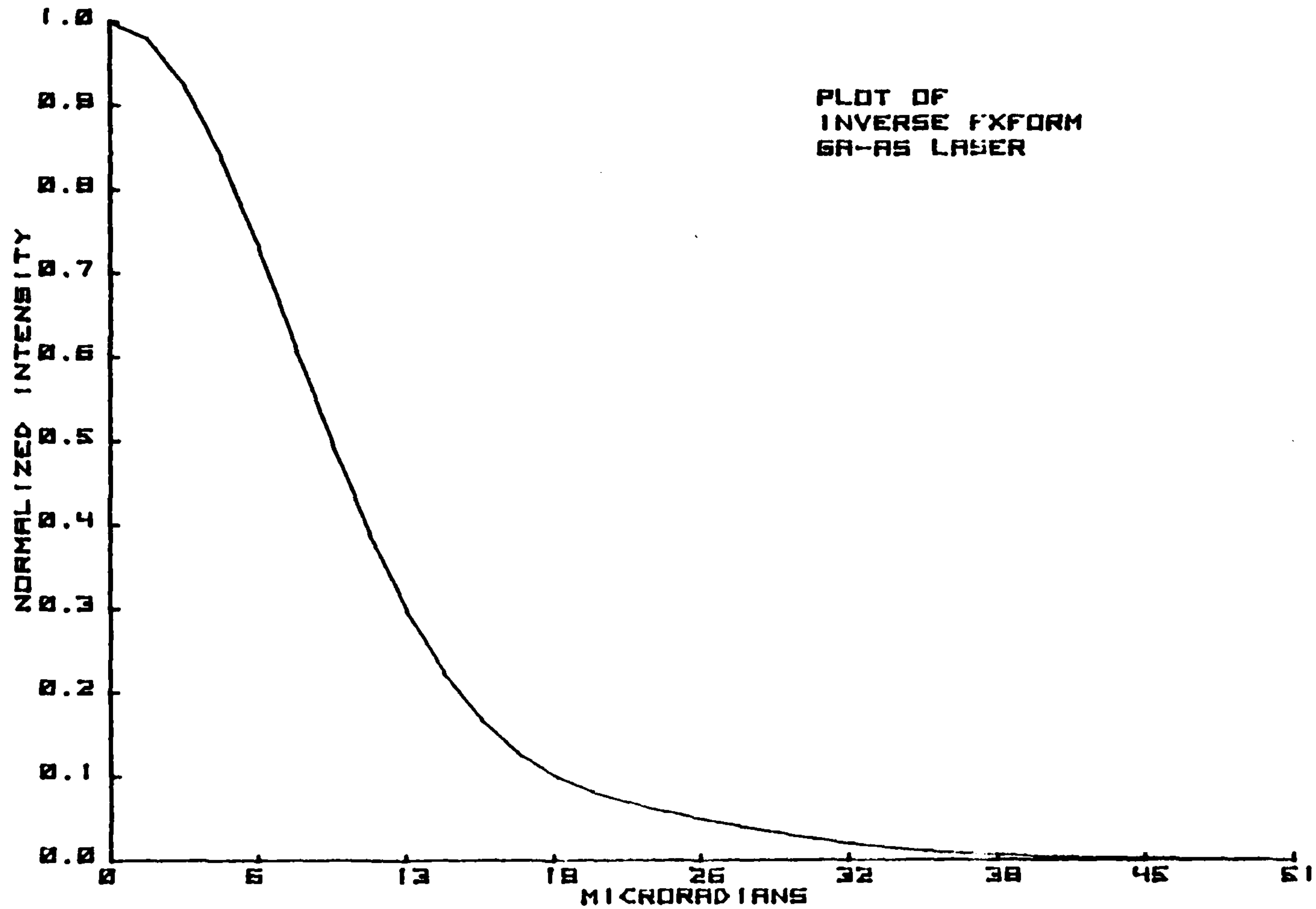

Fig. 3.28 Plot of Inverse Fourier Transform for Ga-As Laser

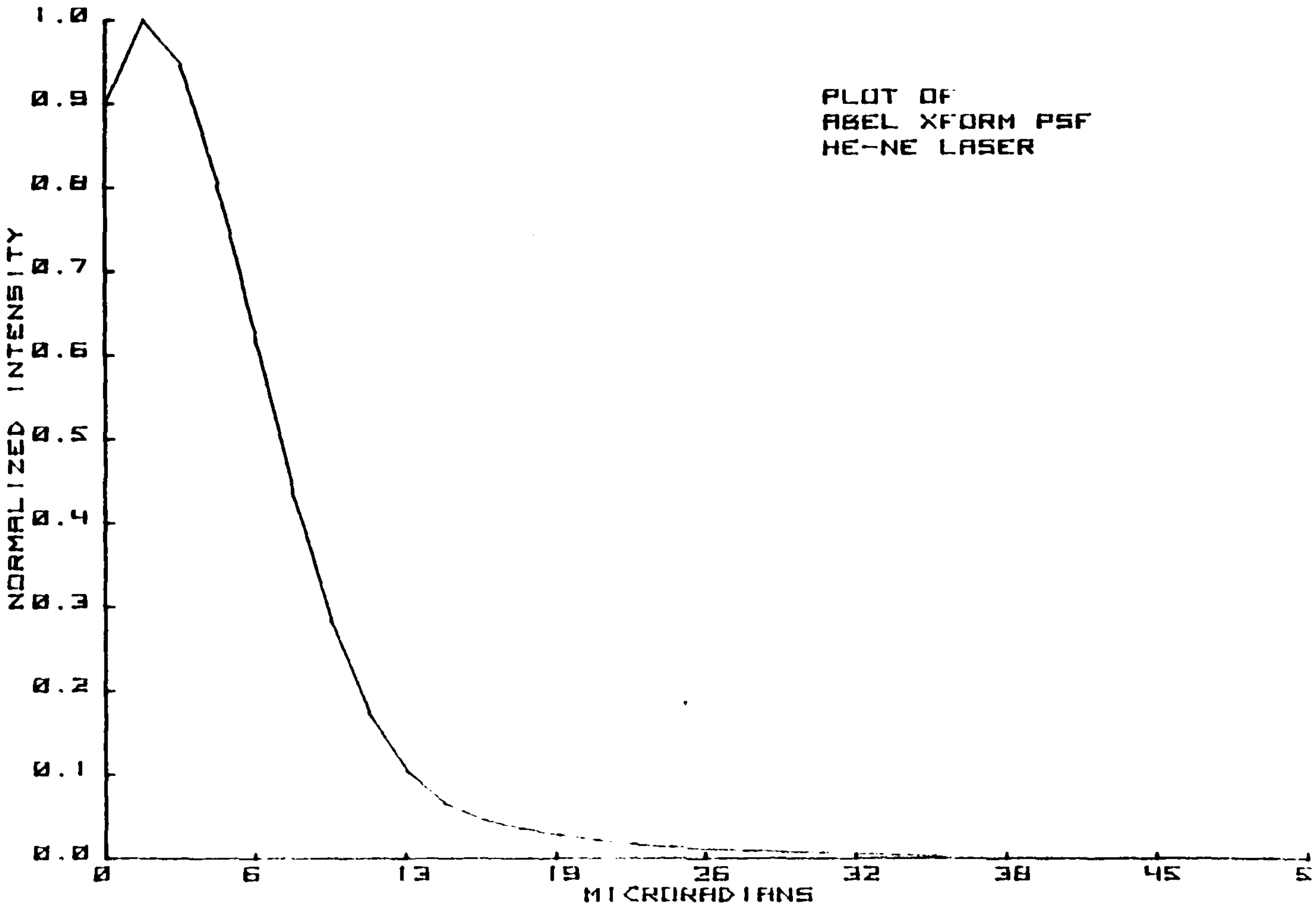

Fig. 3.27 Plot of Abel Transform for He-Ne Laser

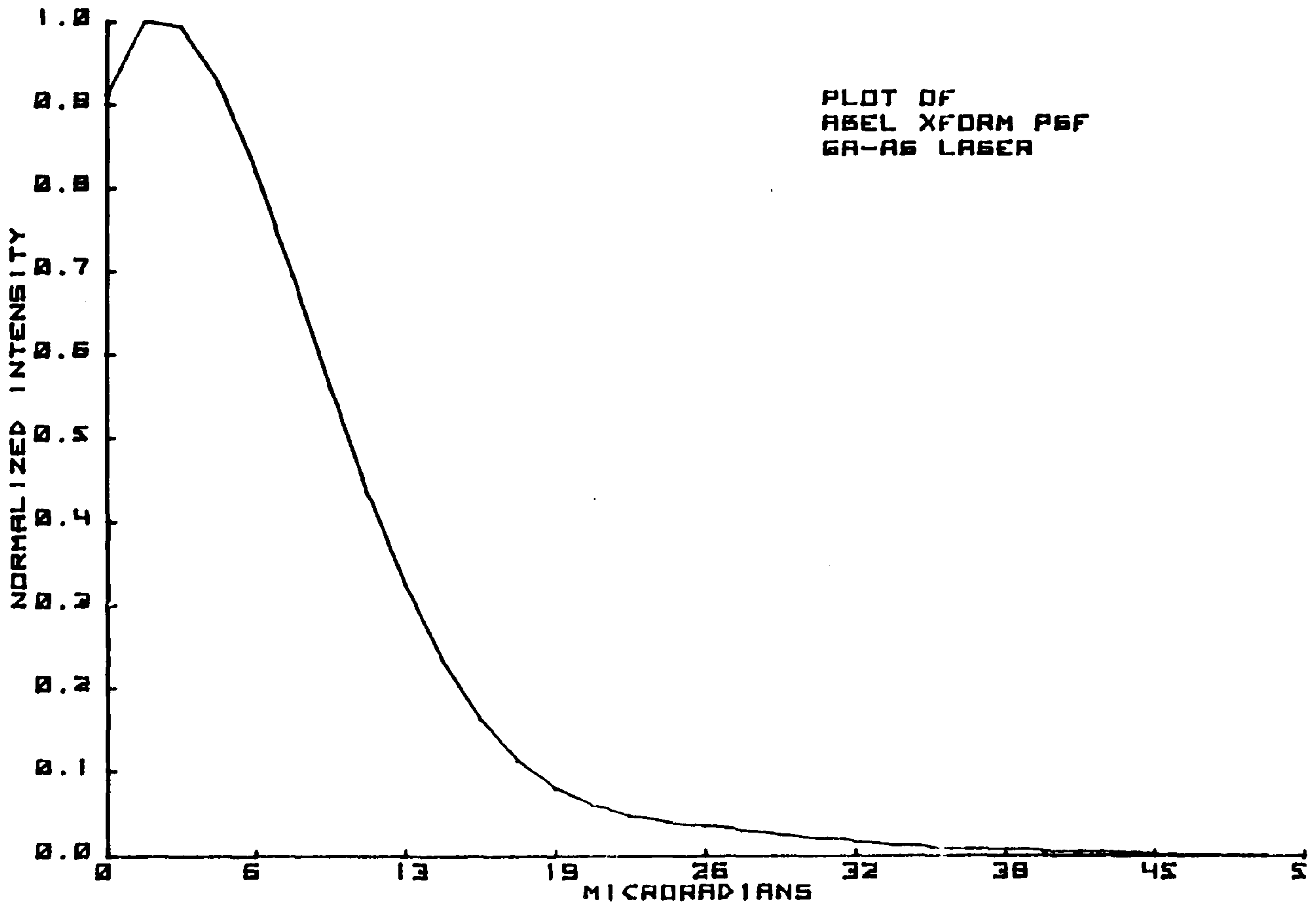

Fig. 3.28 Plot of Abel Transform for Ga-As Laser

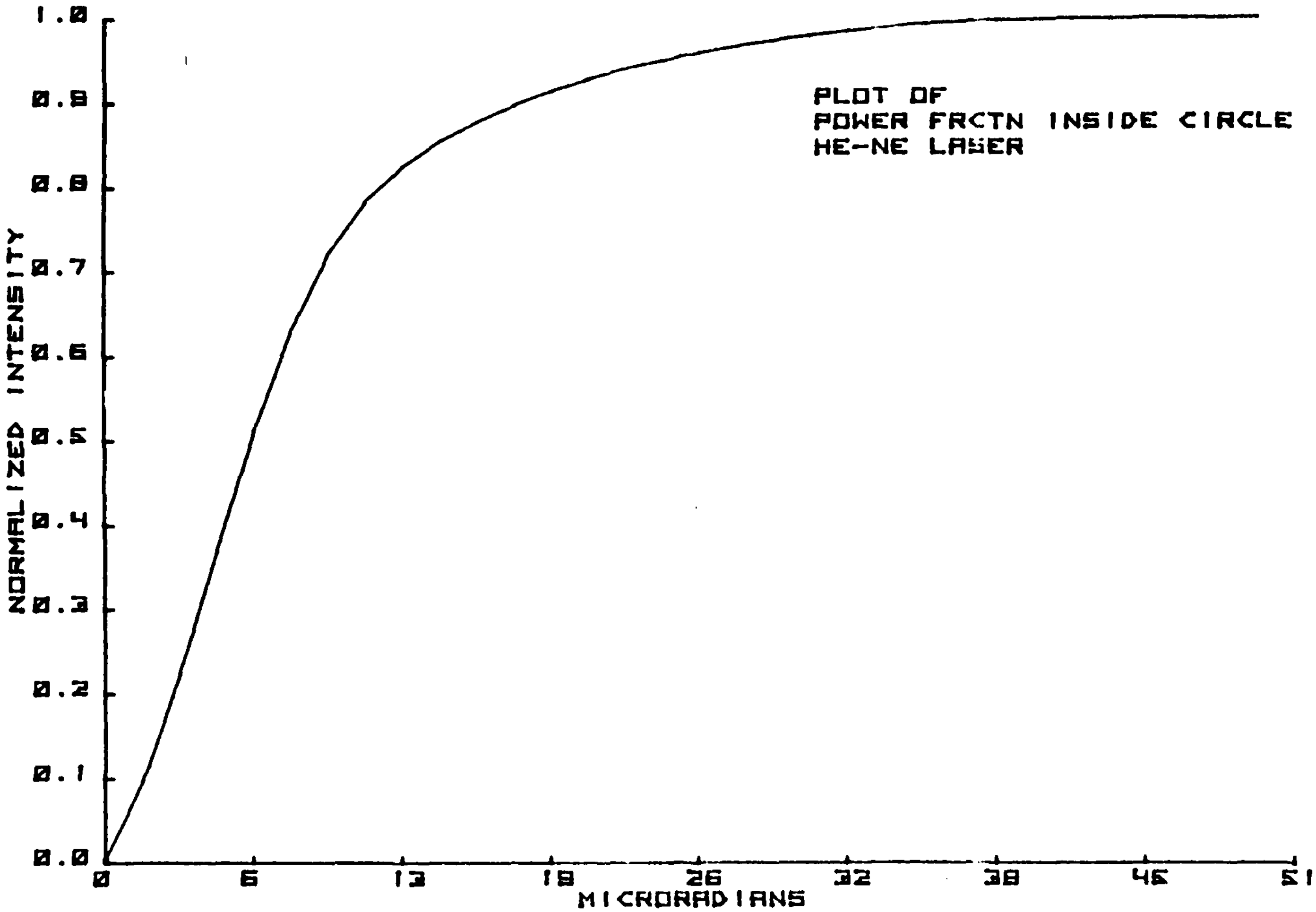

Fig. 3.29 Plot of Power Fraction Inside Circle of Radius R for He-Ne Laser

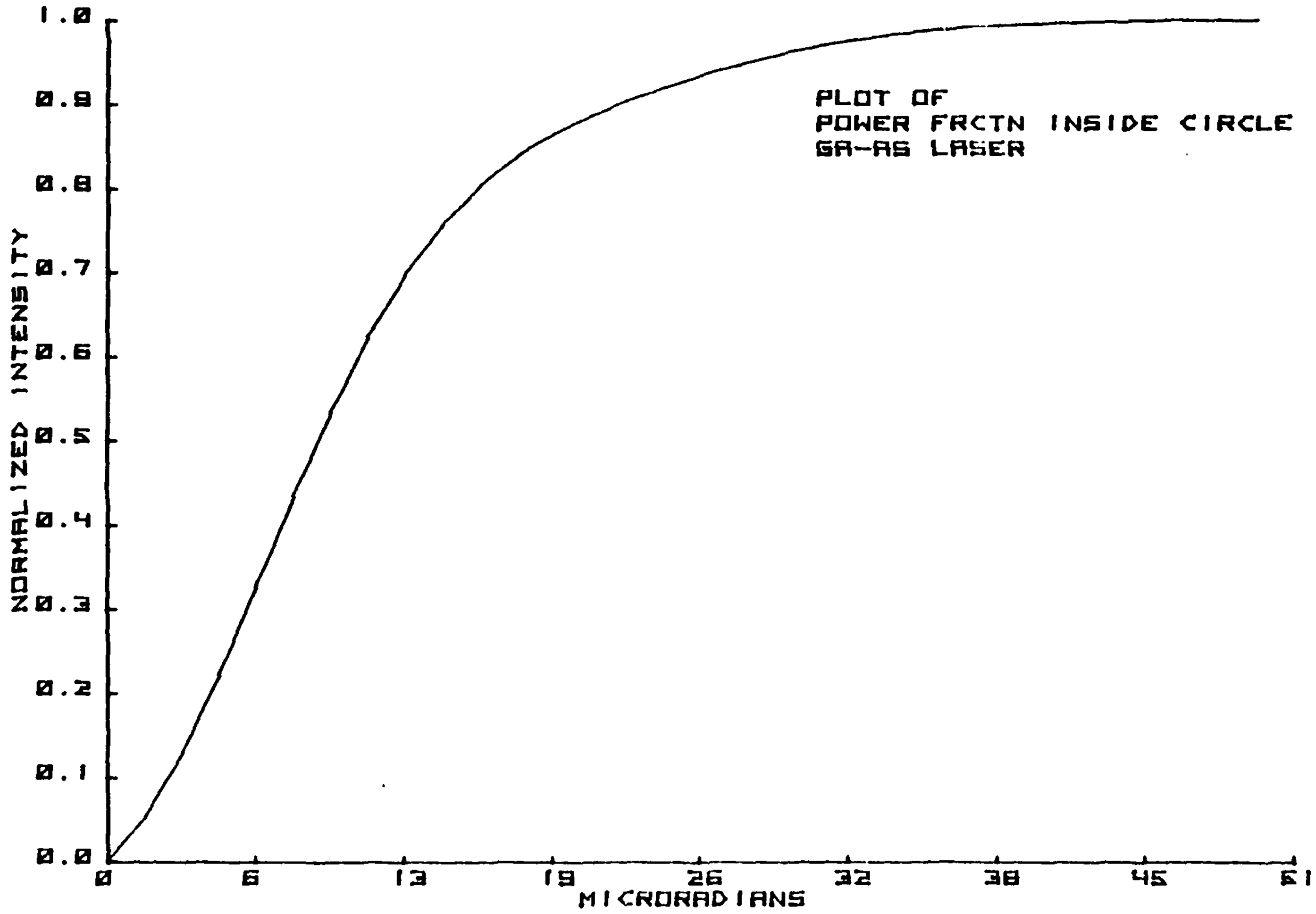

Fig. 3.30 Plot of Power Fraction Inside Circle of Radius R for Ga-As Laser

IV. COMPUTER PROGRAM IN ALGORITHMIC LANGUAGE

The program presented here is written in the algorithmic language as outlined by Graham [Ref. 9]. It is intended that the language in use here be machine independent. Comments appear in parentheses.

```
Algorithm_Laser
 (Input which laser is used.)
    Input Laser_Wavelength
    ESTRING<== Type_of_Laser
```

(Input if the particular laser source data are recorded. The following lines determine if the laser source data are already recorded. If the source data are not recorded then the program goes to the transfer subroutine to allow interfacing with the 468 to effect a data transfer. The parameters passed to the Plot subroutine have the following significance: the first parameter determines the horizontal index, for example 512 points or the number of microradians. The second parameter tells the computer which file the data are recorded on so the data can be loaded into memory. The final parameter determines the labeling of the horizontal axis either in data points, microradians, or lines per microradian.)

```
If Laser_Source_not_recorded then
    Call Transfer(Source_File)
    Call Plot(512,Source_File,0)
End If
```

(Input if the particular laser scale data are recorded. Scale data are recorded with the diffraction grating in place. If the scale data need to be recorded, the subroutine Transfer is called and the scale data are stored on a separate file.)

```
If Laser_Scale_not_recorded then
    Call Transfer(Scale_File)
    Call Plot(512,Scale_file,0)
End If
Input Scale_Factor
```

(Calculation of the scale factor is detailed in Chapter III. Comparison of the time base of the recorded data is necessary to ensure that the data recorded have the same time scale on the oscilloscope. If the time scales are different the program stops and displays an error message. A file is loaded, the waveform preamble is searched for the

"XUNITS" or "XINCR" oscilloscope settings and the particular data are stored. This is done for each of the 3 recorded files: source, scale, and collimated data. Collimated data refer to the same laser recorded under controlled conditions. The laser beam is projected in a collimator and recorded on tape. This data could be used to remove any non-linearities of the video recorder, electronic equipment, or receiving optics. Data elements are compared to ensure consistency of inputs.)

```
Input Laser_source
B<== pos(Laser_Source,'R:')
R1<== val('B+2',B+4')
B<== pos(Laser_Source,'IT:)
ASTRING<== Laser_Source('B+3','B+4')
Input(Laser_Scale)
B<== pos(Laser_Scale,'R:')
R2<== val('B+2',B+4')
B<== pos(Laser_Scale,'IT:')
BSTRING<== Laser_Scale('B+3','B+4')
Input(Collimated_Source)
B<== pos(Collimated_Source,'R:')
R3<== val('B+2','B+4)
B<== pos(Collimated_Source,'IT:')
```

```
   CSTRING<== Collimated_Source('B+3','B+4')
   If R1=R2=R3  then
        If ASTRING = BSTRING = CSTRING then
             Input RDATA(File_Number)
        End If
   Else
        Output 'ERROR IN TIME SCALE'
        Stop
   End If
   A<==B<==C<==0
(Array is initialized to 0)
   Do for I = 1 to 512
        YDATA(I)<== RDATA(I)
   End Do
(This section takes the data from the waveform message as
transferred from the 468 and removes any DC background from
an image as well as subtracting the minimum value in order
to "zero"  the data. This makes y=0 as the starting point
for both calculation and plotting purposes. Data up to 51
and greater than 463 are summed and stored in B.
This represents the  "wings" of the curve. This
process removes the DC background from an image.)
   Do for I = 1 to 512
```

```
        A<== A+YDATA(I)
        If I < 51 then
             B<== YDATA(I) + B
        End If
        If I > 463 then
             B<== YDATA(I) + B
        End If
   End Do
(Output for debugging)
   Output A,B
(Average of the sum of data values in the "wings".)
   D<== B/100
(This is the total sum of all data less the "wings" value.)
   A<== A-512*D
(All data are summed and stored in C. Each data
is compared with the previous total divided by 2.
This will find the index value, I, for which
the maximum value exists.)
   Do for I = 1 to 512
        YDATA(I)<== YDATA(I)-D
        C<== YDATA(I) + C
        If C < A/2 then
             J<== I
```

```
        End If
    End Do
   (Output for debugging.)
    Output C,J
  (The curve is shifted so that the maximum value starts
  at the origin of the horizontal axis. This is called
  the point spread function and is recorded as RDATA.)
    Do for K = 1 to 256
        IDATA(K)<==
YDATA((J-K+1)mod512+1)+YDATA((K+J-1)mod512+1)
    End Do
    Do for I = 257 to 512
        RDATA(I)<== 0
    End Do
    Do for I = 1 to 256
        RDATA(I)<== IDATA(I)
    End Do
  (Determines if tabular or plotted data are desired.)
    If PSF_OUTPUT_wanted then
        Call Table(RDATA)
    End If
    If PSF_PLOT_wanted then
        Call Plot(32,RDATA,1)
```

```
   End If
(Calculates the line spread function from the point
spread function.)
   Call LSF
(Determines if tabular or plotted data are desired.)
   If LSF_OUTPUT_wanted then
        Call Table(RDATA)
   Else If LSF_PLOT_wanted then
        Call Plot(32,RDATA,1)
   End If
(Calculation of Fourier Transform of LSF.)
   Input RDATA
(The maximum value of the array IDATA is at I=1. This
is put back into array RDATA and folded over so that
IDATA(257) to IDATA(512)  is the mirror image of
IDATA(1) to IDATA(255). Then this array is recorded
as RDATA and the Fourier transform calculated.)
   Do for I = 257 to 512
        RDATA(I)<== 0
   End Do
   Do for I = 1 to 256
        RDATA(514-I)<== RDATA(I)
   End Do
```

```
   RDATA(257) <== RDATA(256)
   Call FXFORM
(Determines if tabular or plotted data are desired.)
   If FXFORM_OF_LSF_OUTPUT_wanted then
        Call Table(RDATA)
   Else If FXFORM_OF_LSF_PLOT_wanted then
        Call Plot(32,RDATA,2)
   End If
  (Dia of Obscur/Dia of Obj Lens in meters,RATIO=.064/.164)
  (This is the measurement of the ratio of
  diameters of obscuration to telescope.)
  (R1= Scale of data in microradians=1.60)
  (Diameter of telescope Obj Lens in meters,OBJECT=
  0.164 meters)
   If Laser_Source = He-Ne then
        Wavelength<== 6.328*e-7
   Else
        Wavelength<== 9.05*e-7
   End If
(This begins the calculation of the Fourier transform
of the optics using the  Airy function. All of the
data regarding the optics are recorded on a separate file.)
(These next four statements fix the constants in the
```

```
argument of the optics function.)
   R1<== Scale_Factor
   D<== RATIO**2
   H<== 1-D
   Z<== PI*Scale_Factor*Object*1*e-6/Wavelength
   Do for I = 1 to 256
        Y<== Z*(I-1)
        If Y > 30 then
             RDATA(I) <== 0
        Else
             RDATA(I) <== (AIRY(Y)-D*AIRY(Y*RATIO))**2/H**2
        End If
        K<== I
   End Do
  (Record RDATA on separate file)
(Determines if a plot of the optics function is desired.)
   If OPTICS_FUNCTION_PLOT wanted then
        Call Plot(32,RDATA,1)
   End If
(Calculates the line spread function of the optics
function.)
   Call LSF
(Determines if a plot of the LSF of the optics function is
```

```
desired.)
   If PLOT_OF_LSF_OPTICS wanted then
        Call Plot(32,RDATA,1)
    End If
   Do for I = 257 to 512
        RDATA(I)<== 0
   End Do
(Data are folded over again and the Fourier transform
calculated.)
   Do for I = 1 to 256
        RDATA(514-I)<== RDATA(I)
   End Do
   RDATA(257)<== RDATA(256)
  (Record RDATA)
  (Fourier transform of the LSF of Optics is calculated.)
   Call FXFORM
  (Determines if plot of Fourier transform of Optics
  function is desired.)
   If PLOT_OF_FXFORM_OF_OPTICS wanted then
        Call Plot(256,RDATA,2)
   End If
  (Calculation of the quotient of two Fourier transforms.)
  (This section takes the Fourier transform of the system
```

and divides it, point by point, by the Fourier transform of the optics. This yields the modulation transfer function (MTF) of the atmosphere.)

```
 Input RDATA_OF_FXFORM_OF_SOURCE
 Do for I = 257 to 512
      RDATA(I)<== 0
 End Do
 Do for I = 1 to 256
      RDATA(514-I)<== RDATA(I)
 End Do
 Input RDATA_OF_FXFORM_OF_OPTICS
 Do for I = 1 to 256
      RDATA(I)<== IDATA(I)/RDATA(I)
 End Do
(Determines if a plot of the MTF is desired.)
 If PLOT_OF_MTF_OF_ATMOS_wanted then
      Call Plot(32,RDATA,1)
 End If
```

(Calculation of C_n^2 by curve fitting.
This procedure is described in Chapter III.)
(All "R" variables used in this calculation are initialized to 0.)

```
 R17<==R18<==R19<==R20<==R21<==R22<==R23<==R24<==R25<==0
```

(Analysis of data shows that computer time is wasted beyond 96 points.)

```
   Do for I = 1 to 96
```

(R18 - when summed is the $(f(i))^{10/3}$. This is the total of the angular spatial frequencies squared.)

```
        R18<== ((I-1)*Scale_Factor)**(10/3)
        R17<== R17 + R18
```

(R19 - when summed is the $(f(i))^{5/3}$. This is the total of the angular spatial frequencies.)

```
        R19<== ((I-1)*Scale_Factor)**(5/3)
        R20<== R19 + R20
```

(R21 - is the total number of points.)

```
        R21<== I
        Do While RDATA(I) > 0
```

(R22 - when summed is the total of the product of the natural logarithm of each point with R19.)

```
              R22<== ln(RDATA(I))*R19
              R23<== R22 + R23
```

(R24 - when summed is the total of the natural logarithm of each point.)

```
              R24<== ln(RDATA(I))
              R25<== R24 + R25
        End Do
```

```
  End Do
(Output matrix values for debugging.)
  Output R17,R20,R21,R23,R25
 (Assign value to matrix.
 This section takes the above calculated values and
 sets up a matrix. The matrix equation solved is
 B = A-1*C.)
 (Create 3 matrices A(2,2),B(2,1),C(2,1).)
  A(1,1)<== R20
  A(1,2)<== R21
  A(2,1)<== R17
  A(2,2)<== R20
  INVERT_MATRIX_A
  C(1,1)<== R25
  C(2,1)<==R23
  B<== A*C
 (Output matrix values for debugging.)
  Output B(1,1),B(1,2)
 (Calculation of Cn2 using equation(2.3).)
  R22<== B(1,1)/(-21.49*Range*R20*(Wavelength**(-.33333)))
  Output 'CNSQ=',R22
 (The program now starts the prediction phase.  It
 calculates a source assumed to have a Gaussian
```

distribution by means of the computed source pattern below. Using similar Fourier transform techniques the program uses the calculated value of C_n^2 and predicts the power incident on the target.)

(Computed Source Pattern:A=A0*exp(-x**2/2*Sigma**2)

(This is an "arbitrary" Gaussian source pattern with a standard deviation for Sigma set equal to 2.)

```
 A0<== A_ZERO
 C<== Sigma*Scale_Factor
 Do for I = 1 to 256
      F<== (I-1)*Scale_Factor
      G<== F**2/(2*C**2)
      Do While G > 13
           RDATA(I) <== 0
      End Do
      RDATA(I)<==A0*exp(-G)
 End Do
```

(Record RDATA. This records the computed source.)

(Determines if plot of computed source is desired.)

```
 If PLOT_OF_COMPUTED_SOURCE_wanted then
      Call Plot(32,RDATA,0)
 End If
```

(Calculates the line spread function of the computed

```
source.)
   Call LSF
(Determines if a plot of the LSF of the computed source
is desired.)
   If PLOT_OF_LSF_OF_COMP_SOURCE = 1 then
        Call Plot(32,RDATA,0)
   End If
  (Calculation of the Fourier transform of LSF of computed
  source.)
   Do for I = 257 to 512
        RDATA(I)<== 0
   End Do
   Do for I = 1 to 256
        RDATA(514-I)<== RDATA(I)
   End Do
   RDATA(257<== RDATA(256)
   Call FXFORM
(Determines if a plot of the Fourier transform of the
LSF of the computed source is desired.)
   If PLOT_OF_FXFORM_OF_COMPUTED_SOURCE_wanted then
        Call Plot(256,RDATA,2)
   End If
  (Calculation of the product of two Fourier transforms.)
```

```
(This is the Fourier transform of the computed source
with the MTF of the atmosphere.)
 Do for I = 1 to 256
      RDATA(I)<==
      RDATA(I)_COMPUTED_SOURCE*RDATA(I)_FXFM_OF_MTF
 End Do
(Product of FXFORMS of Source*Atmosphere*Optics.)
 RDATA(I)<==
 RDATA(1)_PRODUCT_OF_2_FXFMS*RDATA(1)_FXFM_OF_OPTICS
 Do for I =  2 to 256
      RDATA(I)<==
      RDATA(I)_PRODUCT_OF_2_FXFMS*RDATA(I)_FXFM_OF_OPTICS
      RDATA(514-I)<==RDATA(I)
 End Do
 RDATA(257)<== RDATA(256)
(The above data predicts what the Fourier transform
of the entire system is, using the calculated
value of Cn² for the atmospheric turbulence.)
(Determines if a plot of the result of Fourier transform
is desired.)
 If PLOT_OF_FXFORM_PRODUCTS_wanted then
      Call Plot(32,RDATA,2)
 End If
```

```
  (Inverse Fourier transform gives target LSF.)
   Call INVERSE_FXFORM
(Determines if a plot of the inverse Fourier transform
is desired.)
   If PLOT_OF_INVERSE_FXFROM_wanted then
        Call Plot(32,RDATA,0)
   End If
(Converts target's one dimensional LSF to a
two dimensional PSF by Abel transform.)
   Call ABEL
(Determines if a plot of the Abel transform is desired.)
   If PLOT_OF_ABEL_XFORM_wanted then
        Call Plot(32,RDATA,0)
   End If
  (Calculates the fraction of power inside circle of radius
  R. This predicts the fraction of power that will be
  incident on target.)
   RDATA(1)<== 0.25*PI*RDATA(1)
   Do for I = 2 to 256
        RDATA(I)<== 2*PI*RDATA(I)+RDATA(I-1)
   End Do
(Determines if a plot of the fraction of power is desired.)
   If PLOT_OF_POWER_wanted then
```

```
        Call Plot(32,RDATA,0)
    End If
End Laser
```

(The following subroutines are used in the Algorithm Laser.)

Subroutine_Transfer(File_Number)

(The transfer subroutine gets raw data, both preamble and data from the waveform message sent by the 468. It processes the message by finding the minimum value of the array then subtracting this value from each element in the array. This "zeros" the array.)

```
    Output 'Ensure Equipment set up properly'
    Output 'Continue when ready'
    E<== (-1)
    Do While E = -1
```

("DATA" is the I/O buffer where the data from the 468 are sent. The status of the buffer is read while data are being transferred. When the transfer is complete, the interface is cleared.)

```
        Data<== Transferred_Data
        If Data_Transfer_Complete then
            E<== 0
        End If
```

```
End Do
Clear_Interface
N<== 1
(This is where header format stops and data begin.)
A<== pos(Data,'%')
Do for I = A+2 to 687 by 16
     Do for J = 1 to 16
          If J+I>688 then
               RJ<== 0
               N<== N+1
          End If
          RJ<== num(Data(I+J))
(The numerical values of each element are stored in YDATA.)
          YDATA(N) <== RJ
          N<== N+1
     End Do
End Do
E<== minimum(YDATA)
Do for I = 1 to 512
  YDATA(I) <== YDATA(I)-E
  RDATA(I) <== YDATA(I)
End Do
Store_RDATA(File_Number)
```

```
   Return
End Transfer
(This subroutine calculates the Line Spread Function
for the previously recorded point spread function
by using equation (1.1).)
   Subroutine_LSF
(Depending on which file number has been passed down
from the calling subroutine, either scale or source
data are loaded.)
   If File_Number = Scale_Data then
        Input Scale_Data
        RDATA<==SCALE_DATA
   Else
        Input RDATA
   End If
   Do for I = 1 to 512
        IDATA(I)<== 0
   End Do
   Do for I = 1 to 256
        IDATA(I)<== RDATA(I)
   End Do
(Plots have shown that computer time is lost and no
valuable information is gained  beyond about 24 points.)
```

```
    Do for I = 1 to 24
        J<== 1
        Output I
        Q<== IDATA(I)
        Do While R < 24
            R<== SQRT(I*I+J*J)
            Q<==
            Q+2*((1-fraction(R))*I(int(R))+fraction(R)*I(int(R)+1))
            J<== J+1
        End Do
        IDATA(I)<== Q
    End Do
    Do for I = 1 to 24
        RDATA(I)<== IDATA(I)
    End Do
    If File_Number = Scale_Data then
        Store_Scale_Data
    Else
        Store_RDATA
    End If
    Return
End LSF
```

(This subroutine calculates the Fourier transform of the given data using the Cooley-Tukey Algorithm. If the inverse statement is true, then the inverse Fourier transform is calculated.)

```
Subroutine_FXFORM
   Set_Radian_Mode
  (2**9=512 which is the number of points.)
   N<== 9
   Do for I = 1 to 512
        IDATA(I)<== 0
   End Do
   If File_Number = Scale_Data then
        Input Scale_Data
   Else
        Input RDATA
   End If
   T<== PI/2**(N-1)
        Do for J = 0 to 2**(N-1)-1
(BI is a bit inversion subroutine.)
             Call BI(J,P,N-1)
             C<== cos(P*T)
             If INVERSE_FXFORM = True then
                  Flg7<== 1
```

```
            Else
                 Flg7<== 0
            End If
            P<== sin(P*T)*(1-2*Flg7)
            Do for I = 2*R0*J+1 to 2*R0*J+R0
                 R1<== RDATA(I)
                 R2<== RDATA(I+R0)
                 R3<== IDATA(I)
                 R4<== IDATA(I+R0)
                 RDATA(I)<== R1+R2*C+R4*P
                 IDATA(I)<== R3+R4*C-R2*P
                 RDATA(I+R0)<== R1-R2*C-R4*P
                 IDATA(I+R0)<== R3-R4*C+R2*P
            End Do
       End Do
       Output M
End Do
(This section is for re-ordering the block.)
Do for I = 0 to 2**N-1
       Call BI(I,J,N)
       Do While I-J < or = 0
            Do While I # J
                 P<== RDATA(I+1)/SQRT(2**N)
```

```
            Z<== IDATA(I+1)/SQRT(2**N)
            RDATA(I+1)<== RDATA(J+1)
            IDATA(J+1)<== IDATA(J+1)
            RDATA(J+1)<== P
            IDATA(J+1)<== Z
        End Do
        RDATA(I+1)<== RDATA(I+1)/SQRT(2**N)
        IDATA(I+1)<== IDATA(I+1)/SQRT(2**N)
    End Do
    If File_Number = Scale_Data then
        Store_Scale_Data(File_Number)
    Else
        Store_RDATA(File_Number)
    End If
  End Do
  Set_Degrees_Mode
  Return
End FXFORM
```

(This subroutine takes the binary number P1 containing P3 bits and inverts it end for end, e.g. 010111 becomes 111010.)

```
Subroutine BI(P1,P2,P3)
  P2<== 0
```

```
   P4<== P1
   Do for Z = 1 to P3
         P4<== P4/2
         P2<== 2*P2
         If fraction(P4) # 0 then
               P2<== P2 + 1
         End If
         P4<== int(P4)
   End Do
   Return
End BI
```

(This function calculates Airy(x)=2*J1(x)/x where J1(x) is the Bessel function of order one.)

```
   Function AIRY(P1)
   If P1 < 0 then
         Output 'ERROR-ARGUMENT LESS THAN 0'
         Stop
   End If
   If P1 = 0 then
         R4<== 1
         Return R4
   End If
   R5<== 0
```

```
If P1 > 15 then
     R6<== 90 + P1/2
     R12<== 1.4*P1 + 60/P1
End If
If P1 < 5 then
     R6<== 20 + 10*P1-P1**2/3
     R12<== 6 + P1
Else
     R6<== 20 + 10*P1-P1**2/3
     R12<== 1.4*P1 + 50/P1
End If
R12<== maximum(int(R12),int(3+P1/4))
Do for M = R12 to R6 by 3
     R8<== 1*e-28
     R13<==R14<== 0
     If M/2 = int(M/2) then
          Flg10<== 0
     Else
          Flg10<== 1
     End If
     Do for J = 1 to M-2
          R15<== 2*(M-J)*R8/P1-R13
          R13<== R8
```

```
            R8<==R13
            If M-J-2 = 0 then
                R4<== R15
            End If
            If Flg10 = 0 then
                Flg10<== 1
            Else
                Flg10<== 0
            End If
            R14<== R14+2*R8*Flg10
        End Do
        R15<== 2*R8/P1-R13
        R14<== R14+R15
        R4<==R4/R14
        If (abs(R4-R5)-abs(R4*1*e-6)) < or = 0 then
            R4<== 2*R4/P1
        End If
        Return R4
        R5<== R4
    End Do
    Output 'ACCURACY NOT OBTAINED'
    Return R4
End AIRY
```

```
(The subroutine Abel takes a one-dimensional
line spread function and calculates a two
dimensional point spread function.)
Subroutine ABEL(File_Number)
    N<== RDATA(1)
    RDATA(1)<== 1.4*RDATA(1)-1.3*RDATA(2)+.4*RDATA(3)
    Do for I = 2 to 54
          M<== RDATA(I)
          RDATA(I)<== .4*N+.2*M-.6*RDATA(I+1)
          N<== M
    End Do
    Do for I = 1 to 54
          RDATA(I)<== RDATA(I)/(2*SQRT((I+.1)**2-I*I))
          Do for J = 1 to 54
                RDATA(I) <==
RDATA(I)+RDATA(J)/SQRT((J+.1)**2-I*I)
          End Do
          RDATA(I)<== RDATA(I)/PI
          Output I
    End Do
    Return
End ABEL
```

```
(This subroutine prints out data in tabular form.)
Subroutine_TABLE(File_Number)
   Input RDATA(File_Number)
   Do for I = 1 to 32
        Do for J = 1 to 15
        Output RDATA(16(I-1)+J)
   End Do
   Output RDATA(16*I)
   Return
End TABLE

(This subroutine plots the desired data.)
(Each time a plot is called, this subroutine
plots the particular graph and labels it.
The horizontal axis is labeled according to the first
and last parameters passed by the calling subroutine.)
Subroutine_PLOT(P1,File_Number,P3)
   Input RDATA(File_Number)
   A<== 0
   B<== P1
   C<== minimum(RDATA)
   D<== maximum(RDATA)
   XMIN<== -.1*(B-A)
```

```
XMAX<== B+.05*(B-A)

YMIN<== C-.1*(D-C)

YMAX<== D+.05*(D-C)

E<== B

F<== 10

(Using the value of P1, the horizontal increment for
plotting and labeling is determined.)

If P1 = 512 then

     G<== 64

Else If P1 = 256 then

     G<== 32

Else If P1 = 64 then

     G<== 8

Else

     G<== 4

End If

Plot B,C,1

(This lines and places tic marks on the horizontal axis.)

Do for I = E to 0 by -G

     Plot I*(B-A)/E+A,C,2

     Plot I*(B-A)/E+A,C+(D-C)/150,2

     Plot I*(B-A)/E+A,C,2

End Do
```

(This lines and places tic marks on the vertical axis.)

```
Do for I = 0 to F
     Plot A,I*(D-C)/F+C,2
Plot A+(B-A)/150,I*(D-C)/F+C,2
Plot A,I*(D-C)/F+C,2
End Do
Character_Size 1.2,1,.7,0
```

(This numerically labels the vertical axis.)

```
Do for I = F to 0 by -1
     Plot A-.075*(B-A),I*(D-C)/F+C,1
     Label I/F
End Do
```

(This sets up a character string for labeling the vertical axis.)

```
If P3 = 0 then
     ASTRING<== 'DATA POINTS"
     L<== 1
Else If P3 = 2 then
     ASTRING<== 'LINES/MICRORADIAN'
     L<== 1/(2*L)
End If
```

(This numerically labels the horizontal axis.)

```
Do for I = 0 to E by 3
```

```
      Plot A+(I/E-.025)*(B-A),C-.025*(D-C),1
      Label I*L
  End Do
  If P3 # 0 then
      L<== Scale_Factor
  End If
(This labels the horizontal axis.)
  Plot .4*(B-A)+A,.05*(D-C)+C,1
  Label ASTRING
  Plot -.07*(B-A)+A,.3*(D-C)+C,1
  Character_Size = 1.2,1,.7,90
  ASTRING<== 'NORMALIZED INTENSITY'
  Label ASTRING
  Character_Size = .5,1,1.5,0
(This plots data.)
  I<== 0
  Plot I,maximum(RDATA(I)),1
  Do for I = 1 to P1
      Plot I-1,RDATA(I)
  End Do
  If P3 = 0 then
      Input PLOT_LABEL
      ISTRING<== PLOT_LABEL
```

```
    End If
    Plot .6*B,.9*D,1
    Label 'PLOT OF'
    Plot .6*B,.87*D,1
    Label ISTRING
    Plot .6*B,.84*D,1
    Label ESTRING, ' Laser'
    Return
End PLOT
```

V. SUMMARY

The work reported in this thesis supports the model predicted and measured in Crittenden, and others, for the long exposure case [Ref. 2]. The vidicon, in replacing the mechanical slit scanning system, shows no degrading of the signal data. It also demonstrates that a good approximation for the point spread function may be made by recording a single TV line through a laser spot. This line is then used to calculate the one-dimensional line spread function. The linearity of the video tape recorder is seen in the results of the MTF and C_n^2. The 468 oscilloscope is the workhorse for the entire system. It effectively displays, stores, digitizes, and transfers data on a real time basis.

The overall system does not have the capability of the system described by Crager. However, the relative simplicity of the structured programming technique coupled with a lower equipment cost demonstrates that comparable measurements and data evaluation using this equipment can be made. Further investigation should include use of the Data Precision 6000 digital waveform analyzer thereby allowing data to be sampled and analyzed on a near real time basis.

ANNEX A - PROGRAM LISTING

```
0: "HE-NE:SOURCE ON 9,SCALE ON 7,& COLLIMATED ON 5":
1: "GA-AS:SOURCE ON 8,SCALE ON 6,&COLLIMATED ON 4":
2: ent "SELECT CODE FOR PRINTER",A;dev "print",A
3: fmt 1,z,c;fmt 2,f8.1,z;fmt 3,f8.1
4: dim I$[1024],R[512],Y[512],C$[20],D$[20],E$[20]
5: dim I[512],A$[32],B$[20],A[2,2],B[2,1],C[2,1]
6: buf "DATA",I$,3;ina Y,I,R;0→R→W→V→U;1→L;buf "I",I$,3
7: beep;dsp "ENTER  LASER USED";wait 1500
8: ent "HE-NE=1,GA-AS=0",W
9: if W=1;"HE-NE"→E$;9→Q;jmp 2
10: "GA-AS"→E$;8→Q
11: beep;dsp E$&" SOURCE DATA RECORDED?";wait 1500
12: ent "1=YES,0=NO",V
13: if V=0 and W=1;sfg 0;cll 'TRANSFER'(Q);jmp 2
14: if V=0 and W=0;sfg 0;cll 'TRANSFER'(Q)
15: beep;ent "PLOT OF SOURCE?,1=YES,0=NO",R
16: if R=1;cll 'PLOT'(512,Q,0)
17: beep;dsp E$&" SCALE DATA RECORDED?";wait 1500
18: beep;ent "1=YES,0=NO",U
19: if U=0 and W=1;sfg 0;cll 'TRANSFER'(7→Q);jmp 2
20: if U=0 and W=0;sfg 0;cll 'TRANSFER'(6→Q)
21: beep;dsp "WHAT IS SCALE FACTOR?";wait 1000
22: ent "SCALE FACTOR=?;0 GETS PLOT",S
23: if S=0 and U#0;Q-2→Q;cll 'PLOT'(512,Q,0)
24: if S=0 and U=0;cll 'PLOT'(512,Q,0)
25: if S=0;jmp -3
26: S→L
27: if W=1;9→T→Q;jmp 2
28: 8→T→Q
29: ldf T,I$,R[*]
30: pos(I$,"R:")→B
31: val(I$[B+2,B+4])→r1
32: pos(I$,"IT:")→B
33: I$[B+3,B+4]→A$
34: ldf T-2,I$,R[*]
35: pos(I$,"R:")→B
36: val(I$[B+2,B+4])→r2
37: pos(I$,"IT:")→B
38: I$[B+3,B+4]→B$
```

```
39: ldf T-2,I$,R[*]
40: pos(I$,"R:")→B
41: val(I$[B+2,B+4])→r3
42: pos(I$,"LT:")→B
43: I$[B+3,B+4]→C$
44: if r2=r1 and A$=B$ and r2=r3 and B$=C$;jmp 2
45: beep;dsp "ERROR IN TIME SCALE";stp
46: "B":ldf Q,I$,R[*];ina Y;ara R→Y;0→A→B→C
47: for I=1 to 512
48: A+Y[I]→A;if I<51;B+Y[I]→B
49: if I>463;B+Y[I]→B
50: next I;prt A,B
51: B/100→D;A-512*D→A
52: for I=1 to 512;Y[I]-D→Y[I];C+Y[I]→C
53: if C<A/2;I→J
54: next I;prt C,J
55: for K=1 to 256
56: Y[(J-K+1)mod512+1]+Y[(K+J-1)mod512+1]→I[K]
57: next K;ina R;ara I→R
58: "IMAGE POINT SPREAD FCN"→I$;rcf 10,I$,R[*]
59: beep;ent "PSF OUTPUT=1 AND/OR CONT",Z
60: beep;ent "PSF PLOT=1 AND/OR CONT",Y
61: if Z=1;cll ''TABLE'(10)
62: if Y=1;cll ''PLOT'(32,10,1)
63: min(I[*])→r22;max(I[*])→r23
64: prt r22,r23
65: beep;ent "LSF OUTPUT=1 AND/OR CONT",Z
66: beep;ent "LSF PLOT=1 AND/OR CONT",Y
67: cll 'LSF';"IMAGE LINE SPREAD FCN"→I$;rcf 10,I$,R[*]
68: if Z=1;cll ''TABLE'(10)
69: if Y=1;cll ''PLOT'(32,10,1)
70: "CALCULATION OF FXFORM OF LSF":ldf 10,I$,R[*];ina I
71: ara R→I
72: I[1]→R[1];for I=2 to 256
73: I[I]→R[I]→R[514-I];next I
74: R[256]→R[257];rcf 10,I$,R[*]
75: cll 'FXFORM';"FXFORM OF IMAGE LSF"→I$;rcf 10,I$,R[*]
76: beep;ent "FXFORM OF LSF OUTPUT=1 AND/OR CONT",Z
77: beep;ent "FXFORM OF LSF PLOT=1 AND/OR CONT",Y
78: if Z=1;cll ''TABLE'(10)
79: if Y=1;cll ''PLOT'(32,10,2)
80: "B=DIA OF OBSCUR/DIA OF OBJ LENS IN METERS":
81: "B=0.064/.164":
82: "r1=SCALE OF DATA IN MICRORADIANS,r1→1.60":
83: "O=DIA OF OBJ LENS IN METERS;O=0.164M":
84: "W=WAVELENGTH IN METERS":
```

```
85: "CALC OF DIFFRACTION LIMIT POINT SPREAD FCN":
86: ina R;if w=1;6.328e-7→W;jmp 2
87: 9.05e-7→W
88: .064/.164→B;.164→O;L→r1
89: B^2→D;1-D→H;π*r1*O*1e-6/W→Z
90: for I=1 to 256
91: Z*(I-1)→Y;if Y>30;gto +3
92: ('AIRY'(Y)-D*'AIRY'(Y*B))^2/H^2→R[I]
93: I→K;gto +2
94: 0→R[I]
95: fxd 5;dsp R[I];next I;"OPTICS FUNCTION"→I$
96: rcf 11,I$,R[*]
97: beep;ent "OPTICS FCN PLOT=1 AND/OR CONT",Y
98: if Y=1;cll 'PLOT'(32,11,1)
99: sfg 5;cll 'LSF';"LSF OF OPTICS FCN"→I$;rcf 11,I$,R[*]
100: beep;ent "PLOT OF LSF OF OPTICS FCN=1 AND/OR CONT",Y
101: if Y=1;cll 'PLOT'(32,11,1)
102: sfg 5;ina I;ara R→I;I[1]→R[1]
103: for I=2 to 256;I[I]→R[I]→R[514-I];next I
104: R[256]→R[257];rcf 11,I$,R[*]
105: cll 'FXFORM';"FXFORM OF LSF OF OPTICS"→I$;rcf 11,I$,R[*]
106: beep;ent "PLOT OF FXFM OF OPTICS=1 AND/OR CONT",Y
107: if Y=1;cll 'PLOT'(256,11,2)
108: "CALCULATION OF QUOTIENT OF TWO FOURIER TRANSFORMS":
109: ldf 10,I$,R[*];ina I;ara R→I
110: ldf 11,I$,R[*]
111: for I=1 to 256
112: I[I]/R[I]→R[I];next I
113: "MTF OF SYSTEM"→I$;rcf 10,I$,R[*]
114: beep;ent "PLOT OF MTF OF SYS=1 AND/OR CONT",Y
115: if Y=1;cll 'PLOT'(32,10,1)
116: 0→r17→r18→r19→r20→r21→r22→r23→r24→r25
117: for I=1 to 96
118: ((I-1)*L)^(10/3)→r18
119: r18+r17→r17
120: ((I-1)*L)^(5/3)→r19
121: r19+r20→r20
122: I→r21
123: if R[I]<=0;gto "CC"
124: (ln(R[I])→r24)*r19+r23→r23
125: r24+r25→r25
126: "CC":next I
127: prt r17,r20,r21,r23,r25
128: r20→A[1,1];r21→A[1,2];r17→A[2,1];r20→A[2,2]
129: r25→C[1,1];r23→C[2,1]
130: inv A→A;mat A*C→B;flt 5;aprt B
131: "CALCULATION OF CNSQ":
132: B[1,1]/(-21.49*145*r20*W^(-.33333))→r22
133: prt "CNSQ=",r22;stp
```

```
134: cfg ;ldf 2
135: "TRANSFER":beep;dsp "ENSURE EQUIP. SET UP PROPERLY"
136: wait 1500
137: dsp "PRESS CONTINUE WHEN READY";stp
138: dsp "waiting";wait 1500
139: buf "DATA";0→Z
140: tfr 703,"DATA"
141: dsp "transferring"
142: rds("DATA")→E;if E=-1;jmp 0
143: clr 703
144: dsp "setting output"
145: pos(I$,"%")→A;1→N
146: for I=A+2 to 687 by 16
147: for J=1 to 16;if J+I>688;0→rJ;jmp 3
148: num(I$[I+J])→rJ
149: rJ→Y[N]
150: N+1→N
151: next J
152: next I
153: min(Y[*])→E;for I=1 to 512;Y[I]-E→Y[I];next I
154: ina R;ara Y→R;rcf pl,I$,R[*];ret
155: "LSF":if flg5;ldf 11,I$,R[*];jmp 2
156: ldf 10,I$,R[*]
157: ina I;ara R→I;for I=1 to 24
158: 1→J;dsp I;L[I]→Q
159: √(I*I+J*J)→R
160: 2*((1-frc(R))*I[int(R)]+frc(R)*I[int(R)+1])+Q→Q
161: J+1→J;if R<24;jmp -2
162: Q→L[I]
163: next I;ina R;ara I→R;if flg5;rcf 11,I$,R[*];cfg ;ret pl
164: ret pl
165: "FXFORM":rad;9→N;ina I;if flg5;ldf 11,I$,R[*];jmp 2
166: ldf 10,I$,R[*]
167: π/2^(N-1)→T
168: for M=1 to N;2^(N-M)→r0
169: for J=0 to 2^(M-1)-1;cll 'BI'(J,P,N-1)
170: cos(P*T)→C;sin(P*T)*(1-2*flg7)→P
171: for I=2*r0*J+1 to 2*r0*J+r0
172: R[I]→r1;R[I+r0]→r2
173: I[I]→r3;I[I+r0]→r4
174: r1+r2*C+r4*P→R[I];r3+r4*C-r2*P→I[I]
175: r1-r2*C-r4*P→R[I+r0];r3-r4*C+r2*P→I[I+r0]
176: next I;next J;dsp M;next M
177: for I=0 to 2^N-1;cll 'BI'(I,J,N)
178: if I-J>0;gto "BB"
179: if I=J;gto "INC"
180: R[I+1]/√(2^N)→P;I[I+1]/√(2^N)→Z
181: R[J+1]→R[I+1];I[J+1]→I[I+1]
182: P→R[J+1];Z→I[J+1]
```

```
183: "INC":R[I+1]/√(2^N)→R[I+1];I[I+1]/√(2^N)→I[I+1]
184: "BB":next I
185: if flg5;fcr 11,I$,R[*];deg;ret
186: deg;ret
187: "BI":0→p2;p1→p4
188: for Z=1 to p3
189: p4/2→p4;2*p2→p2
190: if frc(p4)#0;p2+1→p2
191: int(p4)→p4
192: next Z;ret
193: "AIRY":if p1<0;beep;dsp "error-argument<0";stp
194: if p1=0;1→r4;ret r4
195: 0→r5;if p1>15;jmp 2
196: 20+10*p1-p1^2/3→r6;jmp 2
197: 90+p1/2→r6
198: if p1<5;6+p1→r12;jmp 2
199: 1.4*p1+60/p1→r12
200: max(int(r12),int(3+p1/4))→r12
201: for M=r12 to r6 by 3;1e-26→r8;0→r13→r14
202: sfg 10;if M/2=int(M/2);cfg 10
203: for J=1 to M-2;2*(M-J)*r8/p1-r13→r15;r8→r13
204: r15→r8;if M-J-2=0;r15→r4
205: cmf 10;r14+2*r8*flg10→r14;next J
206: 2*r8/p1-r13→r15
207: r14+r15→r14;r4/r14→r4
208: if abs(r4-r5)-abs(r4*1e-6)<=0;2*r4/p1→r4;ret r4
209: r4→r5;next M
210: beep;dsp "ACCURACY NOT OBTAINED";wait 1500;ret r4
211: "TABLE":ldf p1,I$,R[*]
212: for I=1 to 32;for J=1 to 15
213: wrt "print.2",R[16(I-1)+J];next J
214: wrt "print.3",R[16I];next I;ret 0→Z
215: "PLOT":ldf p2,I$,R[*]
216: 0→A;p1→B;min(R[*])→C;max(R[*])→D
217: scl A-.1(B-A),B+.05(B-A),C-.1(D-C),D+.05(D-C)
218: B→E;10→F
219: if p1=512;64→G
220: if p1=256;32→G
221: if p1=64;8→G
222: if p1=32;4→G
223: plt B,C,1
224: for I=E to 0 by -G
225: plt I(B-A)/E+A,C,2
226: plt I(B-A)/E+A,C+(D-C)/150,2
227: plt I(B-A)/E+A,C,2
228: next I
229: for I=0 to F
230: plt A,I(D-C)/F+C,2
231: plt A+(B-A)/150,I(D-C)/F+C,2
```

```
232: plt A,I(D-C)/F+C,2
233: next I;pen
234: csiz 1.2,1,.7
235: fxd 1
236: for I=F to 0 by -1
237: plt A-.075(B-A),I(D-C)/F+C,1
238: lbl I/F
239: next I
240: fxd 0
241: if p3=0;"DATA POINTS"→A$;1→L
242: if p3=2;"LINES/MICRORADIAN"→A$;1/(2*L)→L
243: for I=0 to E by G
244: plt A+(I/E-.025)(B-A),C-.025(D-C),1
245: lbl I*L
246: next I;if p3#0 and p3#2;"MICRORADIANS"→A$
247: if p3=2;S→L
248: plt .4(B-A)+A,-.05(D-C)+C;lbl A$
249: plt -.07(B-A)+A,.3(D-C)+C;csiz 1.2,1,.7,90
250: "NORMALIZED INTENSITY"→A$;lbl A$
251: csiz .5,1,1.5,0;0→I
252: plt I,max(R[*]),1
253: for I=1 to p1;plt I-1,R[I];next I
254: csiz 1.2,1,.7,0
255: if p3#0;gto +2
256: beep;ent "PLOT LABEL?",I$
257: plt .6B,.9D,1;lbl "PLOT OF"
258: plt .6B,.87D,1;lbl I$
259: plt .6B,.84D,1;lbl E$," LASER"
260: pen;cfg ;ret 0→Y
*28629
```

```
0: "COMPUTED SOURCE PATTERN":
1: ina R;1000→A;2*L→C;trk 1;fdf 10
2: for I=1 to 256
3: L*(L-1)→F
4: F^2/(2*C^2)→G
5: if G>13;jmp 2
6: A*exp(-G)→R[I];I→K;jmp 2
7: 0→R[I]
8: next I
9: "COMPUTED SOURCE"→I$
10: rcf 10,I$,R[*]
11: beep;ent "PLOT OF COMPUTED SOURCE=1 AND/OR CONT",Y
12: if Y=1;cll 'PLOT'(32,10,0)
13: "CONVERTS PSF TO LSF":
14: cll 'LSF'
15: "LSF OF COMPUTED SOURCE"→I$
16: rcf 10,I$,R[*]
17: beep;ent "PLOT OF LSF OF COMP SOURCE=1 AND/OR CONT",Y
18: if Y=1;cll 'PLOT'(32,10,0)
19: "CALCULATION OF FXFORM OF LSF OF COMPUTED SOURCE":
20: ina I;ara R→I
21: I[1]→R[1]
22: for I=2 to 256
23: I[I]→R[I]→R[514-I];next I
24: R[256]→R[257];rcf 10,I$,R[*]
25: cll 'FXFORM'
26: "FXFORM OF LSF OF CALC SOURCE"→I$;rcf 10,I$,R[*]
27: beep;ent "PLOT OF FXFM OF CALC SRCE=1 AND/OR CONT",Y
28: if Y=1;cll 'PLOT'(256,10,2)
29: "CALCULATION OF PRODUCT OF 2 FXFORMS":
30: ldf 10,I$,R[*];ina I;ara R→I;trk 0
31: ldf 10,I$,R[*]
32: for I=1 to 256
33: R[I]*I[I]→R[I];next I
34: rcf 10,I$,R[*]
35: "TRANSFER FCN OF SOURCE*ATMOSPHERE*OPTICS":
36: ldf 11,I$,R[*];ina I;ara R→I
37: I[1]*R[1]→R[1]
38: for I=2 to 256
39: R[I]*I[I]→R[I]→R[514-I]
40: next I
41: R[256]→R[257]
42: "FXFM OF SOURCE*ATMOS*OPTICS"→I$
43: rcf 10,I$,R[*]
44: beep;ent "PLOT OF FXFM PRODUCTS=1 AND/OR CONT",Y
45: if Y=1;cll 'PLOT'(32,10,2)
```

```
46: "INVERSE FXFORM GIVES TARGET LSF":
47: sfg 7;cll 'FXFORM';cfg 7;"INVERSE FXFORM"→I$
48: rcf 10,I$,R[*]
49: beep;ent "PLOT OF INV FXFM=1 AND/OR CONT",Y
50: if Y=1;cll 'PLOT'(32,10,0)
51: "CONVERTS LSF TO PSF BY ABEL TRANSFORM":
52: cll 'ABEL';"ABEL XFORM PSF"→I$
53: rcf 10,I$,R[*];sfg 0
54: beep;ent "PLOT OF ABEL XFORM=1 AND/OR CONT",Y
55: if Y=1;cll 'PLOT'(32,10,0);stp
56: "CALCULATES FRACTION OF POWER INSIDE CIRCLE OF RADIUS R":
57: .25*π*R[1]→R[1]
58: for I=2 to 256
59: 2π*I*R[I]+R[I-1]→R[I]
60: next I
61: "POWER FRCTN INSIDE CIRCLE"→I$
62: rcf 10,I$,R[*]
63: beep;ent "PLOT OF POWER=1 AND/OR CONT",Y
64: if Y=1;cll 'PLOT'(32,10,0)
65: stp
66: "LSF":if flg5;ldf 11,I$,R[*];jmp 2
67: ldf 10,I$,R[*]
68: ina I;ara R→I;for I=1 to 24
69: 1→J;dsp I;I[I]→Q
70: √(I*I+J*J)→R
71: 2*((1-frc(R))*I[int(R)]+frc(R)*I[int(R)+1])+Q→Q
72: J+1→J;if R<24;jmp -2
73: Q→I[I]
74: next I;ina R;ara I→R;if flg5;rcf 11,I$,R[*];cfg ;ret pl
75: ret pl
76: "FXFORM":rad;9→N;ina I;if flg5;ldf 11,I$,R[*];jmp 2
77: ldf 10,I$,R[*]
78: π/2^(N-1)→T
79: for M=1 to N;2^(N-M)→r0
80: for J=0 to 2^(M-1)-1;cll 'BI'(J,P,N-1)
81: cos(P*T)→C;sin(P*T)*(1-2*flg7)→P
82: for I=2*r0*J+1 to 2*r0*J+r0
83: R[I]→r1;R[I+r0]→r2
84: I[I]→r3;I[I+r0]→r4
85: r1+r2*C+r4*P→R[I];r3+r4*C-r2*P→I[I]
86: r1-r2*C-r4*P→R[I+r0];r3-r4*C+r2*P→I[I+r0]
87: next I;next J;dsp M;next M
88: for I=0 to 2^N-1;cll 'BI'(I,J,N)
89: if I-J>0;gto "BB"
90: if I=J;gto "INC"
91: R[I+1]/√(2^N)→P;I[I+1]/√(2^N)→Z
92: R[J+1]→R[I+1];I[J+1]→I[I+1]
93: P→R[J+1];Z→I[J+1]
94: "INC":R[I+1]/√(2^N)→R[I+1];I[I+1]/√(2^N)→I[I+1]
```

```
95: "EB":next I
96: deg;ret
97: "BI":0→p2;p1→p4
98: for Z=1 to p3
99: p4/2→p4;2*p2→p2
100: if frc(p4)#0;p2+1→p2
101: int(p4)→p4
102: next Z;ret
103: "ABEL":ina R;ldf 10,I$,R[*];R[1]→N
104: 1.4*R[1]-1.8*R[2]+.4*R[3]→R[1]
105: for I=2 to 64
106: R[I]→M
107: .4*N+.2*M-.6*R[I+1]→R[I];M→N;next I
108: for I=1 to 64
109: R[I]/(2*√((I+.1)^2-I*I))→R[I]
110: for J=I+1 to 64
111: R[I]+R[J]/√((J+.1)^2-I*I)→R[I]
112: next J
113: if R[I]<.01;0→R[I]
114: R[I]/π→R[I];dsp I;next I
115: for I=65 to 512;0→R[I];next I;ret
116: "PLOT":ldf p2,I$,R[*]
117: 0→A;p1→B;min(R[*])→C;max(R[*])→D
118: scl A-.1(B-A),B+.05(B-A),C-.1(D-C),D+.05(D-C)
119: B→E;10→F;if flg0;prt A,B,C,D
120: if p1=512;64→G
121: if p1=256;32→G
122: if p1=64;8→G
123: if p1=32;4→G
124: plt B,C,1
125: for I=E to 0 by -G
126: plt I(B-A)/E+A,C,2
127: plt I(B-A)/E+A,C+(D-C)/150,2
128: plt I(B-A)/E+A,C,2
129: next I
130: for I=0 to F
131: plt A,I(D-C)/F+C,2
132: plt A+(B-A)/150,I(D-C)/F+C,2
133: plt A,I(D-C)/F+C,2
134: next I;pen
135: csiz 1.2,1,.7
136: fxd 1
137: for I=F to 0 by -1
138: plt A-.075(B-A),I(D-C)/F+C,1
139: lbl I/F
140: next I
141: fxd 0
142: if p3=2;"LINES/MICRORADIAN"→A$;1/(2*L)→L
143: for I=0 to E by G
```

AD-A144 858 OPTICAL TURBULENCE MEASUREMENT - INVESTIGATIONS FOR ANALYSIS OF LASER DES..(U) ARMY ELECTRONIC PROVING GROUND FORT HUACHUCA AZ E C CRITTENDEN ET AL. MAY 83 3/3

UNCLASSIFIED USAEPG-FR-1226 F/G 20/6 NL

END
DATE
FILMED
9-84
DTIC

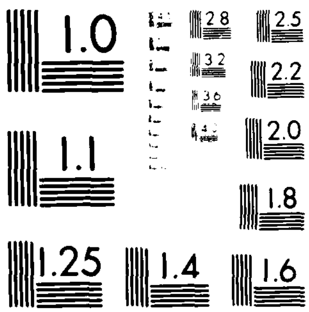

MICROCOPY RESOLUTION TEST CHART

```
144: plt A+(I/E-.025)(B-A),C-.025(D-C),1
145: lbl I*L
146: next I;if p3#2;"MICRORADIANS"→A$
147: if p3=2;S→L
148: plt .4(B-A)+A,-.05(D-C)+C;lbl A$
149: plt -.07(B-A)+A,.3(D-C)+C;csiz 1.2,1,.7,90
150: "NORMALIZED INTENSITY"→A$;lbl A$
151: csiz .5,1,1.5,0;0→I
152: plt I,max(R[*]),1
153: for I=1 to p1;plt I-1,R[I];next I
154: csiz 1.2,1,.7,0
155: plt .6B,.9D,1;lbl "PLOT OF"
156: plt .6B,.87D,1;lbl I$
157: plt .6B,.84D,1;lbl E$," LASER"
158: "RET":pen;ctg ;ret 0→Y
*17524
```

LIST OF REFERENCES

1. Tatarski, V.I., *The Effects of the Turbulent Atmosphere on Wave Propagation*, U.S. Department of Commerce, NTIS, Springfield, Va, 1971.

2. Crittenden, E.C., and others, *Optical Resolution in the Turbulent Atmosphere of the Marine Boundary Layer*, Naval Postgraduate School Report 61-78-003, February, 1978.

3. Crittenden, E.C., Milne, E.A., and Rodeback, G.W., *Systems for Analysis for Laser Designator Spot Wander and Profile*, Naval Postgraduate School Informal Report, November, 1982.

4. Crager, S.R., *A Computer Program for Investigating Atmospheric Effects on Laser Designators*, Master's Thesis, Naval Postgraduate School, Monterey, Cailifornia, March, 1982.

5. Lutomirski, R.F., and Yura, H.T., "Propagation of a Finite Optical Beam in an Inhomogeneous Medium", *Applied Optics*, v. 10, p. 1652, July, 1973.

6. Fried, D.L., "Optical Resolution through a Randomly Inhomogeneous Medium for Very Long and Very Short Exposures", *Journal of Optical Society of America*, v. 56, p. 1372, October, 1966.

7. Griem, H., *Plasma Spectroscopy*, p. 176, McGraw-Hill, 1964.

8. *468 Digital Storage Oscilloscope*, v.I, Tektronix, Inc., Beaverton, Oregon, 1981.

9. Graham, N., *Introduction to Computer Science, A Structured Approach*, 2nd ed., West, 1982.

APPENDIX E REFERENCES

1. Crittenden, Cooper, Milne, Rodeback, Armstead, Kalmbach, Land, and Katz; Optical Resolution to the Turbulent Atmosphere of the Marine Boundary Layer, Naval Postgraduate School Report, NPS61-78-003, February 1978.

2. Crittenden, Cooper, Milne, Rodeback, Kalmbach, and Armstead, Effects of Turbulence on Imaging Through the Atmosphere, SPIE Proceedings, 142, 130, March 1978.

3. Crittenden, Cooper, Milne, Rodeback, and Kalmbach, Multiwave Extinction and Index Fluctuation Measurements, AGARD Proceedings, No. 300, 13, 6 April 1981.

4. Fried, D. L., Optical Resolution through a Randomly Inhomogeneous Medium for Very Long and Very Short Exposures, Journal of the Optical Society of America, 56, 10, 1372, 1966.

5. Crager, Scott R., A Computer Program for Investigating Atmospheric Effects on Laser Designators, M.S. Thesis, Naval Postgraduate School, March 1982.

6. Connors, John, Analysis of Turbulence Utilizing a Video Tape Recorder and Digital Storage Oscilloscope, M.S. Thesis, Naval Postgraduate School, December 1982.

APPENDIX F. DISTRIBUTION LIST

Addressee	Number of Copies
Commander US Army Test and Evaluation Command ATTN: DRSTE-AD-M Aberdeen Proving Ground, Maryland 21005	4
Commander US Army Materiel Systems Analysis Activity ATTN: DRXSY-CC Aberdeen Proving Ground, Maryland 21005	1
Commander Defense Technical Information Center Cameron Station Alexandria, Virginia 22314	2
Commander US Army White Sands Missile Range ATTN: STEWS-TE-P White Sands Missile Range, New Mexico 88002	1
Commander Yuma Proving Ground ATTN: STEYP-TE Yuma, Arizona 85364	1
Commander US Army Tropic Test Center ATTN: STETC-TD-M P.O. Drawer 942 Fort Clayton, Canal Zone 09827	1
Commander Aberdeen Proving Ground ATTN: STEAP-MT-M Aberdeen Proving Ground, Maryland 21005	1
Commander Dugway Proving Ground ATTN: STEDP-MT-DA Dugway, Utah 84022	1
Commander US Army Arctic Test Center ATTN: STEAC-PL-MI APO Seattle, Washington 98733	1
Commandant Naval Postgraduate School ATTN: Code 61CT (Dr. E. Crittenden) Monterey, California 93940	2

Addressee	Number of Copies
US Army Atmospheric Sciences Laboratory ATTN: DELAS-SY-S White Sands Missile Range, New Mexico 88002	1
Commander US Army Electronics R&D Command ATTN: DELCS-S Fort Monmouth, New Jersey 07703	1
Commander/Director US Army Combat Survl and Target Acquisition Laboratory ATTN: DELCS-D Fort Monmouth, New Jersey 07703	1
Director Night Vision & Electro-Optics Laboratory ATTN: DELNV-L Fort Belvoir, Virginia 22060	1
Commander US Army Missile Command ATTN: DRSMI-OG Redstone Arsenal, Alabama 35809	1
Commander Harry Diamond Laboratories ATTN: DELHD-CO 2800 Powder Mill Road Adelphi, Maryland 20783	1
Naval Weapons Center ATTN: Code 3918 China Lake, California 93555	1
Air Force Geophysics Laboratory ATTN: LCC Hanscom AFB, Massachusetts 01731	1
Chief, Atmospheric Sciences Div Code ES-81 NASA Marshall Space Flight Center, Alabama 35812	1
Director NOAA/ERL/APCL R31 RB3-Room 567 Boulder, Colorado 80302	1